THE QUARTERLY JOURNAL OF

MECHANICS AND APPLIED MATHEMATICS

VOLUME XI PART 1

FEBRUARY 1958

OXFORD

AT THE CLARENDON PRESS

1958

Price 18*s. net*

PRINTED IN GREAT BRITAIN BY CHARLES BATEY AT THE UNIVERSITY PRESS, OXFORD

THE QUARTERLY JOURNAL OF MECHANICS AND APPLIED MATHEMATICS

THE QUARTERLY JOURNAL OF MECHANICS AND APPLIED MATHEMATICS is published at 18*s.* net for a single number with an annual subscription (for four numbers) of 60*s.* post free.

NOTICE TO CONTRIBUTORS

1. *Communication.* Papers should be communicated to Dr. D. M. A. Leggett, Department of Mathematics, King's College, Strand, London, W.C. 2.

If possible, to expedite publication, papers should be submitted in duplicate.

2. *Presentation.* Papers should be typewritten (double spacing) and should be preceded by a summary not exceding 300 words in length. References to literature should be given in standard order, *author, title of journal, volume number, date, page.* These should be placed at the end of the paper and arranged according to the order of reference in the paper.

3. *Diagrams.* The number of diagrams should be kept to the minimum consistent with clarity. The lines of the figures should be drawn in ink either on draughtsman's paper or on good quality white paper. Each individual line in the figure should bear reducing to one-half of the size of the original, and great care should be exercised to see that the lines are regular in thickness, especially where they meet. Lettering of the figure should be in pencil and should be sufficient to define clearly the lines and curves in it. The writing of formulae or of explanations on the diagram itself should be avoided. All explanations of symbols, etc., should be given in underline. Contributors should indicate on their manuscripts where figures should be inserted.

4. *Tables.* Tables should preferably be arranged so that they can be printed with the columns parallel to the longer edge of the page.

5. *Notation.* All single letters used to denote vectors in the manuscript should be marked by underlining with a wavy line. Scalar and vector products should be denoted by $\underset{\sim}{a} . \underset{\sim}{b}$ and $\underset{\sim}{a} \wedge \underset{\sim}{b}$ respectively. Real and imaginary parts of complex quantities should be denoted by re and im respectively.

6. *Offprints.* Authors of papers will be entitled to 25 free offprints. This number is available for sharing between authors of joint papers.

7. All correspondence other than that dealing with contributions should be addressed to the publishers:

OXFORD UNIVERSITY PRESS
AMEN HOUSE, LONDON, E.C. 4

THE QUARTERLY JOURNAL OF MECHANICS AND APPLIED MATHEMATICS

THE QUARTERLY JOURNAL OF MECHANICS AND APPLIED MATHEMATICS is published at 18*s.* net for a single number with an annual subscription (for four numbers) of 60*s.* post free.

NOTICE TO CONTRIBUTORS

1. *Communication.* Papers should be communicated to Dr. D. M. A. Leggett, Department of Mathematics, King's College, Strand, London, W.C. 2.

If possible, to expedite publication, papers should be submitted in duplicate.

2. *Presentation.* Papers should be typewritten (double spacing) and should be preceded by a summary not exceeding 300 words in length. References to literature should be given in standard order, *author, title of journal, volume number, date, page.* These should be placed at the end of the paper and arranged according to the order of reference in the paper.

3. *Diagrams.* The number of diagrams should be kept to the minimum consistent with clarity. The lines of the figures should be drawn in ink either on draughtsman's paper or on good quality white paper. Each individual line in the figure should bear reducing to one-half of the size of the original, and great care should be exercised to see that the lines are regular in thickness, especially where they meet. Lettering of the figure should be in pencil and should be sufficient to define clearly the lines and curves in it. The writing of formulae or of explanations on the diagram itself should be avoided. All explanations of symbols, etc., should be given in underline. Contributors should indicate on their manuscripts where figures should be inserted.

4. *Tables.* Tables should preferably be arranged so that they can be printed with the columns parallel to the longer edge of the page.

5. *Notation.* All single letters used to denote vectors in the manuscript should be marked by underlining with a wavy line. Scalar and vector products should be denoted by $\underset{\sim}{a} . \underset{\sim}{b}$ and $\underset{\sim}{a} \wedge \underset{\sim}{b}$ respectively. Real and imaginary parts of complex quantities should be denoted by re and im respectively.

6. *Offprints.* Authors of papers will be entitled to 25 free offprints. This number is available for sharing between authors of joint papers.

7. All correspondence other than that dealing with contributions should be addressed to the publishers:

OXFORD UNIVERSITY PRESS
AMEN HOUSE, LONDON, E.C. 4

Some Non-Linear Problems in the Theory of Automatic Control

By A. I. LUR'E

A translation from the Russian, covering seven years' work published in the Soviet Journal, *Applied Mathematics and Mechanics*, and elsewhere. It is intended for engineers and scientific workers engaged on the calculation and construction of systems of automatic control in various spheres of engineering. **17s. 6d.** (*post* 11*d.*)

HMSO

from the Government Bookshops or through any bookseller

AN APPLICATION OF CROCCO'S STREAM FUNCTION TO THE STUDY OF ROTATIONAL SUPERSONIC FLOW PAST AIRFOILS†

By ABRAHAM KOGAN‡

(*Technion—Israel Institute of Technology, Haifa, Israel*)

[Received 25 October 1956]

SUMMARY

A method of successive approximations to the ideal flow around airfoils at high supersonic Mach numbers is developed, based on the concept of Crocco's stream function.

Taking the undisturbed flow as a starting-point, a second approximation to the flow in the whole region surrounding the airfoil is derived, and the results for velocity and pressure distribution at the airfoil surface are compared with the corresponding expressions obtained by potential flow theory.

The flow behind a plane shock wave is next chosen as zero-order approximation in order to obtain better results for the flow in the vicinity of the leading edge. The first approximation gives expressions for the shock-wave curvature and for the derivative of the pressure coefficient at the leading edge, which check similar results obtained by other investigators. The second approximation yields expressions for the derivative of the shock-wave curvature and for the second derivative of the pressure coefficient at the leading edge.

Nomenclature

A, B, C	constants defined by equations (78).
G, H, L	constants defined by equations (56).
a_{ij}, b_{ij}	coefficients in expansions of velocity perturbations.
c	speed of sound, in units of limiting velocity.
c_v	specific heat at constant volume.
c_p	pressure coefficient.
$g(x)$	airfoil profile.
$G(x)$	airfoil profile form function.
K_{w_0}, K_{sh_0}	airfoil and shock curvature at leading edge, respectively.
M	Mach number.
P	function of w, defined by equation (11).
P_{ij}	coefficients in expansion of P in powers of ψ_y and ψ_x.

† Abstracted from a doctoral dissertation submitted by the author in the Department of Aeronautical Engineering, Princeton University. The work was sponsored by the U.S. Air Force, under contract AF61(514)–870.

The author gratefully acknowledges the helpful suggestions of Professor Sydney Goldstein, under whose supervision this research was carried out.

‡ Senior Lecturer, Department of Aeronautics.

p pressure.
S entropy.
T temperature.
x, y cartesian coordinates.
u, v components of w in x- and y-directions.
u', v' components of velocity perturbations.
w velocity, in units of limiting velocity.
$\alpha_1, \alpha_2, \alpha_3$ constants defined by equations (81).
α $\sqrt{(M_1^2-1)}$.
β $\sqrt{(M_2^2-1)}$.
$\Delta_1, \Delta_2, \Delta_3, \Delta_4, \Delta_5$ determinants defined by equations (88).
δ flow inclination to undisturbed stream.
ϵ thickness parameter.
η $M_1^2 \sin^2\nu$.
$\eta_0, \eta_1, \ldots$ coefficients in expansion of η in powers of ϵ or Ψ.
μ_2 $\sin^{-1}(1/M)$.
ν shock-wave inclination to undisturbed stream.
ρ density.
σ length parameter along shock profile.
τ slope of shock-wave profile.
$\tau_0, \tau_1, \tau_2, \ldots$ coefficients in expansion of τ in powers of x.
Ψ Crocco's stream function.
ψ perturbation stream function.
$\psi_1, \psi_2, \ldots$ terms in expansion of ψ.
ν_0, δ_0 shock and flow inclination at leading edge.
M_0, u_0 zero-order approximations to M and u.
p_0, S_0, T_0, ρ_0 stagnation values of p, S, T, and ρ.
$p_1, S_1, T_1, \rho_1, M_1, u_1, v_1, w_1, c_1$ values of respective parameters in undisturbed flow.
$p_2, S_2, T_2, \rho_2, M_2, u_2, v_2, c_2$ values of respective parameters behind plane shock wave.

1. Introduction

THE potential flow approximation to the supersonic flow around airfoils gives a fair estimate of the actual flow when the airfoils considered are thin and the free stream Mach number small enough. However, when the thickness ratio of the airfoils and the free stream Mach number are increased, the vorticity generated by the curved shock wave attached to the leading edge becomes an important factor, and approximations obtained by potential flow theory become rather poor. In fact, when the thickness ratio and the free stream Mach number are increased to the point at which the free

stream Mach angle equals the tip wedge angle, potential flow perturbation solutions lose their physical meaning altogether (**1**).

Since the method of characteristics, which is capable of giving exact solutions of the ideal flow, is rather lengthy and provides results only in numerical form, attempts have been made in recent years to devise approximate methods which should simplify the treatment of high supersonic flows without neglecting the main rotationality effect (**2–5**; see also **16** and **17**).

The study of flow behind a curved shock wave in the vicinity of the leading edge of airfoils is particularly interesting, since essential features of the high supersonic flow may be explained by such studies. Also the approximate methods for the calculation of the whole flow field take the flow in the region of the leading edge as a starting-point.

The aim of the present investigation is to develop a method of successive approximations for the study of flow at high supersonic Mach numbers, based on the use of Crocco's stream function.

A first and second approximation to the flow in the whole region surrounding the airfoil are calculated, starting from the undisturbed flow as the zero-order approximation. The well-known results obtained by Busemann (**6**, **7**) and Van Dyke (**1**) by potential flow theory are obtained, but it is shown that their validity extends to much higher values of the free stream Mach number and of the leading edge angle.

Then taking the flow behind a plane shock wave as zero-order approximation, the flow in the vicinity of the leading edge is studied. The solution of the first approximation gives expressions for the shock-wave curvature and for the slope of the pressure coefficient at the leading edge which check the results obtained by the method of characteristics (**8–12**). The second approximation yields formulae for the derivative of the shock-wave curvature and for the second derivative of the pressure coefficient at the leading edge.

2. Crocco's equation for two-dimensional flow

Consider a sharp-nosed airfoil placed in a uniform supersonic flow of an ideal and perfect gas. Crocco (**13**) showed that it is possible to define a stream function Ψ by the equations

$$\left.\begin{aligned} \Psi_y &= u(1-w^2)^{1/(\gamma-1)} \\ \Psi_x &= -v(1-w^2)^{1/(\gamma-1)} \end{aligned}\right\}, \tag{1}$$

where suffixes denote derivatives.

The continuity equation is satisfied identically by Ψ, and the momentum and energy equations lead to Crocco's equation

$$(c^2-u^2)\Psi_{xx}-2uv\Psi_{xy}+(c^2-v^2)\Psi_{yy} = (1-w^2)^{(\gamma+1)/(\gamma-1)}(w^2-c^2)f(\Psi) \tag{2}$$

p pressure.
S entropy.
T temperature.
x, y cartesian coordinates.
u, v components of w in x- and y-directions.
u', v' components of velocity perturbations.
w velocity, in units of limiting velocity.
$\alpha_1, \alpha_2, \alpha_3$ constants defined by equations (81).
α $\sqrt{(M_1^2-1)}$.
β $\sqrt{(M_2^2-1)}$.
$\Delta_1, \Delta_2, \Delta_3, \Delta_4, \Delta_5$ determinants defined by equations (88).
δ flow inclination to undisturbed stream.
ϵ thickness parameter.
η $M_1^2 \sin^2\nu$.
$\eta_0, \eta_1, \ldots$ coefficients in expansion of η in powers of ϵ or Ψ.
μ_2 $\sin^{-1}(1/M)$.
ν shock-wave inclination to undisturbed stream.
ρ density.
σ length parameter along shock profile.
τ slope of shock-wave profile.
$\tau_0, \tau_1, \tau_2, \ldots$ coefficients in expansion of τ in powers of x.
Ψ Crocco's stream function.
ψ perturbation stream function.
$\psi_1, \psi_2, \ldots$ terms in expansion of ψ.
ν_0, δ_0 shock and flow inclination at leading edge.
M_0, u_0 zero-order approximations to M and u.
p_0, S_0, T_0, ρ_0 stagnation values of p, S, T, and ρ.
$p_1, S_1, T_1, \rho_1, M_1, u_1, v_1, w_1, c_1$ values of respective parameters in undisturbed flow.
$p_2, S_2, T_2, \rho_2, M_2, u_2, v_2, c_2$ values of respective parameters behind plane shock wave.

1. Introduction

THE potential flow approximation to the supersonic flow around airfoils gives a fair estimate of the actual flow when the airfoils considered are thin and the free stream Mach number small enough. However, when the thickness ratio of the airfoils and the free stream Mach number are increased, the vorticity generated by the curved shock wave attached to the leading edge becomes an important factor, and approximations obtained by potential flow theory become rather poor. In fact, when the thickness ratio and the free stream Mach number are increased to the point at which the free

stream Mach angle equals the tip wedge angle, potential flow perturbation solutions lose their physical meaning altogether (**1**).

Since the method of characteristics, which is capable of giving exact solutions of the ideal flow, is rather lengthy and provides results only in numerical form, attempts have been made in recent years to devise approximate methods which should simplify the treatment of high supersonic flows without neglecting the main rotationality effect (**2–5**; see also **16** and **17**).

The study of flow behind a curved shock wave in the vicinity of the leading edge of airfoils is particularly interesting, since essential features of the high supersonic flow may be explained by such studies. Also the approximate methods for the calculation of the whole flow field take the flow in the region of the leading edge as a starting-point.

The aim of the present investigation is to develop a method of successive approximations for the study of flow at high supersonic Mach numbers, based on the use of Crocco's stream function.

A first and second approximation to the flow in the whole region surrounding the airfoil are calculated, starting from the undisturbed flow as the zero-order approximation. The well-known results obtained by Busemann (**6**, **7**) and Van Dyke (**1**) by potential flow theory are obtained, but it is shown that their validity extends to much higher values of the free stream Mach number and of the leading edge angle.

Then taking the flow behind a plane shock wave as zero-order approximation, the flow in the vicinity of the leading edge is studied. The solution of the first approximation gives expressions for the shock-wave curvature and for the slope of the pressure coefficient at the leading edge which check the results obtained by the method of characteristics (**8–12**). The second approximation yields formulae for the derivative of the shock-wave curvature and for the second derivative of the pressure coefficient at the leading edge.

2. Crocco's equation for two-dimensional flow

Consider a sharp-nosed airfoil placed in a uniform supersonic flow of an ideal and perfect gas. Crocco (**13**) showed that it is possible to define a stream function Ψ by the equations

$$\left.\begin{aligned} \Psi_y &= u(1-w^2)^{1/(\gamma-1)} \\ \Psi_x &= -v(1-w^2)^{1/(\gamma-1)} \end{aligned}\right\}, \tag{1}$$

where suffixes denote derivatives.

The continuity equation is satisfied identically by Ψ, and the momentum and energy equations lead to Crocco's equation

$$(c^2-u^2)\Psi_{xx}-2uv\Psi_{xy}+(c^2-v^2)\Psi_{yy} = (1-w^2)^{(\gamma+1)/(\gamma-1)}(w^2-c^2)f(\Psi) \tag{2}$$

where
$$f(\Psi) = \frac{1}{2\gamma}\frac{dS}{c_v\, d\Psi}. \tag{3}$$

The only restrictions made in deriving (2) are the assumptions of a two-dimensional steady flow and of a frictionless perfect gas. Equation (2) is valid for compressible and rotational flow. It is suitable therefore for the treatment of two-dimensional flow behind shock waves.

It is remarkable that (1) define Ψ only by velocity components. No thermodynamical state property of flow appears explicitly in them. This feature of Crocco's stream function gives it the advantage over the ordinary stream function for compressible flow. It is also interesting to observe that since by the energy equation

$$1-w^2 = \frac{2}{\gamma-1}c^2 = \frac{T}{T_0}, \tag{4}$$

equations (1) may be written in the form

$$\Psi_y = \left(\frac{T}{T_0}\right)^{1/(\gamma-1)} u = \exp\left(\frac{S-S_0}{R}\right)\left(\frac{\rho}{\rho_0}\right)u,$$

$$\Psi_x = -\left(\frac{T}{T_0}\right)^{1/(\gamma-1)} v = -\exp\left(\frac{S-S_0}{R}\right)\left(\frac{\rho}{\rho_0}\right)v,$$

so in the case of isentropic flow Crocco's stream function becomes identical with the ordinary stream function for compressible flow. They are really different only in the case of a rotational flow.

Equations (1) may be written in the form

$$d\Psi = (1-w^2)^{1/(\gamma-1)}(u\,dy - v\,dx), \tag{5}$$

which shows that Ψ is a constant along streamlines and that it increases continually when we move from the airfoil surface towards more remote streamlines; Ψ can therefore be used as a coordinate along the shock wave profile. In particular, the shock-wave parameter $\eta = M_1^2 \sin^2\nu$ is a function of Ψ:

$$\eta = \eta(\Psi). \tag{6}$$

It is convenient to express $f(\Psi)$ in (3) explicitly through η. The following equations relate the entropy increase through a shock wave to the shock-wave parameter η:

$$\frac{S-S_1}{c_v} = \ln(p/p_1)+\gamma\ln(\rho_1/\rho),$$

$$\frac{p}{p_1} = \frac{2\gamma}{\gamma+1}\left(\eta-\frac{\gamma-1}{2\gamma}\right); \qquad \frac{\rho_1}{\rho} = \frac{\gamma-1}{\gamma+1}\left(\eta+\frac{2}{\gamma-1}\right)\Big/\eta.$$

Using these relations, we obtain for $f(\Psi)$

$$f(\Psi) = \frac{1}{2\gamma}\frac{dS}{c_v d\eta}\frac{d\eta}{d\Psi} = \frac{1}{2\gamma}Q(\eta)\frac{d\eta}{d\Psi} \tag{7}$$

with
$$Q(\eta) = \frac{(\eta-1)^2}{\eta[\eta-\{(\gamma-1)/2\gamma\}][\eta+\{2/(\gamma-1)\}]}. \tag{8}$$

3. The perturbation stream function

Define a perturbation stream function $\psi(x, y)$ by

$$\Psi = u_0(1-u_0^2)^{1/(\gamma-1)}\{y+\psi(x,y)\}, \tag{9}$$

where u_0 is a constant representing the zero-order approximation to u. Expressed in terms of ψ, (2) becomes

$$\frac{2}{\gamma-1}(1-u_0^2)^{-1}\{(c^2-u^2)\psi_{xx}-2uv\psi_{xy}+(c^2-v^2)\psi_{yy}\} = P(w)Q(\eta)\frac{d\eta}{d\Psi}, \tag{10}$$

where
$$P(w) = \frac{1}{\gamma(\gamma-1)}u_0^{-1}(1-u_0^2)^{-\gamma/(\gamma-1)}(1-w^2)^{(\gamma+1)/(\gamma-1)}(w^2-c^2). \tag{11}$$

We shall choose the coordinate system with the x-axis in the direction of the uniform flow which represents the zero-order approximation. The perturbations of the velocity components $u' = u-u_0$ and $v' = v$ can be expanded by (1) into power series of the first derivatives of ψ

$$u'/u_0 = \sum_{i,j=0}^{\infty} a_{ij}\psi_y^i\psi_x^j, \tag{12}$$

$$v'/u_0 = \sum_{i,j=0}^{\infty} b_{ij}\psi_y^i\psi_x^j. \tag{13}$$

The coefficients a_{ij} and b_{ij} may be expressed through the Mach number M_0 of the zero-order flow approximation. The coefficients up to the second order are

$$\left.\begin{aligned} a_{00} &= a_{01} = a_{11} = b_{00} = b_{10} = b_{20} = b_{02} = 0 \\ a_{10} &= -1/(M_0^2-1) \\ a_{20} &= \tfrac{1}{2}\{M_0^2/(M_0^2-1)^3\}\{(2-\gamma)M_0^2-3\} \\ a_{02} &= -\tfrac{1}{2}M_0^2/(M_0^2-1) \\ b_{01} &= -1 \\ b_{11} &= M_0^2/(M_0^2-1) \end{aligned}\right\}. \tag{14}$$

Equations (12) and (13) will be used subsequently in order to expand the coefficients of (10).

4. Boundary conditions

If the airfoil profile is given by

$$y = g(x) \tag{15}$$

the condition of tangency of flow at the solid boundary may be expressed by

$$\Psi(x, g(x)) = 0.$$

Or, taking the derivative of this equation along the airfoil profile and introducing the perturbation stream function ψ, the tangency condition becomes

$$\psi_x(x, g(x)) + g'(x)\{1 + \psi_y(x, g(x))\} = 0. \tag{16}$$

The Rankine–Hugoniot shock-wave conditions may be expressed as follows:

$$w_t - w_{1t} = 0, \tag{17}$$

$$w_{1n}(w_n - w_{1n}) = \frac{2}{\gamma+1}(c_1^2 - w_{1n}^2), \tag{18}$$

where w_t and w_n are the components of the non-dimensional velocity in a direction tangential and normal to the shock-wave profile respectively, evaluated right behind the shock wave, and the quantities marked by the index $_1$ are evaluated in front of it.

In terms of the velocity components u, v in the x, y coordinate system, and the slope τ of the shock wave, w_t and w_n can be expressed as

$$w_t = \frac{u + \tau v}{\sqrt{(1+\tau^2)}}, \tag{19}$$

$$w_n = \frac{\tau u - v}{\sqrt{(1+\tau^2)}}. \tag{20}$$

When (19) and (20) are inserted in (17) and (18) these become

$$u + \tau v = u_1 + \tau v_1 \tag{21}$$

and

$$(\tau u_1 - v_1)(\tau u - v) = \frac{2}{\gamma+1} c_1^2 (1+\tau^2) + \frac{\gamma-1}{\gamma+1}(\tau u_1 - v_1)^2. \tag{22}$$

Our problem is to find a solution $\psi(x, y)$ of (10) subject to the conditions (16), (21), and (22). The differential equation (10) is of the second order and a solution would be determined by two boundary conditions. Yet the conditions (16), (21), and (22) do not over-determine the system since they contain a new unknown, the shock-wave parameter $\eta = \eta(\Psi)$ or $\tau = \tau(x)$. The problem is further complicated by the fact that the right-hand side of (10) depends itself on the unknown parameter η.

The natural approach seems to be one of successive approximations. We shall assume a zero-order approximation for the velocity field and for the shock profile. Using this approximation, we shall express explicitly the differential equation and the boundary conditions correct to the first

order. This will determine a first-order approximation to the flow field and the shock-wave profile. Then the procedure will be iterated in the hope that we thus obtain a sequence of solutions which converge to the correct result.

Up to this point we have assumed that the zero-order approximation to the flow field is given by a uniform flow

$$w = u_0$$

and consequently by a plane shock wave

$$\tau = \tau_0$$

without specifying, however, the values of u_0 and τ_0. We can expect the results of higher approximations to be better the closer the zero-order approximation itself represents the flow. In the case of very thin airfoils we may hope to obtain good results by taking the undisturbed flow in front of the airfoil as the zero-order approximation. But if the airfoil is thick, the free stream would provide a bad starting-point. In this case the results will be much better if we choose as zero-order approximation the flow behind a straight shock-wave generated by a plane wedge of wedge angle equal to the leading edge angle of the airfoil. We shall consider separately these two cases.

5. First approach: free stream taken as zero-order approximation

According to our convention above, we choose in this case the x-axis in the direction of the undisturbed flow.

Let us introduce a thickness parameter ϵ by writing the airfoil profile equation in the form

$$y = g(x) = \epsilon\, G(x), \tag{23}$$

where

$$G(x)_{\max} = 1.$$

The shock-wave parameters may be expanded in powers of ϵ:

$$\eta = M_1^2 \sin^2\nu = \eta_0 + \eta_1\epsilon + \eta_2\epsilon^2 + \dots \tag{24}$$

or, alternatively,

$$\tau = \tan\nu = \tau_0 + \tau_1\epsilon + \tau_2\epsilon^2 + \dots . \tag{25}$$

The perturbation stream function may be similarly expanded

$$\psi = \psi_1\epsilon + \psi_2\epsilon^2 + \dots . \tag{26}$$

In the present case the zero-order approximation to the second shock condition (22) reduces to

$$M_1^2 = \frac{1+\tau_0^2}{\tau_0^2},$$

or, defining ν_0 by $\tan\nu_0 = \tau_0$,

$$M_1^2 = \frac{1}{\sin^2\nu_0}.$$

This yields

$$\eta_0 = M_1^2 \sin^2\nu_0 = 1. \tag{27}$$

But since $dS/(c_v d\eta)$ contains the factor $(\eta-1)^2$ and $d\eta/d\Psi = O(\epsilon)$, it follows that the right-hand side of the differential equation (10) is at least of third order in ϵ. The first- and second-order expressions for the differential equation reduce therefore to

$$\psi_{1yy}-\alpha^2\psi_{1xx} = 0 \tag{28}$$

and

$$\psi_{2yy}-\alpha^2\psi_{2xx} = -(\gamma+1)\frac{\alpha^2+1}{\alpha^2}\psi_{1y}\psi_{1xx}-2(\alpha^2+1)\psi_{1x}\psi_{1xy}- \\ -(\gamma+1)\frac{\alpha^2+1}{\alpha^2}\psi_{1y}\psi_{1yy}, \tag{29}$$

respectively, where $\alpha^2 = M_1^2-1$.

The tangency condition (16) will be expanded around $y = 0$. Inserting (23) in (16) and equating equal powers of ϵ, we obtain for the first approximation

$$\psi_{1x}(x, 0)+G'(x) = 0 \tag{30}$$

and for the second approximation

$$\psi_{2x}(x, 0)+G(x)\psi_{1xy}(x, 0)+G'(x)\psi_{1y}(x, 0) = 0. \tag{31}$$

The shock-wave conditions should be expressed at the shock-wave profile. But since this is unknown as yet, we may expand quantities at the actual shock line in Taylor series around the zero-order position of the shock line. We thus obtain from (12) and (13) the velocity components on the shock-wave surface as

$$u\left(x, \int_0^x \tau\, dx\right) \\ = u_1\left[1+a_{10}\psi_{1y}\epsilon+\left(a_{10}\int_0^x \tau_1(x)\, dx\, \psi_{1yy}+a_{10}\psi_{2y}+a_{20}\psi_{1y}^2+a_{02}\psi_{1x}^2\right)\epsilon^2+\dots\right] \tag{32}$$

and

$$v\left(x, \int_0^x \tau\, dx\right) \\ = u_1\left[b_{01}\psi_{1x}\epsilon+\left(b_{01}\int_0^x \tau_1(x)\, dx\, \psi_{1xy}+b_{01}\psi_{2x}+b_{11}\psi_{1x}\psi_{1y}\right)\epsilon^2+\dots\right], \tag{33}$$

where ψ_{1x}, ψ_{1y}, ψ_{1xy}, and ψ_{1yy} are evaluated at $y = \tau_0 x$. Since in the present case

$$u_0 = u_1, \qquad v_0 = 0$$

the shock-wave conditions (21) and (22) simplify to

$$\frac{u}{u_1}+\tau\frac{v}{u_1} = 1 \tag{34}$$

and
$$\tau^2\frac{u}{u_1}-\tau\frac{v}{u_1}=\frac{2}{\gamma+1}\frac{c_1^2}{u_1^2}+\left(\frac{2}{\gamma+1}\frac{c_1^2}{u_1^2}+\frac{\gamma-1}{\gamma+1}\right)\tau^2. \tag{35}$$

Inserting here the expansions (32), (33), and (25), we find that (34) is identically satisfied to the zero-order of approximation, and that it gives to the first order
$$a_{10}\psi_{1y}+\tau_0 b_{01}\psi_{1x}=0 \tag{36}$$
and to the second order
$$a_{10}\psi_{2y}+\tau_0 b_{01}\psi_{2x}+(a_{10}\psi_{1yy}+\tau_0 b_{01}\psi_{1xy})\int_0^x \tau_1(x)\,dx+$$
$$+b_{01}\tau_1\psi_{1x}+a_{20}\psi_{1y}^2+a_{02}\psi_{1x}^2+\tau_0 b_{11}\psi_{1x}\psi_{1y}=0. \tag{37}$$
Equation (35) gives to the zero order
$$M_1^2=\frac{1}{\sin^2\nu_0},$$
to the first order
$$\tau_0 a_{10}\psi_{1y}-b_{01}\psi_{1x}=\frac{4}{\gamma+1}\left(\frac{c_1^2}{u_1^2}-1\right)\tau_1 \tag{38}$$
and to the second order
$$\frac{2}{\gamma+1}\left(1-\frac{c_1^2}{u_1^2}\right)(\tau_1^2+2\tau_0\tau_2)+\tau_0^2 a_{10}\psi_{2y}-\tau_0 b_{01}\psi_{2x}+$$
$$+(\tau_0^2 a_{10}\psi_{1yy}-\tau_0 b_{01}\psi_{1xy})\int_0^x \tau_1(x)\,dx+$$
$$+(2\tau_0 a_{20}\psi_{1y}-b_{01}\psi_{1x})\tau_1+\tau_0^2 a_{20}\psi_{1y}^2+\tau_0^2 a_{02}\psi_{1x}^2-$$
$$-\tau_0 b_{11}\psi_{1x}\psi_{1y}=0. \tag{39}$$
Here all derivatives of ψ are evaluated at $y=\tau_0 x$.

The first-order problem is defined by the differential equation (28) with the boundary conditions (30), (36), and (38). The general solution of (28) is
$$\psi_1(x,y)=m_1(x+\alpha y)+n_1(x-\alpha y),$$
where m and n are determined by (30) and (36). We obtain
$$\psi_1(x,y)=-G(x-\alpha y). \tag{40}$$
Using this result in (38), we obtain for τ_1
$$\tau_1=\frac{\gamma+1}{4}\frac{(\alpha^2+1)^2}{\alpha^4}G'(0). \tag{41}$$

Hence to the first order the shock wave is still plane, but it no longer coincides with the Mach wave.

The second-order problem is defined by the differential equation (29) with the boundary conditions (31), (37), and (39). These equations are determined by inserting for ψ_1 and τ_1 the first-order solution (40) and (41).

Equation (29) becomes

$$\psi_{2yy}-\alpha^2\psi_{2xx} = (\gamma+1)\frac{(\alpha^2+1)^2}{\alpha} G'(x-\alpha y)G''(x-\alpha y). \tag{42}$$

The following particular integral $\bar{\psi}_2$ of this equation was found by inspection:

$$\bar{\psi}_2 = -\frac{\gamma+1}{4}\frac{(\alpha^2+1)^2}{\alpha^3}\{G'(x-\alpha y)\}^2 x.$$

The general solution of (42) may be expressed, therefore, in the form

$$\psi_2(x,y) = m_2(x+\alpha y)+n_2(x-\alpha y)-\frac{\gamma+1}{4}\frac{(\alpha^2+1)^2}{\alpha^3}\{G'(x-\alpha y)\}^2 x.$$

The application of the shock-wave condition (37) yields

$$m_2'(x) = 0,$$

and we can put, without loss of generality,

$$m_2 = 0;$$

n_2 is then determined by the tangency condition (31) and we obtain

$$\psi_2(x,y) = -\frac{\gamma+1}{4}\frac{(\alpha^2+1)^2}{\alpha^2}\{G'(x-\alpha y)\}^2 y-\alpha\, G(x-\alpha y)\, G'(x-\alpha y). \tag{43}$$

Finally, inserting this value of ψ_2 into the second shock-wave condition (39), the following expression for τ_2 is found:

$$\tau_2(x) = \frac{(\gamma+1)^2}{32}\frac{(\alpha^2+1)^2}{\alpha^7}\left\{\left(\alpha^4+2\frac{3\gamma-1}{\gamma+1}\alpha^2+5\right)(G'(0))^2+ \right.$$
$$\left. +\frac{8}{\gamma+1}\alpha^4 G(0)G''(0)+2(\alpha^2+1)^2 G'(0)\, G''(0)x\right\}. \tag{44}$$

To the second approximation the shock wave is represented by a parabola. Now using the expressions (40) and (43) for ψ_1 and ψ_2, we can calculate u/u_1 and v/u_1 at a point x, y of the flow, correct to the second order. They depend in general on $G(x-\alpha y)$, $G'(x-\alpha y)$, and $G''(x-\alpha y)$. But at the airfoil surface the terms of u/u_1 containing G'' cancel and we obtain

$$\frac{u(x,\epsilon\, G(x))}{u_1} = 1-\frac{1}{\alpha}G'(x)\epsilon-\frac{\gamma+1}{4}\frac{\alpha^4+2\{(\gamma-1)/(\gamma+1)\}\alpha^2+1}{\alpha^4}\{G'(x)\}^2\epsilon^2. \tag{45}$$

This result is identical with the one obtained by Van Dyke (1) by potential flow theory.

Inserting this and the corresponding expression for v/u_1 into the expanded expression of c_p, we obtain to the second order

$$c_p = \frac{2}{\alpha}G'(x)\epsilon+\frac{(\gamma+1)(\alpha^2+1)^2-4\alpha^2}{2\alpha^4}\{G'(x)\}^2\epsilon^2, \tag{46}$$

which coincides with the well-known result of Busemann (6, 7). Taking the free stream as zero-order approximation, the pressure coefficient at the airfoil surface depends, to the second order, only on the local slope.

As far as conditions at the airfoil surface are concerned the present method does not improve on the results of potential theory. This is due to the fact that no terms representing vorticity appear in the differential equation up to the second-order approximation, and the boundary conditions at the airfoil are also equally approximated by both methods.

But our method also gives good results away from the airfoil, even near the shock wave, where the potential theory fails because of its inherently incorrect application of the shock-wave conditions. A check on our results (27), (41), and (44) for the shock profile may be obtained by expanding the exact shock profile equation of the flow over a plane wedge of wedge angle

$$\delta = \tan^{-1}\epsilon.$$

The exact shock profile equation in this case is

$$\frac{1}{\epsilon} = \left[\frac{\gamma+1}{2}\,\frac{M_1^2}{\{M_1^2\tau^2/(1+\tau^2)-1\}} - 1\right]\tau,$$

where τ is the tangent of the shock angle. Inserting

$$\tau = \tau_0+\tau_1\epsilon+\tau_2\epsilon^2+\ldots$$

and equating equal powers of ϵ, we obtain

$$\tau_0 = \frac{1}{\alpha}, \tag{47}$$

$$\tau_1 = \frac{\gamma+1}{4}\,\frac{(\alpha^2+1)^2}{\alpha^4}, \tag{48}$$

$$\tau_2 = \frac{(\gamma+1)^2}{32}\,\frac{(\alpha^2+1)^2}{\alpha^7}\left\{\alpha^4+2\,\frac{3\gamma-1}{\gamma+1}\,\alpha^2+5\right\}. \tag{49}$$

Equation (47) corresponds with (27). When we insert (47)–(49) in (41) and (44) we find that we must have

$$G'(0) = 1$$

and

$$G''(0) = 0.$$

In this connexion it is interesting to observe that in potential flow theory the region of disturbed flow is bounded, to any order of approximation, by the airfoil surface and by the Mach wave from the tip in the undisturbed flow. And when M_1 and the tip angle δ_0 are so high that

$$\tan\delta_0 = \epsilon\,G'(0) \geqslant \frac{1}{\sqrt{(M_1^2-1)}},$$

the region of definition of disturbed flow shrinks to zero and potential flow

approximations become altogether meaningless. Such a breakdown occurs, to be sure, in the present approach too, but for a given tip angle it is delayed to much higher values of M_1. Thus in the present theory the ratio of the tangents of the shock and airfoil tip angles is given to the first approximation by

$$\frac{\tau}{\tan\delta_0} = \frac{1}{\epsilon\, G'(0)\sqrt{(M_1^2-1)}} + \frac{\gamma+1}{4}\,\frac{M_1^4}{(M_1^2-1)^2}, \tag{50}$$

and in potential theory by

$$\frac{\tau}{\tan\delta_0} = \frac{1}{\epsilon\, G'(0)\sqrt{(M_1^2-1)}}. \tag{51}$$

TABLE 1

	M_1 *for which* $\frac{\tau}{\tan\delta_0} = 1$	
δ_0	*Potential theory*	*Present theory*
5°	11·48	28·8
10°	5·75	14·0
15°	3·86	9·08
20°	2·92	6·58
25°	2·36	4·75

In Table 1 are indicated the values of M_1 for which these ratios become equal to 1 and breakdown of each theory occurs. It shows that Busemann's result for $c_p(x)$ at the airfoil surface is of value beyond the region for which it was originally calculated.

There are no added difficulties in the calculation of a third-order approximation than in the preceding calculation, except for some more lengthy algebra. The third-order approximation to the differential equation will contain a term arising from the right-hand side of (10). This term will depend only on the first-order quantities ψ_1 and η_1, which are known by now. We might expect the next approximation to $c_p(x)$ on the surface of the airfoil not to coincide with the equivalent result obtainable by potential theory.

6. Second approach: flow behind plane shock wave taken as zero-order approximation

For high values of M_1 and of δ_0 our method can be improved by assuming as zero-order approximation the flow behind a plane oblique shock wave generated by a wedge of angle equal to the airfoil tip angle.

It would be interesting in this case also to try to obtain approximations to the flow in the whole disturbed region by expressing airfoil shape, shock profile, and perturbation stream function by (23), (24), (25), and (26). But

since now the vorticity term in (10) gives a contribution in the first-order approximation, the main difficulty of the problem will not be removed by the above expansions: the first-order approximation to the differential equation will contain a term which depends on the first-order solution itself.

In this case we shall therefore investigate only the flow in the vicinity of the tip by expanding the airfoil and shock-wave profiles in Taylor series. Write

$$y = g(x) = \frac{g''(0)}{2}x^2 + \frac{g'''(0)}{6}x^3 + \dots \tag{52}$$

for the airfoil profile, and

$$\eta = M_1^2 \sin^2\nu = \eta_0 + \eta_1 \Psi + \eta_2 \Psi^2 + \dots \tag{53}$$

or

$$\tau = \tan(\nu - \delta_0) = \tau_0 + \tau_1 x + \tau_2 x^2 + \dots . \tag{54}$$

We consider only a region of flow in the vicinity of the leading edge, small enough so that it is justifiable to assume

$$\eta_i \Psi^i = O((\eta_1 \Psi)^i) \quad \text{and} \quad \tau_i x^i = O((\tau_1 x)^i).$$

The constants η_0, η_1, η_2, τ_0, τ_1, and τ_2 are related by the equations

$$\left.\begin{aligned} \eta_0 &= M_1^2 \sin^2\nu_0, \qquad \tau_0 = \tan(\nu_0 - \delta_0) \\ \eta_1 &= G(M_1, \delta_0)\tau_1 \\ \eta_2 &= H(M_1, \delta_0)\tau_1^2 + L(M_1, \delta_0)\tau_2 \end{aligned}\right\} \tag{55}$$

with

$$\left.\begin{aligned} G &= \frac{2\eta_0 \cos^2(\nu_0 - \delta_0)}{\tan\nu_0 \tan(\nu_0 - \delta_0)} \frac{1}{u_2(1-u_2^2)^{1/(\gamma-1)}} \\ H &= \frac{G^2}{4}\left\{\left[\frac{2\gamma}{\gamma-1} - \tan^2\nu_0 - 3\tan\nu_0 \tan(\nu_0 - \delta_0)\right]\frac{1}{\eta_0} - \right. \\ &\qquad \left. - \frac{2\gamma}{(\gamma-1)} \frac{1}{\{\eta_0 + 2/(\gamma-1)\}} - \frac{2}{(\gamma-1)} \frac{1}{\{\eta_0 - (\gamma-1)/2\gamma\}}\right\} \\ L &= \frac{G^2}{2} \frac{\tan\nu_0}{\eta_0 \cos^2(\nu_0 - \delta_0)} \end{aligned}\right\}. \tag{56}$$

We shall also expand the perturbation stream function

$$\psi = \psi_1 + \psi_2 + \psi_3 + \dots \tag{57}$$

and shall assume tentatively

$$\psi_i = O(\psi_1^i),$$

and

$$\psi_{1x} = O(\eta_1 \Psi), \qquad \psi_{1y} = O(\eta_1 \Psi).$$

It will be seen *a posteriori* that all these assumptions are consistent.

It should be borne in mind that according to our convention the x-axis is now chosen in a direction tangent to the airfoil at the tip, and not in the free-stream direction.

The expression $P(w)$ in (10) can be expanded by (12), (13), and (57) into a power series in ψ_{1x} and ψ_{1y}

$$P(w) = P_{00}+P_{10}\psi_{1y}+P_{01}\psi_{1x}+\dots \tag{58}$$

with

$$\left.\begin{aligned} P_{00} &= \frac{1}{\gamma(\gamma-1)}\,\frac{\beta^2}{\beta^2+1}\,u_2(1-u_2^2)^{1/(\gamma-1)} \\ P_{10} &= \frac{\gamma+1}{\gamma(\gamma-1)}\,\frac{\beta^2-1}{\beta^2}\,u_2(1-u_2^2)^{1/(\gamma-1)} \\ P_{01} &= 0 \end{aligned}\right\}. \tag{59}$$

Also

$$Q(\eta) = Q(\eta_0)\left\{1+\frac{Q'(\eta_0)}{Q(\eta_0)}\,\eta_1\,\Psi+\dots\right\} \tag{60}$$

with

$$\left.\begin{aligned} Q(\eta_0) &= \frac{(\eta_0-1)^2}{\eta_0\{\eta_0-(\gamma-1)/2\gamma\}\{\eta_0+2/(\gamma-1)\}} \\ \frac{Q'(\eta_0)}{Q(\eta_0)} &= \frac{2}{\eta_0-1}-\frac{1}{\eta_0}-\frac{1}{\eta_0-(\gamma-1)/2\gamma}-\frac{1}{\eta_0+2/(\gamma-1)} \end{aligned}\right\}. \tag{61}$$

If all the expressions in (10) are similarly expanded by (12), (13), and (57), and terms of equal orders are equated, the following differential equations are obtained for the first and second approximation:

$$\psi_{1yy}-\beta^2\psi_{1xx} = P_{00}\,Q(\eta_0)G\tau_1 \tag{62}$$

$$\left.\begin{aligned} \psi_{2yy}-\beta^2\psi_{2xx} &= P_{10}\,Q(\eta_0)G\tau_1\psi_{1y}+ \\ &+P_{00}\,Q(\eta_0)\left\{\left(\frac{Q'(\eta_0)}{Q(\eta_0)}\,G^2+2H\right)\tau_1^2+2L\tau_2\right\}u_2(1-u_2^2)^{1/(\gamma-1)}y- \\ &-(\gamma+1)\frac{\beta^2+1}{\beta^2}\psi_{1x}\psi_{1xx}-2(\beta^2+1)\psi_{1x}\psi_{1xy}-(\gamma-1)\frac{\beta^2+1}{\beta^2}\psi_{1y}\psi_{1yy} \end{aligned}\right\}. \tag{63}$$

And in general, for the ith approximation, a differential equation is obtained of the form

$$\begin{aligned} &\psi_{iyy}-\beta^2\psi_{ixx} \\ &\quad = F(\psi_{1x},\psi_{1y},\psi_{1xx},\psi_{1xy},\psi_{1yy},\dots,\psi_{i-1yy};\,\eta_0,\eta_1,\dots,\eta_i;\,\psi_{i-2}). \end{aligned} \tag{64}$$

When all the approximations up to the $(i-1)$th are solved, the right-hand side of (64) is a known function of x and y, and we are faced with the problem of solving a differential equation of the form

$$\psi_{yy}-\beta^2\psi_{xx} = \phi(x,y) \tag{65}$$

subject to certain boundary conditions. The general solution of (65) may be put into the form

$$\psi(x,y) = m(x+\beta y)+n(x-\beta y)+\frac{1}{2\beta}\int_0^y d\zeta \int_{x-\beta(y-\zeta)}^{x+\beta(y-\zeta)} \phi(\xi,\zeta)\,d\xi, \tag{66}$$

as can be checked by differentiation.

As for the boundary conditions, the approximate tangency conditions are obtained from (16) by expanding around $y = 0$ and substituting for $g(x)$ from (52). For the first approximation the condition

$$\psi_{1x}(x,0)+g''(0)x = 0 \tag{67}$$

is obtained, and for the second approximation

$$\psi_{2x}(x,0)+g''(0)x\,\psi_{1y}(x,0)+\tfrac{1}{2}g''(0)x^2\psi_{1xy}(x,0)+\tfrac{1}{2}g'''(0)x^2 = 0. \tag{68}$$

The approximate shock-wave conditions are obtained by expanding (21) and (22) using (12), (13), (14), and (54), and by evaluating quantities on the shock profile by their expansions around the plane $y = \tau_0 x$. The zero approximation shock conditions are

$$\frac{u_1}{u_2}+\tau_0\frac{v_1}{u_2} = 1, \tag{69}$$

$$\frac{2}{(\gamma+1)}\frac{c_1^2}{u_2^2} = \frac{\tan\nu_0}{1+\tan^2(\nu_0-\delta_0)}\left\{\tan(\nu_0-\delta_0)-\frac{\gamma-1}{\gamma+1}\tan\nu_0\right\}, \tag{70}$$

the first approximation is given by

$$A_1\psi_{1y}+B_1\psi_{1x}+C_1\tau_1 x = 0, \tag{71}$$

$$A_2\psi_{1y}+B_2\psi_{1x}+C_2\tau_1 x = 0, \tag{72}$$

and the second approximation by

$$A_1\psi_{2y}+B_1\psi_{2x}+C_1\tau_2 x^2+D_1\tau_1^2 x^2 = 0, \tag{73}$$

$$A_2\psi_{2y}+B_2\psi_{2x}+C_2\tau_2 x^2+D_2\tau_1^2 x^2 = 0, \tag{74}$$

where the derivatives of ψ_1 and ψ_2 are evaluated at $y = \tau_0 x$ and the coefficients are given by

$$\left.\begin{aligned}
A_1 &= -\tan^2\mu_2\\
B_1 &= -\tan(\nu_0-\delta_0)\\
C_1 &= \cos^2(\nu_0-\delta_0)\{\tan\nu_0-\tan(\nu_0-\delta_0)\}\\
D_1 &= -\tan^2\mu_2\frac{\psi_{1yy}}{2\tau_1}-\tan(\nu_0-\delta_0)\frac{\psi_{1xy}}{2\tau_1}+a_{20}\left(\frac{\psi_{1y}}{\tau_1 x}\right)^2+\\
&\qquad +a_{02}\left(\frac{\psi_{1x}}{\tau_1 x}\right)^2+b_{11}\tan(\nu_0-\delta_0)\left(\frac{\psi_{1x}}{\tau_1 x}\right)\left(\frac{\psi_{1y}}{\tau_1 x}\right)-\left(\frac{\psi_{1x}}{\tau_1 x}\right)\\
A_2 &= 0\\
B_2 &= 1\\
C_2 &= \frac{\cos^4(\nu_0-\delta_0)}{\tan\nu_0}\left\{\frac{3-\gamma}{\gamma+1}\tan\nu_0+\tan(\nu_0-\delta_0)-\right.\\
&\qquad \left.-\tan\nu_0\tan(\nu_0-\delta_0)[\tan\nu_0-\tan(\nu_0-\delta_0)]\right\}\\
&= \frac{2}{(\gamma+1)}\cos^4(\nu_0-\delta_0)\left\{\frac{\cos^2\mu_2}{\cos^2(\nu_0-\delta_0)}+\frac{1}{\eta_0}\right\}
\end{aligned}\right\}. \tag{75}$$

$$D_2 = \left(\frac{\psi_{1xy}}{2\tau_1}\right) + \frac{1+\delta\tan\nu_0\tan(\nu_0-\delta_0)\cos^2(\nu_0-\delta_0)}{\tan\nu_0}\left(\frac{\psi_{1x}}{\tau_1 x}\right) -$$
$$-b_{11}\left(\frac{\psi_{1x}}{\tau_1 x}\right)\left(\frac{\psi_{1y}}{\tau_1 x}\right) + \frac{2\cos^6(\nu_0-\delta_0)}{\tan\nu_0}\{1+\tan\nu_0\tan(\nu_0-\delta_0)\}\times$$
$$\times\left\{\frac{1}{\gamma+1} - \frac{\gamma}{\gamma+1}\tan\nu_0\tan(\nu_0-\delta_0) + \tan^2(\nu_0-\delta_0)\right\} -$$
$$-\frac{2}{\gamma+1}\cos^4(\nu_0-\delta_0)\tan\nu_0$$

Here again the derivatives of ψ_1 are evaluated at $y = \tau_0 x$.

7. The first approximation

The general solution of the first approximation differential equation (62) is found by application of (66) to be

$$\psi_1(x,y) = m_1(x+\beta y) + n_1(x-\beta y) + \tfrac{1}{2}P_{00}\,Q(\eta_0)\,G\tau_1 y^2. \qquad (76)$$

The functions m_1 and n_1 are determined by the shock-wave conditions, (71) and (72):

$$m_1(x) = \tfrac{1}{2}\mathscr{M}_1\tau_1 x^2,$$
$$m_2(x) = \tfrac{1}{2}\mathscr{N}_1\tau_1 x^2,$$

with

$$\mathscr{M}_1 = \frac{(\Delta_3 - \kappa\tau_0\Delta_1) - \beta\Delta_2}{2\beta\Delta_1(1+\beta\tau_0)},$$
$$\mathscr{N}_1 = \frac{-(\Delta_3 - \kappa\tau_0\Delta_1) - \beta\Delta_2}{2\beta\Delta_1(1-\beta\tau_0)},$$

where (**14**)

$$\kappa = P_{00}\,Q(\eta_0)G = \frac{\cos^4(\nu_0-\delta_0)}{\tan^2\mu_2\tan\nu_0\tan(\nu_0-\delta_0)}[\tan\nu_0 - \tan(\nu_0-\delta_0)]^2,$$

$$\Delta_1 = \begin{vmatrix} A_1 & B_1 \\ A_2 & B_2 \end{vmatrix} = -\tan^2\mu_2,$$

$$\Delta_2 = \begin{vmatrix} A_1 & C_1 \\ A_2 & C_2 \end{vmatrix} = -\frac{2}{\gamma+1}\cos^4(\nu_0-\delta_0)\tan^2\mu_2\left[\frac{\cos^2\mu_2}{\cos^2(\nu_0-\delta_0)} + \frac{1}{\eta_0}\right],$$

$$\Delta_3 = \begin{vmatrix} B_1 & C_1 \\ B_2 & C_2 \end{vmatrix} = -\frac{\cos^4(\nu_0-\delta_0)}{\tan\nu_0}\times$$
$$\times\left[\tan^2\nu_0 + \tan^2(\nu_0-\delta_0) - 2\frac{\gamma-1}{\gamma+1}\tan\nu_0\tan(\nu_0-\delta_0)\right].$$

Hence we may write

$$\psi_1 = (Ax^2 + 2Bxy + Cy^2)\tau_1 \qquad (77)$$

with

$$\left.\begin{aligned}
A &= \tfrac{1}{2}(\mathscr{M}_1+\mathscr{N}_1)\\
&= -\frac{2}{\gamma+1}\,\frac{\cos^4(\nu_0-\delta_0)}{\{1-\tan^2(\nu_0-\delta_0)/\tan^2\mu_2\}}\left\{\frac{\tan^2(\nu_0-\delta_0)}{\tan^2\mu_2}+\frac{1}{2}\left(\frac{\cos^2\mu_2}{\cos^2(\nu_0-\delta_0)}+\frac{1}{\eta_0}\right)\right\}\\
B &= \tfrac{1}{2}\beta(\mathscr{M}_1-\mathscr{N}_1)\\
&= \frac{2}{\gamma+1}\,\frac{\sin(\nu_0-\delta_0)\cos^3(\nu_0-\delta_0)}{\tan^2\mu_2\{1-\tan^2(\nu_0-\delta_0)/\tan^2\mu_2\}}\left\{1+\frac{1}{2}\left(\frac{\cos^2\mu_2}{\cos^2(\nu_0-\delta_0)}+\frac{1}{\eta_0}\right)\right\}\\
C &= \tfrac{1}{2}\beta^2(\mathscr{M}_1+\mathscr{N}_1)+\tfrac{1}{2}\kappa\\
&= \frac{1}{\tan^2\mu_2}\left\{A+\frac{\cos^4(\nu_0-\delta_0)[\tan\nu_0-\tan(\nu_0-\delta_0)]^2}{2\tan\nu_0\tan(\nu_0-\delta_0)}\right\}
\end{aligned}\right\} \tag{78}$$

The tangency condition (67) gives then the relation between τ_1 and $g''(0)$, which determines the ratio of curvatures of the shock wave and the profile of the airfoil at the leading edge. Indeed, the curvature of the airfoil at the leading edge is given by

$$K_{w_0} = g''(0)$$

and the curvature of the shock-wave profile at the leading edge by

$$K_{sh_0} = \frac{(d\tau/dx)_{x=0}}{(1+\tau_0^2)^{\frac{1}{2}}} = \cos^3(\nu_0-\delta_0)\tau_1.$$

Hence, by (67),

$$\begin{aligned}
\frac{K_{sh_0}}{K_{w_0}} &= -\frac{\cos^3(\nu_0-\delta_0)}{2A}\\
&= \frac{(\gamma+1)}{4\cos(\nu_0-\delta_0)}\,\frac{1-\{\tan^2(\nu_0-\delta_0)/\tan^2\mu_2\}}{\{\tan^2(\nu_0-\delta_0)/\tan^2\mu_2\}+\frac{1}{2}\{\cos^2\mu_2/\cos^2(\nu_0-\delta_0)+1/\eta_0\}},
\end{aligned} \tag{79}$$

which is a well-known result (see Kraus (**12**)). Other equivalent formulae have been obtained by Thomas (**10**), Cabannes (**11**), and Schaefer (**8**).

In a similar way, using the first-order results, (77) and (78), in the first-order approximation to c_p, the corresponding relation for $(dc_p/dx)_{x=0}$ in reference (**12**) is obtained.

8. The second approximation

The second approximation differential equation (63) can now be determined by the substitutions

$$\psi_{1x} = 2\tau_1(Ax+By); \qquad \psi_{1y} = 2\tau_1(Bx+Cy)$$
$$\psi_{1xx} = 2\tau_1 A; \qquad \psi_{1xy} = 2\tau_1 B; \qquad \psi_{1yy} = 2\tau_1 C.$$

The resulting equation may be put into the form

$$\psi_{2yy}-\beta^2\psi_{2xx} = \alpha_1\tau_1^2 x+(\alpha_2\tau_1^2+\alpha_3\tau_2)y, \tag{80}$$

where

$$\left.\begin{aligned}\alpha_1 &= 2B\{D-4(\beta^2+1)A\}\\ \alpha_2 &= 2CD-8(\beta^2+1)B^2+EF\\ \alpha_3 &= \frac{1}{\eta_0}\frac{\tan\nu_0}{\cos^2(\nu_0-\delta_0)}E\end{aligned}\right\} \tag{81}$$

with

$$\left.\begin{aligned}D &= \frac{2(\gamma+1)}{\gamma(\gamma-1)}\frac{(1-\tan^2\mu_2)\cos^2(\nu_0-\delta_0)}{\tan\nu_0\tan(\nu_0-\delta_0)}\frac{(\eta_0-1)^2}{\{\eta_0-(\gamma-1)/2\gamma\}\{\eta_0+2/(\gamma-1)\}}-\\ &\qquad -2(1+\tan^2\mu_2)\{(\gamma+1)A+(\gamma-1)C\}\\ E &= \frac{4}{\gamma(\gamma-1)}\frac{\cos^2\mu_2\cos^4(\nu_0-\delta_0)}{\tan^2\nu_0\tan^2(\nu_0-\delta_0)}\frac{\eta_0(\eta_0-1)^2}{\{\eta_0-(\gamma-1)/2\gamma\}\{\eta_0+2/(\gamma-1)\}}\\ F &= \left\{\frac{1}{\gamma-1}-\tfrac{1}{2}\tan^2\nu_0-\tfrac{3}{2}\tan\nu_0\tan(\nu_0-\delta_0)\right\}\frac{1}{\eta_0}+\\ &\qquad +\frac{2}{\eta_0-1}-\frac{(2\gamma-1)}{(\gamma-1)}\frac{1}{\{\eta_0+2/(\gamma-1)\}}-\frac{\gamma}{(\gamma-1)}\frac{1}{\{\eta_0-(\gamma-1)/2\gamma\}}\end{aligned}\right\}. \tag{82}$$

The second-order shock-wave conditions (73) and (74) are determined similarly by the first-order solution. We obtain for D_1 and D_2

$$\left.\begin{aligned}D_1 &= -C\tan^2\mu_2-B\tan(\nu_0-\delta_0)+4a_{20}(B+\tau_0 C)^2+\\ &\qquad +4a_{02}(A+\tau_0 B)^2+4b_{11}\tan(\nu_0-\delta_0)(A+\tau_0 B)(B+\tau_0 C)-\\ &\qquad\qquad -2(A+\tau_0 B)\\ D_2 &= B-4b_{11}(A+\tau_0 B)(B+\tau_0 C)+\\ &\qquad +2\frac{\cos^2(\nu_0-\delta_0)}{\tan\nu_0}(A+\tau_0 B)[1+3\tan\nu_0\tan(\nu_0-\delta_0)]+\\ &\qquad +2\frac{\cos^6(\nu_0-\delta_0)}{\tan\nu_0}[1+\tan\nu_0\tan(\nu_0-\delta_0)]\times\\ &\qquad \times\left[\frac{1}{\gamma+1}-\frac{\gamma}{\gamma+1}\tan\nu_0\tan(\nu_0-\delta_0)+\tan^2(\nu_0-\delta_0)\right]-\\ &\qquad -\frac{2}{\gamma+1}\cos^4(\nu_0-\delta_0)\tan\nu_0\end{aligned}\right\}. \tag{83}$$

Finally, the second-order tangency condition (68) becomes, after substitution of the first approximation terms,

$$\psi_{2x}(x,0)+[3B\tau_1 g''(0)+\tfrac{1}{2}g'''(0)]x^2=0. \tag{84}$$

The second-order shock wave and tangency conditions, as well as the expanded expression for $c_p(x)$, involve only derivatives of ψ_2. Since we are mainly interested in determining $c_p(x)$ to the second order, it is not necessary to calculate ψ_2 by (66). It will be sufficient, instead, to determine ψ_{2x} and

ψ_{2y}. Using

$$\phi(x,y) = \alpha_1\tau_1^2 x + (\alpha_2\tau_1^2 + \alpha_3\tau_2)y, \tag{85}$$

the following expressions are obtained for these derivatives:

$$\left.\begin{aligned} \psi_{2x} &= m_2'(x+\beta y) + n_2'(x-\beta y) + \frac{\alpha_1\tau_1^2 y^2}{2} \\ \psi_{2y} &= \beta[m_2'(x+\beta y) - n_2'(x-\beta y)] + \alpha_1\tau_1^2 xy + (\alpha_2\tau_1^2 + \alpha_3\tau_2)y^2 \end{aligned}\right\}. \tag{86}$$

As in the case of the first-order approximation, so in the second approximation, the functions $m_2'(x)$ and $n_2'(x)$ are determined by the shock-wave conditions (73) and (74):

$$\left.\begin{aligned} m_2'(x) &= -\frac{[(\alpha_1\tau_0 + \tfrac{1}{2}\alpha_2\tau_0^2 + \Delta_5/\Delta_1) + (\tfrac{1}{2}\alpha_1\tau_0^2 + \Delta_4/\Delta_1)\beta]\tau_1^2 + \\ &\qquad + [(\tfrac{1}{2}\alpha_3\tau_0^2 - \Delta_3/\Delta_1) + \beta\Delta_2/\Delta_1]\tau_2}{2\beta(1+\beta\tau_0)^2} x^2 \\ n_2'(x) &= \frac{[(\alpha_1\tau_0 + \tfrac{1}{2}\alpha_2\tau_0^2 + \Delta_5/\Delta_1) - (\tfrac{1}{2}\alpha_1\tau_0^2 + \Delta_4/\Delta_1)\beta]\tau_1^2 + \\ &\qquad + [(\tfrac{1}{2}\alpha_3\tau_0^2 - \Delta_3/\Delta_1) - \beta\Delta_2/\Delta_1]\tau_2}{2\beta(1-\beta\tau_0)^2} x^2 \end{aligned}\right\}, \tag{87}$$

where

$$\left.\begin{aligned} \Delta_1 &= \begin{vmatrix} A_1 & B_1 \\ A_2 & B_2 \end{vmatrix}, \quad \Delta_2 = \begin{vmatrix} A_1 & C_1 \\ A_2 & C_2 \end{vmatrix}, \quad \Delta_3 = \begin{vmatrix} B_1 & C_1 \\ B_2 & C_2 \end{vmatrix} \\ \Delta_4 &= \begin{vmatrix} A_1 & D_1 \\ A_2 & D_2 \end{vmatrix}, \quad \Delta_5 = \begin{vmatrix} B_1 & D_1 \\ B_2 & D_2 \end{vmatrix} \end{aligned}\right\}. \tag{88}$$

Here τ_2 is still unknown and must be determined by the tangency condition (84). The substitution of the above expressions for $m_2'(x)$ and $n_2'(x)$ in (84) yields the following result for τ_2:

$$Z_1(M_1,\nu_0)\tau_2 + Z_2(M_1,\nu_0)\tau_1^2 = g'''(0) \tag{89}$$

with

$$\left.\begin{aligned} Z_1 &= \frac{1}{\beta}\left\{\frac{(\tfrac{1}{2}\alpha_3\tau_0^2 - \Delta_3/\Delta_1) + \beta\Delta_2/\Delta_1}{(1+\beta\tau_0)^2} - \frac{(\tfrac{1}{2}\alpha_3\tau_0^2 - \Delta_3/\Delta_1) - \beta\Delta_2/\Delta_1}{(1-\beta\tau_0)^2}\right\} \\ Z_2 &= \frac{1}{\beta}\left\{\frac{(\alpha_1\tau_0 + \tfrac{1}{2}\alpha_2\tau_0^2 - \Delta_5/\Delta_1) + (\tfrac{1}{2}\alpha_1\tau_0^2 + \beta\Delta_4/\Delta_1)}{(1+\beta\tau_0)^2} - \right. \\ &\qquad \left. - \frac{(\alpha_1\tau_0 + \tfrac{1}{2}\alpha_2\tau_0^2 - \Delta_5/\Delta_1) - (\tfrac{1}{2}\alpha_1\tau_0^2 + \beta\Delta_4/\Delta_1)}{(1-\beta\tau_0)^2}\right\} + 12AB \end{aligned}\right\}. \tag{90}$$

The derivatives ψ_{2x} and ψ_{2y} are thus completely determined by (86) to (90).

A second approximation to the pressure coefficient can now be evaluated. By definition

$$c_p = \frac{2}{\gamma M_1^2}\left(\frac{p}{p_1} - 1\right). \tag{91}$$

But since the flow along the airfoil is isentropic,

$$\frac{p}{p_1} = \frac{p_2}{p_1}\left(\frac{T}{T_2}\right)^{\gamma/(\gamma-1)} = \frac{p_2}{p_1}\left(\frac{1-w^2}{1-u_2^2}\right)^{\gamma/(\gamma-1)}. \tag{92}$$

This expression can be expanded by (12), (13), and (57), and the values of the derivatives of ψ_1 and ψ_2 on the airfoil surface, which appear in this expansion can be further expanded around $y = 0$. We obtain, to the second order of approximation,

$$\left(\frac{1-w^2}{1-u_2^2}\right)^{\gamma/(\gamma-1)} = 1 + \frac{\gamma M_2^2}{M_2^2-1}\psi_{1y}(x,0) +$$

$$+ \frac{\gamma M_2^2}{2(M_2^2-1)}\left\{\frac{(\gamma-1)M_2^4 + M_2^2 + 1}{(M_2^2-1)^2}\psi_{1y}^2(x,0) + \psi_{1x}^2(x,0) + \right.$$

$$\left. + 2\psi_{2y}(x,0) + 2g(x)\psi_{1yy}(x,0)\right\}. \tag{93}$$

The functions ψ_1 and ψ_2 determine the first and second derivative of $c_p(x)$ at the leading edge.

A check of the results can be obtained by calculating the approximate shape of the shock-wave profile by

$$y = \tau_0 x + \frac{\tau_1}{2}x^2 + \frac{\tau_2}{3}x^3 + \ldots$$

and comparing the result with the curve obtained by characteristics (**4**, **15**). Fig. 1 shows this comparison for a 10 per cent thick parabolic biconvex airfoil placed symmetrically in a uniform stream at $M_1 = \infty$. In the figure are plotted the shock-wave profile obtained by the method of characteristics, the results of the present first and second approximation, and the curve obtained by the shock expansion method (**4**). The second-order curve is closer to the curve obtained by characteristics even relatively far from the leading edge.

Fig. 2 is a plot of the results for c_p for the same airfoil and flow. In Fig. 3 are plotted values of c_p for the same airfoil in a uniform stream at $M_1 = 10$. Our second approximation curve coincides with the curve obtained by characteristics (**15**) up to $x/c = 0{\cdot}35$ within an order of 2 per cent.

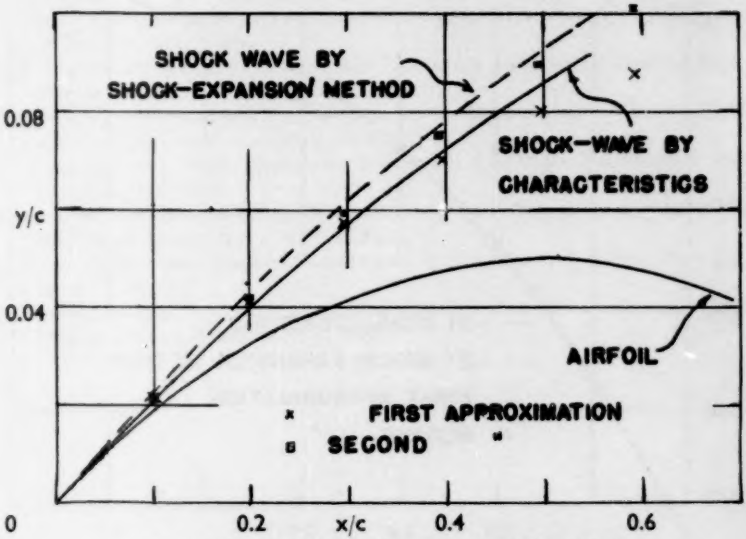

FIG. 1. Shock profile for biconvex parabolic airfoil

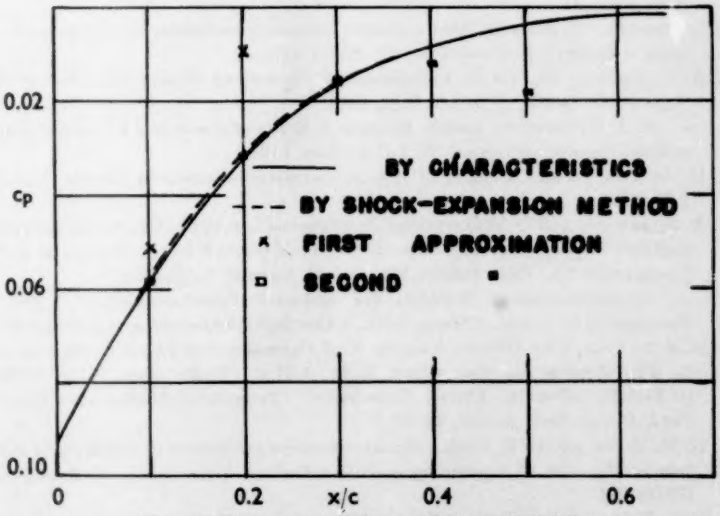

FIG. 2. Pressure coefficient on biconvex airfoil

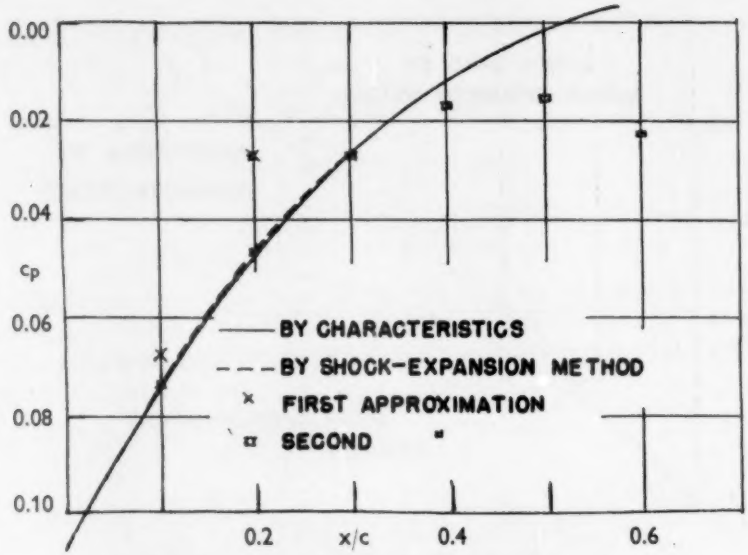

FIG. 3. Pressure coefficient on biconvex parabolic airfoil

REFERENCES

1. M. D. VAN DYKE, *A Study of Second-order Supersonic Flow Theory*, N.A.C.A. Rep. 1081, 11.
2. L. CROCCO, 'Singolarità della corrente gassosa iperacustica nell' intorno di una prora a diedro', *L'Aerotecnica*, **17** (1937) 519.
3. A. J. EGGERS, JR., *On the Calculation of Flow about Objects travelling at High Supersonic Speeds*, N.A.C.A. T.N. 2811.
4. —— C. A. SYVERSTON, and S. KRAUS, *A Study of Inviscid Flow about Airfoils at High Supersonic Speeds*, N.A.C.A. Rep. 1123.
5. M. D. VAN DYKE, *A Study of Hypersonic Small-disturbance Theory*, N.A.C.A. T.N. 3173.
6. A. BUSEMANN and O. WALCHNER, 'Profileigenschaften bei Ueberschallgeschwindigkeit', *Forsch. Geb. Ing.-Wes.* **4** (1933). (Available in translation as R.T.P. Translation No. 1786, British Ministry of Aircraft Production.)
7. —— 'Aerodynamischer Auftrieb bei Ueberschallgeschwindigkeit', *Atti dei Convegni* 5, *R. Accad. d'Italia*, 1936. (Also *Luftfahrtforschung*, **12** (1935) 210.)
8. M. SCHAEFER, *The Relation between Wall Curvature and Shock Front Curvature in Two-dimensional Gas Flow*, A.F., A.M.C., Tech. Rep. F–TS–1202–IA (G.D.A.M. A9–T–9), Brown University. (Technische Hochschule Dresden, 1942, *Peenemunde Archiv*, **44** (8).)
9. M. M. MUNK and R. C. PRIM, 'Surface pressure gradient and shock front curvature at the edge of a plane ogive with attached shock front', *J. Aero. Sci.* **15** (1948) 691.
10. T. Y. THOMAS, 'Calculation of the curvature of attached shock waves', *J. Math. Phys.* **27** (1949) 279.

11. H. CABANNES, 'Détermination de l'onde de choc attachée lorsque la vitesse aval à la pointe est subsonique', *Actes du Colloque International de Méchanique*, 2 (Poitiers, 1950), 181.
12. S. KRAUS, *An Analysis of Supersonic Flow in the region of the Leading Edge of Curved Airfoils*, N.A.C.A. T.N. 2729, 15.
13. L. CROCCO, 'Eine neue Stromfunktion für die Erforschung der Bewegung der Gase mit Rotation', *Z.A.M.M.* 17 (1937) 1.
14. Ames Research Staff, *Equations, Tables and Charts for Compressible Flow*, N.A.C.A. Rep. 1135.
15. A. J. EGGERS, JR., and C. A. SYVERTSON, *Inviscid Flow about Airfoils at High Supersonic Speeds*, N.A.C.A. T.N. 2646.
16. K. O. FRIEDRICHS, 'Formation and decay of shock waves', *Comm. Pure Appl. Math.* 1 (1948) 211.
17. M. J. LIGHTHILL, *High Speed Aerodynamics and Jet Propulsion*, vol. vi, Section E, Princeton Univ. Press, 1955, p. 345.

ON THE DEFLEXION OF JETS BY AEROFOILS

By L. C. WOODS†

(*N.S.W. University of Technology, Australia*)

[Received 7 February 1957]

SUMMARY

A two-dimensional jet of incompressible, inviscid fluid is deflected by an aerofoil immersed in it. The relation between the aerofoil incidence and jet deflexion angle, the extent to which the aerofoil displaces the jet from the position it would occupy in the aerofoil's absence, and the ratio of the fluid flowing above the aerofoil to that flowing below are calculated in this paper. Other results, such as the velocity distribution over the aerofoil and the shape of the free surface of the jet, are also given.

1. Introduction

FREE jets of air and water are frequently used to test the performance of aero- and hydrofoils, and an 'exact' theory for dealing with this type of flow is of some interest.

One application of such a theory is to flexible walled wind tunnels (**1**). In these tunnels the walls are first adjusted in shape until the pressure on them is constant, and the flow then corresponds to that of a free jet about an aerofoil (neglecting the effect of the boundary layer on the walls). The walls are next moved according to a rule—which must be derived from theoretical considerations—until they lie along the streamlines appropriate to an infinite stream. The existing theory for a lifting aerofoil is based on the theory of a vortex in a free jet (**1**); this could be improved with the aid of the theory given in the present paper.

Havelock (**2**) has given a theory which applies to a thin aerofoil between free surfaces, but in this theory the free surface boundary condition is applied on lines parallel to the y-axis instead of on the free surface itself. But even the assumption that the aerofoil's incidence—and hence the jet deflexion angle—is very small, must still mean that downstream of the aerofoil the jet diverges further and further from the y-axis by an amount which increases infinitely. There is some *a priori* doubt, therefore, as to whether Havelock's solution is relevant to the free jet and aerofoil problem; in any case the validity of his approximate boundary condition ought to be checked by a theory in which the existence of a finite deflexion angle is taken properly into account.

† Nuffield Research Professor in mechanical engineering.

It is found in this paper that (see section 11) even in the limit as the jet deflexion angle tends to zero the author's results are not in agreement with those given by Havelock. This is found to be due to a discrepancy between the number assumed by Havelock to be the incidence and the real incidence, and a simple modification to Havelock's incidence brings the results into agreement.

The main difficulty of an exact theory of the aerofoil and jet problem is that the position of the free surfaces is not known initially, and furthermore this position is dependent on the circulation about the aerofoil. It is therefore necessary to assign a value to the circulation from the beginning, but as the theory is developed sufficient relations emerge to enable the circulation and other similar parameters to be eliminated in favour of geometrical variables such as the incidence, jet width, and chord length. These relations are summarized in section 10, and readers concerned only with the application of the theory can turn immediately to this section.

2. The conformal transformations

The transformations and planes used in the subsequent theory are shown in Fig. 1. The z-plane ($z = x+iy$) is the 'real' or physical plane; in this plane the aerofoil ($ABCB'A'$) is shown deflecting a free jet ($EF_\infty GF'_\infty E'$) through some angle β, say. There will be a circulation about the aerofoil, so in the w-plane ($w = \phi+i\psi$) of equipotentials ($\phi =$ constant) and streamlines ($\psi =$ constant) it is necessary to have a jump in potential across some barrier such as AE or $B'F'_\infty$, which reduces the connectivity of the region. AE is the most suitable choice in the general case, for then the w-plane can be arranged symmetrically as shown in the figure, and this in turn simplifies the subsequent transformations. The origin in the w-plane is placed at C, a point midway (in the w-plane) between the front and rear stagnation points B and B' at $\phi = -2a$, $2a$ respectively. If one side of the barrier, $A'E'$ say, is at $\phi = \frac{1}{2}\Gamma$, and the other side, AE, is at $\phi = -\frac{1}{2}\Gamma$, then the circulation will equal Γ.

From the point of view of potential theory the shape of the w-plane shown in Fig. 1 is rather awkward. A more convenient shape is obtained by mapping the w-plane into the rectangle shown in the ζ-plane ($\zeta = \gamma+i\eta$). The t-plane shown in the figure is simply an intermediate mapping used in deriving the relation between the w- and ζ-planes. As each of these planes are (generalized) polygons in shape, each can be mapped on to the t-plane by the Schwarz–Christoffel mapping, and then eliminating t from the two resulting mapping equations yields the relation between the ζ- and w-planes. The following table gives the values of w and ζ at corresponding points, and

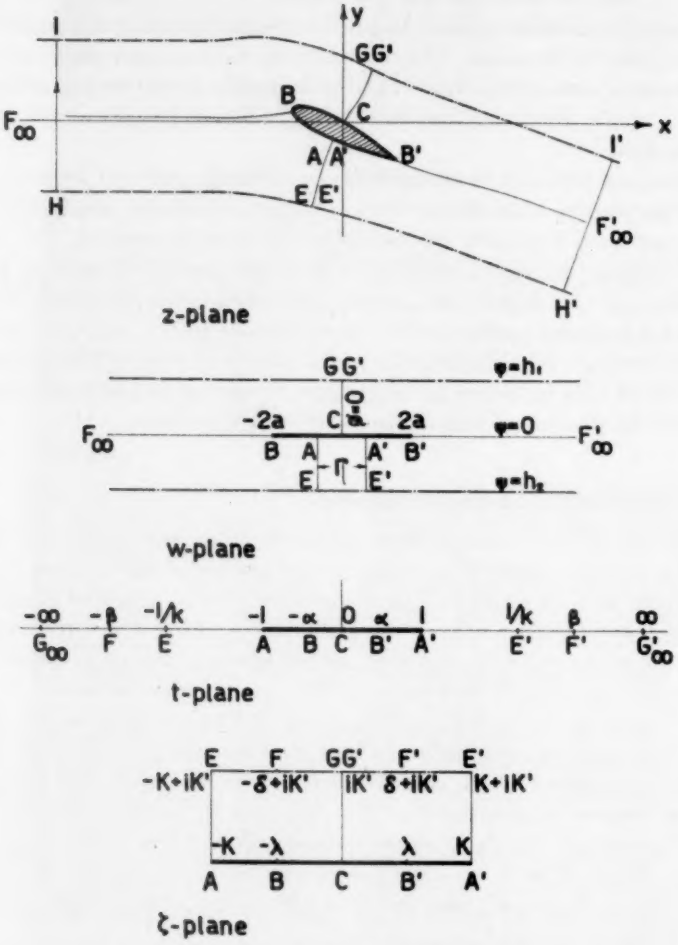

FIG. 1. The transformations

together with Fig. 1 serves to define all the constants introduced in the mapping.

Point	*C*	*B'*	*B*	*A'*	*A*	*E'*	*E*	*F'*	*F*	*G*
w-plane	0	$2a$	$-2a$	$\frac{1}{2}\Gamma$	$-\frac{1}{2}\Gamma$	$\frac{1}{2}\Gamma-ih_2$	$-\frac{1}{2}\Gamma-ih_2$	$\infty+i0$	$-\infty+i0$	ih_1
ζ-plane	0	λ	$-\lambda$	K	$-K$	$K+iK'$	$-K+iK'$	$\delta+iK'$	$-\delta+iK'$	iK'
t-plane	0	α	$-\alpha$	1	-1	$1/k$	$-1/k$	β	$-\beta$	$\pm\infty$

In terms of the symbols defined in this table the relation between ζ and w is readily found to be

$$w = \frac{1}{\pi}(h_1+h_2)[\{2Z(\delta)+Z(\lambda-\delta)-Z(\delta+\lambda)\}\zeta-2\Pi(\zeta,\delta)], \tag{1}$$

where $Z(x)$ is Jacobi's zeta function, and $\Pi(x,a)$ is Jacobi's incomplete elliptic integral of the third kind (see (3), pp. 518–23), i.e.

$$\Pi(x,a) \equiv \int_0^x \frac{k^2 \operatorname{sn} a \operatorname{cn} a \operatorname{dn} a \operatorname{sn}^2 x}{1-k^2\operatorname{sn}^2 a \operatorname{sn}^2 x}\, dx. \tag{2}$$

The real and imaginary quarter-periods of the Jacobian elliptic function involved here are the numbers K and K' introduced in the table above, while k is the modulus of these functions.

We shall assume for the moment that a, Γ, h_1, and h_2 are known quantities (it will be shown in section 7 how these are determined) so that our mapping into the ζ-plane introduces three unknown constants, viz. δ, λ, and k (K', K are determined uniquely by k). Relations defining these constants are found by substituting the corresponding values of w and ζ at points A', B', and E' in equation (1). It is found that

$$\frac{2\pi a}{h_1+h_2} = \{2Z(\delta)+Z(\lambda-\delta)-Z(\delta+\lambda)\}\lambda-2\Pi(\lambda,\delta), \tag{3}$$

$$\frac{\pi\Gamma}{2(h_1+h_2)} = \{Z(\lambda-\delta)-Z(\delta+\lambda)\}K, \tag{4}$$

and

$$2\delta = \left\{1+\frac{h_2-h_1}{h_1+h_2}\right\}K+\frac{\Gamma K'}{h_1+h_2}. \tag{5}$$

In the next section we shall also need the result

$$\frac{dw}{d\zeta} = \frac{2}{\pi}(h_1+h_2)\frac{k^2 \operatorname{sn}\delta \operatorname{cn}\delta \operatorname{dn}\delta}{1-k^2\operatorname{sn}^2\delta \operatorname{sn}^2\lambda}\left\{\frac{\operatorname{sn}^2\lambda-\operatorname{sn}^2\zeta}{1-k^2\operatorname{sn}^2\delta \operatorname{sn}^2\zeta}\right\} d\zeta, \tag{6}$$

which follows from (1), (2), and the relation

$$2Z(\delta)+Z(\lambda-\delta)-Z(\delta+\lambda) = \frac{2k^2 \operatorname{sn}^2\lambda \operatorname{sn}\delta \operatorname{cn}\delta \operatorname{dn}\delta}{1-k^2\operatorname{sn}^2\delta \operatorname{sn}^2\lambda}.$$

The importance of the ζ-plane is that it arranges the mixed boundary conditions of the flow problem in a very simple pattern—the known aerofoil shape lies on $\eta = 0$, $-K \leqslant \gamma \leqslant K$, the constant pressure surface is on $\eta = K'$, $-K \leqslant \gamma \leqslant K$, while any function $f(\gamma,\eta)$ characteristic of the flow satisfies $f(-K,\eta) = f(K,\eta)$, $0 \leqslant \eta \leqslant K'$. We shall therefore adopt the ζ-plane as the plane of *independent* variables.

Before introducing the dependent variables we mention here one important special case of (1) that has been used previously (for example, (4)

and (5)). This is the case in which the circulation is zero, i.e. $\Gamma = 0$, and the stagnation streamline $\psi = 0$ lies midway between the free boundaries of the jet, i.e. $h_1 = h_2$. With these values (5) reduces to $\delta = \frac{1}{2}K$, then (4) shows that λ also equals $\frac{1}{2}K$. Putting $a = \frac{1}{2}K$ in (2) and making use of Landen's transformation (see (3), p. 508), we find that

$$\Pi(\zeta, \tfrac{1}{2}K) = -Z(\tfrac{1}{2}K)\zeta - \tfrac{1}{4}\ln\left(\frac{1+k_1\,\mathrm{sn}\{(2K_1/K)\zeta, k_1\}}{1-k_1\,\mathrm{sn}\{(2K_1/K)\zeta, k_1\}}\right), \tag{7}$$

where the modulus of the elliptic functions appearing here is

$$k_1 = \frac{1-k'}{1+k'}, \tag{8}$$

k' being the complementary modulus $(1-k^2)^{\frac{1}{2}}$. The corresponding quarter period K_1 is related to K by $K_1 = \frac{1}{2}K(1+k')$. Equation (7) permits (1) to be rewritten

$$\tanh\frac{\pi w}{2h} = k_1\,\mathrm{sn}\left(\frac{2K_1}{K}, k_1\right), \tag{9}$$

where $h = \frac{1}{2}(h_1+h_2)$. Similarly (3) reduces to

$$k_1 = \tanh\frac{\pi a}{h}. \tag{10}$$

The importance of this special case lies in the fact that the stagnation streamline $B'F'_\infty$ now lies on the *straight* line $\gamma = \frac{1}{2}K$, so the transformation $\zeta' = \zeta + \frac{1}{2}K$ shifts $B'F'$ to $\zeta' = \pm K$. In the general case the stagnation streamline cannot be placed on opposite sides of the rectangle in the ζ-plane in this way. Having the trailing edge streamline on $\zeta' = -K+0$, $\zeta' = K-0$, enables us to deal with small *unsteady* perturbations of the flow, for such unsteadiness produces a vortex sheet of calculable strength lying along the stagnation streamline, i.e. a jump in velocity from $\zeta' = K-0$ to $\zeta' = -K+0$. And this type of boundary condition can be treated (5) by an extension of the theory for steady flow given in the next section.

3. The general theory of the flow of a jet past an aerofoil

The only satisfactory dependent variable to use in the theory is that defined by

$$f \equiv \ln\left(\frac{U\,dz}{dw}\right) = \ln\left(\frac{U}{q}\right) + i\theta, \tag{11}$$

where (q, θ) is the velocity vector in polar coordinates, and U is the (constant) velocity at the free surface of the jet. The angle θ will be measured from the positive direction of the x-axis. By (1) and (11) the complex function f is an analytic function of z, w (as $w = w(z)$) and of ζ. Thus, in the rectangle in the ζ-plane we have to find an analytic function $f(\zeta)$ such that $\mathrm{im}\,f = \theta_a$, the known slope of the aerofoil surface, on $\eta = 0$, $\mathrm{re}\,f = 0$ on the free surface $\eta = K'$, and $f(-K, \eta) = f(K, \eta)$.

The solution to the mixed boundary value problem just defined is known to be (6)

$$f(\zeta) = \frac{K_1}{\pi K}\int_{-K}^{K} \theta_a(\gamma^*)\frac{\mathrm{sn}'}{\mathrm{sn}}\left\{\frac{K_1}{K}(\gamma^*-\zeta), k_1\right\} d\gamma^*$$

$$= \frac{1}{\pi}\int_{-K}^{K} \theta_a\, d\left\{\ln\left[\mathrm{sn}\left(\frac{K_1}{K}(\gamma^*-\zeta), k_1\right)\right]\right\}, \tag{12}$$

where K_1, K, and k_1 are the numbers defined in section 2, and by $\mathrm{sn}'/\mathrm{sn}(u, k_1)$ is meant $(d/du)\ln\{\mathrm{sn}(u, k_1)\}$. (The result given in the author's earlier paper is actually the special case of (12) in which $K = 2K_1$.)

A more convenient form of (12) can be obtained by applying Landen's transformation. As $K_1/K = \frac{1}{2}(1+k')$, it is found that the transformation enables (12) to be written

$$f(\zeta) = \frac{1}{\pi}\int_{-K}^{K} \theta_a\, d\{\ln(\mathrm{sn}[\tfrac{1}{2}(\gamma^*-\zeta), k]\mathrm{cd}[\tfrac{1}{2}(\gamma^*-\zeta), k])\}$$

$$= \frac{1}{2\pi}\int_{-K}^{K} \theta_a\, d\{\ln(\mathrm{sn}^2[\tfrac{1}{2}(\gamma^*-\zeta)]\mathrm{cd}^2[\tfrac{1}{2}(\gamma^*-\zeta)])\}$$

$$= \frac{1}{2\pi}\int_{-K}^{K} \theta_a\, d\left\{\ln\left[\frac{1-\mathrm{cn}(\gamma^*-\zeta)}{1+\mathrm{dn}(\gamma^*-\zeta)}\,\frac{1+\mathrm{cn}(\gamma^*-\zeta)}{1+\mathrm{dn}(\gamma^*-\zeta)}\right]\right\},$$

where the modulus of the elliptic functions k is omitted for brevity. The modulus of all elliptic functions appearing below is also k, so there is no ambiguity involved in the abbreviated notation sn u, etc., which will be used in the remainder of this paper.

Performing the differentiation in the last expression for $f(\zeta)$ we arrive at the concise result

$$f(\zeta) = \frac{1}{\pi}\int_{-K}^{K} \theta_a\,\mathrm{cs}(\gamma^*-\zeta)\, d\gamma^*, \tag{13}$$

which is the required general solution of our boundary value problem.

4. The jet deflexion angle

Let the jet be deflected through an angle β in the sense shown in Fig. 2, and let the x-axis be selected so that upstream at infinity the flow is parallel to it, i.e. $\theta_{\phi=-\infty} = 0$. Then $\theta_{\phi=+\infty} = -\beta$.

On the free surface $\zeta = \gamma + iK'$, and on substituting this in (13) it is found that the slope of the free surface is given by

$$\theta(\gamma) = \frac{1}{\pi}\int_{-K}^{K} \theta_a\,\mathrm{dn}(\gamma^*-\gamma)\, d\gamma^*. \tag{14}$$

The point upstream at infinity is at $\gamma = -\delta$ (cf. Fig. 1), and at this point $\theta = 0$, so that from (14) we have

$$0 = \frac{1}{\pi} \int_{-K}^{K} \theta_a \, \mathrm{dn}(\gamma^* + \delta) \, d\gamma^*. \tag{15}$$

Similarly, $\theta(\delta) = -\beta$, so that

$$\beta = -\frac{1}{\pi} \int_{-K}^{K} \theta_a \, \mathrm{dn}(\gamma^* - \delta) \, d\gamma^*. \tag{16}$$

Equation (15) serves to define the position of the front stagnation point relative to some fixed point on the aerofoil (e.g. the leading edge), while (16) determines the jet deflexion angle.

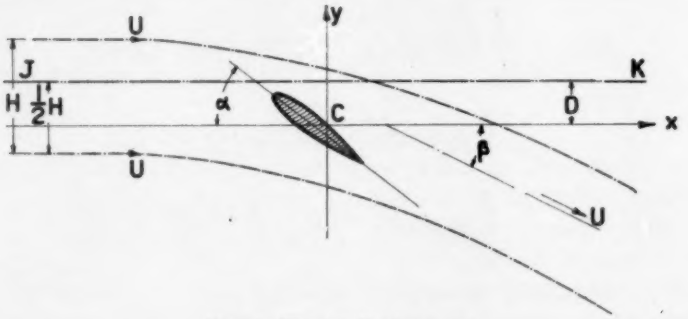

FIG. 2. The jet displacement

5. The closure conditions

No restriction has so far been placed on the magnitude of the deflexion angle β. However, a restriction is necessary if the relation $z = z(\zeta)$ is to be expressed in a tractable form. Then the closure conditions, i.e. that $\oint dz = 0$ about any circuit enclosing the aerofoil, can also be expressed simply. Thus, for mathematical reasons we now restrict β to be of first order in magnitude, and ignore second and higher order terms. From a practical point of view this is not an important restriction, for the aerofoil incidence α must always exceed the deflexion angle (see equation (44) below), and the usual restriction on α, i.e. that it be less than the stalling angle, will also restrict β.

If the z-plane origin is at C (Fig. 1) where $w = \zeta = 0$, then (11) and (6) yield

$$Uz = \int_0^{\zeta} e^{f(\zeta)} \frac{dw}{d\zeta} \, d\zeta = \frac{2}{\pi}(h_1 + h_2) \frac{k^2 \, \mathrm{sn}\,\delta \, \mathrm{cn}\,\delta \, \mathrm{dn}\,\delta}{1 - k^2 \mathrm{sn}^2\delta \, \mathrm{sn}^2\lambda} \int_0^{\zeta} e^{f} \frac{\mathrm{sn}^2\lambda - \mathrm{sn}^2\zeta}{1 - k^2 \mathrm{sn}^2\delta \, \mathrm{sn}^2\zeta} \, d\zeta. \tag{17}$$

The closure condition, namely $\oint dz = 0$, can be written (see Fig. 1)

$$\int_{-K+i\eta}^{K+i\eta} e^{f(\zeta)}\left(\frac{dw}{d\zeta}\right) d\zeta = 0, \tag{18}$$

where η is any number between 0 and K'. On the jet surface and at large distances from the aerofoil it follows from (11) that $f = i\theta$, where $\theta \leqslant \beta$, so if a value of η nearly equal to K' is used in (18), we can write $e^f \approx 1+f$ to first order in β. Then as $w(\zeta = K+i\eta) - w(\zeta = -K+i\eta)$ equals the circulation Γ, (18) becomes

$$\Gamma + \int_{-K+i\eta}^{K+i\eta} f(\zeta)\left(\frac{dw}{d\zeta}\right) d\zeta = 0,$$

or by (13) and (6),

$$\Gamma + \frac{1}{\pi}\int_{-K}^{K} \theta_a\{I(K+i\eta,\gamma^*) - I(-K+i\eta,\gamma^*)\}\, d\gamma^*, \tag{19}$$

where

$$I(\zeta,\gamma^*) = \frac{2}{\pi}(h_1+h_2)\frac{k^2\operatorname{sn}\delta\operatorname{cn}\delta\operatorname{dn}\delta}{1-k^2\operatorname{sn}^2\delta\operatorname{sn}^2\lambda}\int_0^{\zeta}\frac{\operatorname{cs}(\gamma^*-\zeta)(\operatorname{sn}^2\lambda-\operatorname{sn}^2\zeta)}{1-k^2\operatorname{sn}^2\delta\operatorname{sn}^2\zeta}\, d\zeta. \tag{20}$$

This integral can be evaluated by using the formula

$$\operatorname{cs}(\zeta-\gamma^*) = \frac{\operatorname{sn}\zeta\operatorname{cn}\zeta\operatorname{dn}\gamma^* + \operatorname{sn}\gamma^*\operatorname{cn}\gamma^*\operatorname{dn}\zeta}{\operatorname{sn}^2\gamma^* - \operatorname{sn}^2\zeta}.$$

It is found that

$$\begin{aligned} I(\zeta,\gamma^*) = {} & \frac{1}{\pi}(h_1+h_2)\frac{k^2\operatorname{sn}\delta\operatorname{cn}\delta\operatorname{dn}\delta}{1-k^2\operatorname{sn}^2\delta\operatorname{sn}^2\lambda}\times \\ & \times\left\{\frac{\operatorname{sn}^2\gamma^*-\operatorname{sn}^2\lambda}{1-k^2\operatorname{sn}^2\delta\operatorname{sn}^2\gamma^*}\ln\left[\frac{1-\operatorname{dn}(\gamma^*-\zeta)}{1+\operatorname{dn}(\gamma^*+\zeta)}\frac{1+\operatorname{dn}\gamma^*}{1-\operatorname{dn}\gamma^*}\right] + \right. \\ & + \frac{2(1-k^2\operatorname{sn}^2\delta\operatorname{sn}^2\lambda)}{1-k^2\operatorname{sn}^2\delta\operatorname{sn}^2\gamma^*}\left[\frac{\operatorname{sn}\gamma^*\operatorname{cn}\gamma^*}{\operatorname{dn}\delta}\tan^{-1}(\operatorname{sc}\zeta\operatorname{dn}\delta) - \right. \\ & \left.\left. - \frac{\operatorname{dn}\gamma^*}{k^2\operatorname{sn}\delta\operatorname{cn}\delta}\{\tan^{-1}(\operatorname{dn}\zeta\operatorname{sc}\delta) - \tan^{-1}(\operatorname{sc}\delta)\}\right]\right\}. \end{aligned} \tag{21}$$

On taking account of the periodic properties of the various functions in this expression, we obtain

$$\begin{aligned} & I(K+i\eta,\gamma^*) - I(-K+i\eta,\gamma^*) \\ & \quad = \frac{1}{\pi}(h_1+h_2)\frac{k^2\operatorname{sn}\delta\operatorname{cn}\delta\operatorname{dn}\delta}{(1-k^2\operatorname{sn}^2\delta\operatorname{sn}^2\lambda)(1-k^2\operatorname{sn}^2\delta\operatorname{sn}^2\gamma^*)}\times \\ & \qquad \times\left\{2\pi i(\operatorname{sn}^2\gamma^*-\operatorname{sn}^2\lambda) + 2\pi(1-k^2\operatorname{sn}^2\delta\operatorname{sn}^2\lambda)\frac{\operatorname{sn}\gamma^*\operatorname{cn}\gamma^*}{\operatorname{dn}\delta}\right\}. \end{aligned}$$

Substituting this into (19) the imaginary part gives

$$\int_{-K}^{K} \theta_a \frac{\mathrm{sn}^2\gamma^* - \mathrm{sn}^2\lambda}{1-k^2\mathrm{sn}^2\delta\,\mathrm{sn}^2\gamma^*}\,d\gamma^* = 0, \tag{22}$$

and the real part gives

$$\Gamma + \frac{1}{\pi}(h_1+h_2)\int_{-K}^{K} \theta_a \frac{2k^2\mathrm{sn}\,\delta\,\mathrm{cn}\,\delta\,\mathrm{sn}\,\gamma^*\mathrm{cn}\,\gamma^*}{1-k^2\mathrm{sn}^2\delta\,\mathrm{sn}^2\gamma^*}\,d\gamma^* = 0,$$

or

$$\Gamma - \frac{1}{\pi}(h_1+h_2)\int_{-K}^{K} \theta_a\{\mathrm{dn}(\gamma+\delta) - \mathrm{dn}(\gamma-\delta)\}\,d\gamma = 0.$$

Applying (15) and (16) to this result we get the concise relation

$$\Gamma = (h_1+h_2)\beta = HU\beta, \tag{23}$$

where H is the width of the jet at infinity and U is the corresponding velocity (h_1+h_2 is the total change in the stream function across the jet, and therefore equals HU).

Equations (22) and (23) are the required closure conditions, but it must be remembered that they are valid only for small β.

6. The relation between z and ζ

Equations (13) and (17) together give the exact relation between z and ζ, but, except for some special cases, the integration must be performed numerically. The approximation $e^f \approx 1+f$ can be applied to (17) only if the incidence is small, and if the path of integration does not terminate near the leading or trailing edges where $|f|$ is apt to be large. This restriction on α is more stringent than that imposed in the previous section, as β is always less than α, and for a wide jet is much less than α.

When the approximation is valid it follows from equations (13), (17), and (20) that

$$Uz = w + \frac{1}{\pi}\int_{-K}^{K} \theta_a\, I(\zeta, \gamma^*)\,d\gamma^*.$$

Now equations (15) and (16) may be combined and written in the form

$$\beta = -\frac{2}{\pi}\int_{-K}^{K} \frac{\theta_a\,\mathrm{dn}\,\gamma^*\,\mathrm{dn}\,\delta\;d\gamma^*}{1-k^2\mathrm{sn}^2\delta\,\mathrm{sn}^2\gamma^*} = -\frac{2}{\pi}\int_{-K}^{K} \frac{\theta_a\,k^2\mathrm{sn}\,\gamma^*\,\mathrm{cn}\,\gamma^*\,\mathrm{sn}\,\delta\,\mathrm{cn}\,\delta\;d\gamma^*}{1-k^2\mathrm{sn}^2\delta\,\mathrm{sn}^2\gamma^*},$$

so that when (21) is substituted into the equation for Uz the result can be written

$$Uz = w - \frac{1}{\pi}(h_1+h_2)\beta\{\tan^{-1}(\operatorname{sc}\zeta\,\operatorname{dn}\delta) - \tan^{-1}(\operatorname{dn}\zeta\,\operatorname{sc}\delta) + \tan^{-1}(\operatorname{sc}\delta)\} + \\ + \frac{1}{\pi^2}(h_1+h_2)\frac{k^2\operatorname{sn}\delta\,\operatorname{cn}\delta\,\operatorname{dn}\delta}{1-k^2\operatorname{sn}^2\delta\,\operatorname{sn}^2\lambda}\int_{-K}^{K}\theta_4\frac{\operatorname{sn}^2\gamma^*-\operatorname{sn}^2\lambda}{1-k^2\operatorname{sn}^2\delta\,\operatorname{sn}^2\gamma^*}\times \\ \times\ln\left(\frac{1-\operatorname{dn}(\gamma^*-\zeta)}{1+\operatorname{dn}(\gamma^*-\zeta)}\,\frac{1+\operatorname{dn}\gamma^*}{1-\operatorname{dn}\gamma^*}\right)d\gamma^*. \quad (24)$$

7. Position of the aerofoil within the jet

The actual position of the aerofoil relative to the jet will obviously depend on both the aerofoil incidence α, and the position of the aerofoil centre relative to the jet position upstream at infinity. Let JK in Fig. 2 be the centre line of the jet in its undisturbed upstream position, and let the vertical distance from C (origin of the z-plane) to JK be D. Then if D is fixed h_1/h_2 will clearly decrease with increasing α. The relation between these variables can be found from equation (24).

Let ϵ be a small *positive* number, then $\lim_{\epsilon\to 0}\operatorname{im} z(\zeta = \epsilon-\delta+iK')$ is the value of y on the *upper* free surface upstream at infinity. The jet centre-line JK is a distance $\frac{1}{2}H$ below this free surface, and it therefore follows that

$$D = \lim_{\epsilon\to 0}\operatorname{im} z(\zeta = \epsilon-\delta+iK') - \tfrac{1}{2}H, \quad (25)$$

where z is given by equation (24). We shall take the limits of the terms in (24) separately.

First, combining equations (1), (4), and (23) we find that

$$w = \frac{1}{2K}(h_1+h_2)\beta\zeta + \frac{1}{\pi}(h_1+h_2)\ln\left\{\frac{\vartheta_4\{(\pi/2K)(\zeta+\delta)|(iK'/K)\}}{\vartheta_4\{(\pi/2K)(\zeta-\delta)|(iK'/K)\}}\right\}, \quad (26)$$

where $2\{\Pi(\zeta,\delta)-\zeta Z(\delta)\}$ has been replaced by the logarithmic term involving the theta functions (see (3), pp. 479 and 523). Thus, from the quasi-periodic properties of the theta functions,

$$\lim_{\epsilon\to 0} w(\zeta = \epsilon-\delta+iK') \\ = \frac{\beta(h_1+h_2)(iK'-\delta)}{2K} + \frac{1}{\pi}(h_1+h_2)\lim_{\epsilon\to 0}\ln\left[\frac{-e^{-i\delta/K}\vartheta_1(\pi\epsilon/2K)}{\vartheta_1(\pi\delta/K)}\right],$$

the parameter of the theta functions ($\tau = iK'/K$) being omitted for brevity. Equations (5) and (23) permit this limit to be expressed as

$$\lim_{\epsilon\to 0} w(\zeta = \epsilon-\delta+iK') = ih_1 + \frac{1}{\pi}(h_1+h_2)\lim_{\epsilon\to 0}\ln\left[\frac{\vartheta_1(\pi\epsilon/2K)}{\vartheta_1(\pi\delta/K)}\right]. \quad (27)$$

Secondly,

$$\lim_{\epsilon\to 0}\{\tan^{-1}\mathrm{sc}(\epsilon-\delta+iK')\mathrm{dn}\,\delta-\tan^{-1}\mathrm{dn}(\epsilon-\delta+iK')\mathrm{sc}\,\delta+\tan^{-1}(\mathrm{sc}\,\delta)$$
$$=-\frac{i}{2}\ln\frac{k^2\mathrm{sn}^2\delta\,\mathrm{cn}^2\delta}{\mathrm{dn}^2\delta}-\tan^{-1}(\mathrm{cs}\,\delta), \quad (28)$$

and, finally,

$$\lim_{\epsilon\to 0}\mathrm{im}\ln\left(\frac{1-\mathrm{dn}(\gamma^*-\zeta)}{1+\mathrm{dn}(\gamma^*-\zeta)}\frac{1+\mathrm{dn}\,\gamma^*}{1-\mathrm{dn}\,\gamma^*}\right)=-2\tan^{-1}\mathrm{cs}(\gamma^*+\delta). \quad (29)$$

From (23) to (29) the following expression for D can now be derived:

$$\frac{2D}{H}=\frac{h_1-h_2}{h_1+h_2}+\frac{\beta}{\pi}\ln\left[\frac{k^2\mathrm{sn}^2\delta\,\mathrm{cn}^2\delta}{\mathrm{dn}^2\delta}\right]-$$
$$-\frac{4}{\pi^2}\frac{k^2\mathrm{sn}\,\delta\,\mathrm{cn}\,\delta\,\mathrm{dn}\,\delta}{1-k^2\mathrm{sn}^2\delta\,\mathrm{sn}^2\lambda}\int_{-K}^{K}\theta_a\frac{\mathrm{sn}^2\gamma^*-\mathrm{sn}^2\lambda}{1-k^2\mathrm{sn}^2\delta\,\mathrm{sn}^2\gamma^*}\tan^{-1}\mathrm{cs}(\gamma^*+\delta)\,d\gamma^*. \quad (30)$$

Another important geometric number is the chord to jet-width ratio, c/H. A simple expression for this can also be derived from (24) provided it is assumed that the distance between the front and rear stagnation points is a sufficiently close measure of the chord length (always true for aerofoil shapes at moderate incidences). In this case

$$c=z(\zeta=\lambda)-z(\zeta=-\lambda),$$

and so (24) yields

$$\frac{c}{H}=\frac{4a}{h_1+h_2}+\frac{2\beta}{\pi}\tan^{-1}(\mathrm{sc}\,\delta)+\frac{1}{\pi^2}\frac{k^2\mathrm{sn}\,\delta\,\mathrm{cn}\,\delta\,\mathrm{dn}\,\delta}{1-k^2\mathrm{sn}^2\delta\,\mathrm{sn}^2\lambda}\times$$
$$\times\int_{-K}^{K}\theta_a\frac{\mathrm{sn}^2\gamma^*-\mathrm{sn}^2\lambda}{1-k^2\mathrm{sn}^2\delta\,\mathrm{sn}^2\gamma^*}\ln\left|\frac{1-\mathrm{dn}(\gamma^*-\lambda)}{1+\mathrm{dn}(\gamma^*-\lambda)}\frac{1+\mathrm{dn}(\gamma^*+\lambda)}{1-\mathrm{dn}(\gamma^*+\lambda)}\right|d\gamma^*. \quad (31)$$

It will be recalled that in section 2 we assumed temporarily that a, Γ, h_1, h_2 were known quantities, but of course in a practical problem of an aerofoil in a jet the known quantities are most likely to be c, H, D, and α. However, we now have sufficient relations, viz., equations (16), (23), (30), and (31), to calculate a, Γ, h_1, and h_2 from given values of c, H, D, and α. (The incidence α is implicit in the right-hand side of (16), see section 9.)

8. The lift and circulation

The equation of linear momentum shows that the force on the aerofoil L makes an angle of $\frac{1}{2}(\pi-\beta)$ with the y-axis, and that its magnitude is $2H\rho U^2\sin\frac{1}{2}\beta$, where ρ is the fluid density. Thus, to first order in β we have $L=\rho HU^2\beta$, and it therefore follows from (23) that $L=\rho U\Gamma$, in agreement

with the classical result for an infinite stream. The lift coefficient,

$$C_L \equiv L/(\tfrac{1}{2}\rho c U^2),$$

is given by

$$C_L = 2H\beta/c. \tag{32}$$

9. Thin aerofoil theory

With thin, unflapped, aerofoils we can assume that $\theta_a = -\alpha$, except near the leading edge. At the leading edge the flow is reversed in direction (i.e. $\theta_a = \pi - \alpha$) between the stagnation point at $\zeta = -\lambda$ and the nose at $\zeta = -\lambda + \epsilon$, say. Thus, we can write

$$\theta_a = \begin{cases} -\alpha & (-K \leqslant \gamma \leqslant -\lambda,\ -\lambda+\epsilon \leqslant \gamma \leqslant K) \\ \pi-\alpha & (-\lambda \leqslant \gamma \leqslant -\lambda+\epsilon) \end{cases}, \tag{33}$$

where at moderate incidences ϵ will be a small quantity of the same order as α or β.

From equations (15), (16), and (33) we obtain

$$\left.\begin{aligned} \beta &= -\epsilon\{\mathrm{dn}(\lambda+\delta) - \mathrm{dn}(\lambda-\delta)\} \\ \alpha &= \epsilon\,\mathrm{dn}(\lambda-\delta) \end{aligned}\right\} \tag{34}$$

to first order in ϵ. Thus

$$\beta = \alpha\left\{1 - \frac{\mathrm{dn}(\lambda+\delta)}{\mathrm{dn}(\lambda-\delta)}\right\}. \tag{35}$$

Similarly equations (11), (13), (33), and (34) give

$$\frac{dw}{dz} = U\{1 + i\alpha + \alpha\,\mathrm{cs}(\lambda+\zeta)\mathrm{nd}(\lambda-\delta)\}, \tag{36}$$

and in particular, the velocity on the aerofoil surface is given by

$$\frac{q}{U} = 1 + \alpha\,\mathrm{cs}(\lambda+\gamma)\mathrm{nd}(\lambda-\delta). \tag{37}$$

Equation (22) is satisfied by (33) correctly to first order in ϵ.

In the evaluation of the integral in (24) it will be found that the leading edge term in (33) contributes no first-order term. The integral arising from the incidence term is most easily integrated by first differentiating it with respect to ζ, and then reversing the order of the two integrations now necessary. The final result is

$$Uz = w(1-i\alpha) + \frac{(h_1+h_2)(\beta-2\alpha)}{\pi}\{\tan^{-1}(\mathrm{dn}\,\zeta\,\mathrm{sc}\,\delta) - \tan^{-1}(\mathrm{sc}\,\delta)\} - \\ - \frac{(h_1+h_2)\beta}{\pi}\tan^{-1}(\mathrm{sc}\,\zeta\,\mathrm{dn}\,\delta). \tag{38}$$

The equation corresponding to (30) is most directly obtained from (38) by making use of (27) and (28). It is found that

$$\frac{2D}{H} = \frac{h_1-h_2}{h_1+h_2} + \frac{\beta}{\pi}\ln\left|\frac{1-\mathrm{dn}\,2\delta}{1+\mathrm{dn}\,2\delta}\right| + \frac{2\alpha}{\pi}\ln\left(\frac{\vartheta_1(\pi\delta/K)\,\mathrm{ds}\,\delta\,\mathrm{nc}\,\delta}{(8kk'K/\pi)^{\frac{1}{2}}}\right), \tag{39}$$

as

$$\frac{k^2\mathrm{sn}^2\delta\,\mathrm{cn}^2\delta}{\mathrm{dn}^2\delta} = \frac{1-\mathrm{dn}\,2\delta}{1+\mathrm{dn}\,2\delta},$$

and

$$\lim_{\epsilon\to 0}\vartheta_1\left(\frac{\pi\epsilon}{2K}\right)\Big/\epsilon = \frac{\pi}{2K}\vartheta_1'(0) = \frac{\pi}{2K}\vartheta_2(0)\vartheta_3(0)\vartheta_4(0) = (2kk'K/\pi)^{\frac{1}{2}}.$$

Equation (39) can also be written in the more convenient form

$$\frac{2D}{H} = \frac{h_1-h_2}{h_1+h_2} + \frac{\beta}{\pi}\ln\left[\frac{(1-\mathrm{dn}\,2\delta)\vartheta_4(\pi\delta/K)}{(8k'K/\pi)^{\frac{1}{2}}}\right] + \frac{2\alpha-\beta}{\pi}\ln\left[\frac{(1+\mathrm{dn}\,2\delta)\vartheta_4(\pi\delta/K)}{(8k'K/\pi)^{\frac{1}{2}}}\right]. \tag{40}$$

The equation corresponding to (31) from (38) is found to be

$$\frac{c}{H} = \frac{4a}{h_1+h_2} - \frac{2}{\pi}\beta\tan^{-1}(\mathrm{sc}\,\lambda\,\mathrm{dn}\,\delta),$$

or retaining only the highest order terms, $c/H = 4a/(h_1+h_2)$, which is equivalent to

$$4a/U = c. \tag{41}$$

A similar calculation applied to (26) gives

$$\left.\begin{aligned}\frac{4a}{U} &= \frac{2H}{\pi}\ln\left(\frac{\vartheta_4\{(\pi/2K)(\lambda+\delta)\}}{\vartheta_4\{(\pi/2K)(\lambda-\delta)\}}\right)\\ \text{so by (41)}\qquad \frac{c}{H} &= \frac{2}{\pi}\ln\left(\frac{\vartheta_4\{(\pi/2K)(\lambda+\delta)\}}{\vartheta_4\{(\pi/2K)(\lambda-\delta)\}}\right)\end{aligned}\right\}. \tag{42}$$

10. Summary of equations : examples

The principal equations of the theory are

$$\beta = \frac{2K}{\pi}\{Z(\lambda-\delta) - Z(\delta+\lambda)\}, \tag{43}$$

$$\beta = \alpha\{1-\mathrm{dn}(\lambda+\delta)\mathrm{nd}(\lambda-\delta)\}, \tag{44}$$

$$\frac{h_1-h_2}{h_1+h_2} = 1 - \frac{2\delta}{K} + \frac{\beta K'}{K}, \tag{45}$$

$$\frac{c}{H} = \frac{2}{\pi}\ln\left|\frac{\vartheta_4\{(\pi/2K)(\lambda+\delta)\}}{\vartheta_4\{(\pi/2K)(\lambda-\delta)\}}\right|, \tag{46}$$

and

$$\frac{2D}{H} = \frac{h_1-h_2}{h_1+h_2} + \frac{\beta}{\pi}\ln\left[\frac{(1-\mathrm{dn}\,2\delta)\vartheta_4(\pi\delta/K)}{2\vartheta_4(0)}\right] + \frac{2\alpha-\beta}{\pi}\ln\left[\frac{(1+\mathrm{dn}\,2\delta)\vartheta_4(\pi\delta/K)}{2\vartheta_4(0)}\right]. \tag{47}$$

The first of these five equations follows from (4) and (23), the second is the same as (35), the third follows from (5) and (23), the fourth and last are respectively (42) and (40).

Suppose that we have a given geometric arrangement of jet and aerofoil, then c/H, D/H, and α are known quantities. Equations (43)–(47) fix the values of the five unknowns β, K, λ, δ, and h_1/h_2.

An easier procedure is to assign a set of values to λ, δ, and k. Then β follows immediately from (43), α from (44), h_1/h_2 from (45), and finally (46) and (47) yield c/H and D/H. After a few trial values of λ, δ, and k, it is not hard to find values that will very closely produce any desired aerofoil-jet combination. By way of illustration we consider two examples.

Example 1. *Aerofoil in the centre of the jet*

If the jet is undeflected it follows from (43) and (45) that $\delta = \frac{1}{2}K, \lambda = \frac{1}{2}K$. Then (46) gives

$$\frac{c}{H} = \frac{2}{\pi}\ln\left(\frac{\vartheta_3(0)}{\vartheta_4(0)}\right) = \frac{1}{\pi}\ln\left(\frac{1}{k'}\right). \tag{48}$$

If the aerofoil is now at a small incidence, δ and λ will differ from $\frac{1}{2}K$ only by terms of order α. Thus, to first order in α, (43) gives

$$\beta = \alpha(1-\mathrm{dn}\,K\,\mathrm{nd}\,0) = \alpha(1-k') = (1-e^{-\pi c/H}), \tag{49}$$

and if c/H is small, we find from (32) and (49) that

$$\left(\frac{\partial C_L}{\partial \alpha}\right)_{\alpha=0} = \frac{2H}{c}[1-e^{-\pi c/H}] \approx 2\pi\left\{1-\frac{\pi c}{2H}+\frac{\pi^2}{6}\left(\frac{c}{H}\right)^2\right\}. \tag{50}$$

As $\mathrm{dn}(\lambda+\delta)\mathrm{nd}(\lambda-\delta)$ is a minimum at $\lambda = \frac{1}{2}K$, $\delta = \frac{1}{2}K$, it follows from (43) that $(\partial C_L/\partial\alpha)_{\alpha=0}$ is a maximum when the aerofoil is in the centre of the jet.

Example 2. $k^2 = 0{\cdot}9$, $\delta = 1{\cdot}00$, $\lambda = 1{\cdot}35$

This set of values and equations (43)–(47) yield in turn $\beta = 0{\cdot}1857$ $(= 10{\cdot}64°)$, $\alpha = 0{\cdot}2679$ $(= 15{\cdot}34°)$,

$$(h_1-h_2)/(h_1+h_2) = 0{\cdot}340, \quad c/H = 0{\cdot}372, \quad \text{and} \quad 2D/H = 0{\cdot}268. \tag{51}$$

Clearly only a small computing effort would be required to establish sufficient entries in a table, which would allow interpolation to any desired values of α, c/H, and $2D/H$.

11. Comparison with Havelock's theory

In order to test the theory given by Havelock (2) it is sufficient to compare his result for $(\partial C_L/\partial\alpha)_{\alpha=0}$ with that given by equation (50). As Havelock's results are all given in the form of infinite series (in c/H and D/H)

it is not easy to make an exact comparison; he gives an equation which is equivalent to

$$\left(\frac{\partial C_L}{\partial \alpha}\right)_{\alpha=0} = 2\pi\left\{1-\frac{\pi^2}{12}\left(\frac{c}{H}\right)^2+\frac{\pi^4}{120}\left(\frac{c}{H}\right)^4+O\left(\frac{c}{H}\right)^6\right\}, \tag{52}$$

and therefore is not in agreement with the author's theory. Yet there are no errors apparent in the theory which yields (52).

An equation like (52) *can* be deduced from the author's theory as follows. Replace α in (49) by $\alpha'+\frac{1}{2}\beta$, then by (49)

$$\beta = 2\alpha'\left(\frac{1-k'}{1+k'}\right) = 2\alpha'\tanh\left(\frac{\pi c}{2H}\right),$$

and therefore from (32)

$$\left(\frac{\partial C_L}{\partial \alpha'}\right)_{\alpha'=0} = \frac{4H}{c}\tanh\left(\frac{\pi c}{2H}\right) = 2\pi\left\{1-\frac{\pi^2}{12}\left(\frac{c}{H}\right)^2+\frac{\pi^4}{120}\left(\frac{c}{H}\right)^4+O\left(\frac{c}{H}\right)^6\right\}.$$

This makes it clear that Havelock's incidence is not measured from the upstream jet direction (as implied in his paper), but from the *average* of the upstream and downstream jet directions. This seems to be a reasonable conclusion, for the errors introduced by the misplacement of the free boundary condition downstream of the aerofoil must clearly be balanced by a like displacement upstream of the aerofoil.

As Havelock gives no expression for the jet deflexion his results cannot easily be modified to allow for the discrepancy in the incidence.

REFERENCES

1. C. N. H. Lock and J. A. Beavan, Rep. Memor. Aero. Res. Comm., No. 2005, 1944.
2. T. H. Havelock, *Proc. Roy. Soc.* A, **166** (1938) 178–96.
3. E. T. Whittaker and G. N. Watson, *Modern Analysis* (Cambridge, 1952).
4. R. Timman, *App. Sci. Res.* (1) A, **3** (1951) 31.
5. L. C. Woods, *Proc. Roy. Soc.* A, **229** (1955) 235–50.
6. —— ibid. 63–85.

ON THE MOTION OF A SPHERE ALONG THE AXIS OF A ROTATING FLUID

By K. STEWARTSON

(*Department of Mathematics, The University, Bristol*)

[Received 17 January 1957]

SUMMARY

The motion of a sphere along the axis of an unbounded fluid rotating with uniform angular velocity is discussed on the assumption that the fluid is undisturbed far upstream. It is shown that no wave-like components can then occur upstream of the body. The stream function ψ and the drag are found for various values of the Rossby number ka, defined in (1.1) below. When $ka = 5{\cdot}76$ both these quantities become infinite everywhere and it is inferred that the fluid cannot be undisturbed far upstream when $ka \geqslant 5{\cdot}76$. It is probable that cylindrical flow which must then be present must also occur at smaller values of ka of which the lower bound is not known.

1. Introduction

THE chief hydrodynamic interest in the motion of a sphere along the axis of a uniformly rotating fluid stems from the unusual nature of the flow. The first experiments were made by Taylor (**1, 2**) who found that at small values of the Rossby number

$$2\Omega a/W = ka, \tag{1.1}$$

where Ω is the angular velocity of the fluid, a the radius of the sphere, and W is its velocity, the disturbance in the fluid was similar to that when $\Omega = 0$, dying out as the distance from the sphere tended to infinity. At $ka \approx 2\pi$ the character of the disturbance became markedly different. Ahead of the sphere there appeared a régime, near the axis of rotation and bounded approximately by a circular cylinder C circumscribing the sphere and having its generators parallel to the axis of rotation, where the flow was cylindrical. Inside it the fluid was pushed along in front of the sphere and at the same time it behaved with respect to the fluid outside C as if it were solid. Somewhat similar results were found by Long (**3**) using a body with a spherical nose and a conical tail. He also examined the flow behind this body and found that for all values of the Rossby number the fluid near the boundary passed round to the rear of the body and was not carried along with it.

A theoretical solution when ka is large (**4**) confirms the general features of Taylor's observations (**1, 2**) but not Long's (**3**) on the flow to the rear of the body. The reason for this failure is not known.

Taylor (1) also considered the flow from a theoretical standpoint. Let (r, ϕ, z) be cylindrical polar coordinates of a point P with origin at the centre of the sphere and the axis of rotation as Oz, and let (u, v, w) be the corresponding components of velocity. Further we suppose that the sphere is at rest and that in addition to the rotation the fluid streams past it with uniform velocity $w = -W$ when $z = +\infty$. From the equation of continuity a stream function Ψ may be introduced such that

$$\frac{1}{r}\frac{\partial \Psi}{\partial r} = w, \qquad -\frac{1}{r}\frac{\partial \Psi}{\partial z} = u.$$

Then, provided that the problem is properly posed so that the conditions at infinity can be as specified, we have (3)

$$\frac{\partial^2 \psi}{\partial r^2} - \frac{1}{r}\frac{\partial \psi}{\partial r} + \frac{\partial^2 \psi}{\partial z^2} + k^2 \psi = 0, \tag{1.2}$$

where

$$\psi = \Psi + \tfrac{1}{2} W r^2 \quad \text{and} \quad rv = -k\Psi, \tag{1.3}$$

with boundary conditions

$$\psi \to 0 \text{ as } z \to \infty \quad \text{and} \quad \psi = \tfrac{1}{2} W r^2 \text{ on the sphere.} \tag{1.4}$$

Taylor obtained a solution of this equation which included an arbitrary constant. Long (3) showed that nearly every solution of (1.2) satisfied the boundary condition as $z \to \infty$, so that another boundary condition was needed to complete the solution. The indeterminacy is due to the existence of wave-like solutions of (1.2) which, if the fluid is unbounded, die out as $r^2 + z^2 \to \infty$. If, however, the fluid is confined within a cylinder of fixed radius b $(> a)$ the situation is different. When $kb < 3{\cdot}83$ all acceptable solutions of (1.2) die out exponentially as $z \to \infty$, but if $kb > 3{\cdot}83$ there exist wave-like solutions which cannot die out as $z \to \infty$. Hence if the problem is properly posed so that $\psi \to 0$ as $z \to +\infty$, they must be excluded and there is then a unique solution. Long also carried out experiments which confirmed that there were no wave-like motions ahead of the body, the streamlines only oscillating to its rear.

Starting from a study of sources in a rotating fluid enclosed within such a cylinder Fraenkel (5) obtained a solution to the flow of an unbounded fluid past the sphere when ka is small by letting $b \to \infty$. In adopting this limiting process it is assumed that since no wave-like motions occur ahead of the body when b is finite, neither will they occur when $b = \infty$ but, as pointed out above, this is not self-evident. The difficulty arises because two limiting processes, $b \to \infty$ and $z \to \infty$, are involved and the order in which they are taken is important.

For an unbounded fluid the most general solution of (1.2), free from singularities in $z > 0$ is

$$\psi = r \int_0^\infty A(\sigma) J_1(\sigma r) \exp\{-z(\sigma^2 - k^2)^{\frac{1}{2}}\}\, d\sigma \tag{1.5}$$

where $A(\sigma)$ is an arbitrary function of σ. The wave-like part of this solution when z is large comes from that part of the path of integration in which $\sigma < k$ where the exponential oscillates. If no oscillations occur when z is large

$$A(\sigma) = 0 \quad \text{if} \quad \sigma < k. \tag{1.6}$$

In section 2 of this paper we show that no matter how the motion is started, if ultimately it is nearly uniform a long way ahead of the body, ψ there has the form

$$r \int_k^\infty J_1(\sigma r) A(\sigma) \exp\{-z(\sigma^2 - k^2)^{\frac{1}{2}}\}\, d\sigma + r \int_0^k B(\sigma) J_1(\sigma r)\, d\sigma, \tag{1.7}$$

where A and B have to be found. If $\psi \to 0$ as $z \to +\infty$, $B \equiv 0$ and ψ then satisfies both the differential equation (1.2) and the extra boundary condition (1.6). It is quite possible, however, for B to be non-zero, in which case the motion is cylindrical at large distances upstream and the problem stated in (1.2) and (1.4) is not properly posed. There is thus some theoretical doubt as to whether the motion of an unbounded fluid is uniform a long way ahead of the sphere for any ka. The experiments are against such a cylindrical component to ψ (i.e. independent of z) for small values of ka, Taylor (**2**), for example, finding that it first appeared when $ka \approx 2\pi$. It must be remembered, however, that they were all carried out with fluid inside a tube of finite radius b with a/b small, and it has been argued that a drastic change may take place in the character of the flow as $a/b \to 0$. A reason for not believing this is given below.

The nature of the flow due to a sphere is examined in sections 3 and 4 of this paper assuming that $\psi \to 0$ as $z \to +\infty$ and (1.6) holds. The complete family of solutions ψ_m ($m = 1, 2, \ldots$) of (1.2) satisfying (1.6), of which the first was found by Fraenkel (**5**), is obtained in section 3. On writing

$$\psi = \sum A_m \psi_m \tag{1.8}$$

the solution which satisfies (1.4) in addition may be obtained, the A_m being constants which satisfy an infinite set of linear equations. They are found in section 4 and are displayed in Table 1 there, together with the corresponding drag coefficient C_D as functions of ka. So long as $ka \leqslant 2$ all the A_m except for A_1 are small, but for larger values of ka they rapidly increase in value and the streamlines become greatly distorted. Eventually, at $ka = 5{\cdot}76$ all the A_m become infinite, because the determinant of the

coefficients of the linear equations which they satisfy vanishes. This means that the possible values of ψ on the sphere are restricted and to satisfy (1.4) additional terms, which can only be cylindrical from section 2, must be added to ψ. If $ka > 5{\cdot}76$ the solution given by (1.8) although mathematically consistent is unrealistic. From this and a comparison of C_D with a known solution, it is concluded that a cylindrical component certainly occurs in ψ if $ka \geqslant 5{\cdot}76$, probably if $ka \geqslant 3$, but may occur for all $ka > 0$ although there is then an apparent discrepancy with observation. It is not believed that such a discrepancy would be resolved by considering the fluid to be enclosed in a large but finite container for the following reason.

When ka is infinite the flow, both when $a/b \neq 0$ and when $a/b = 0$, is known to be cylindrical. Now let us suppose that when ka is large (but $< kb$ of course) $\psi \to 0$ as $z \to +\infty$. Then if $kb = \infty$, from (1.5) and (1.6),

$$\psi \sim rJ_1(kr) \int_0^\infty C(\tau) e^{-\tau z}\, d\tau \tag{1.9}$$

near the sphere, where C is an arbitrary function. On the other hand, if kb is large, from the corresponding series for ψ (cf. **3**),

$$\psi \sim rJ_1(\alpha r)\exp\{-z(\alpha^2 - k^2)^{\frac{1}{2}}\}$$

near the sphere, where αb is the smallest of those roots of $J_1(x) = 0$ which are greater than kb. In either case ψ cannot be $\propto r^2$ on the sphere and so a cylindrical term must be present. It is inferred that for sufficiently large kb there is a value $f(kb) < kb$ of ka such that if

$$ka > f(kb)$$

the hypothesis that $\psi \to 0$ as $z \to +\infty$ must break down. The way in which the breakdown occurs when $kb = \infty$ is then likely to be typical, i.e. ψ is equal to the sum of a series of functions corresponding to those in (1.8) and at some finite value of ka their coefficients would all be infinite. The argument used when $kb = \infty$ also applies so that there is a theoretical possibility that ψ has a cylindrical component for all possible ka even when kb is finite. The fact that experiment does not bear this out enables us for the present to regard it only as a remote possibility both for kb finite and kb infinite.

2. Ultimate conditions far upstream of the body

In this section we show that if the flow far upstream of the body is uniform at all times then (1.6) holds, i.e. no wave-like motions occur ahead of the body, no matter how it was started from a state of relative rest.

Let the body be at rest at a large distance downstream of the origin and, in addition, let the motion at an infinite distance upstream ($z \to +\infty$) consist

of a uniform rotation and an axial component of velocity $-W$. Then, however the disturbed motion from this state is started the disturbed components of velocity are already small at $z = 0$. To describe the motion when $z > 0$ it is therefore legitimate to linearize the equations of motion as follows. Using fixed rectangular cartesian coordinates (x, y, z) the velocity components may be written

$$(-\Omega y+q_x,\ \Omega x+q_y,\ -W+q_z), \tag{2.1}$$

where q_x, q_y, q_z are assumed to be small if $z > 0$. Then if p is the pressure, ρ the density, and

$$P = p/\rho-\tfrac{1}{2}\Omega^2(x^2+y^2), \tag{2.2}$$

we have

$$\left(\frac{\partial}{\partial t}-W\frac{\partial}{\partial z}\right)q_x-2\Omega q_y = -\frac{\partial P}{\partial x}, \qquad \left(\frac{\partial}{\partial t}-W\frac{\partial}{\partial z}\right)q_y+2\Omega q_x = -\frac{\partial P}{\partial y},$$

$$\left(\frac{\partial}{\partial t}-W\frac{\partial}{\partial z}\right)q_z = -\frac{\partial P}{\partial z} \quad \text{and} \quad \frac{\partial q_x}{\partial x}+\frac{\partial q_y}{\partial y}+\frac{\partial q_z}{\partial z} = 0. \tag{2.3}$$

From these equations it was shown by Squire (6) that (q_x, q_y, q_z) may be eliminated and a single equation for P obtained, viz.

$$\left(\frac{\partial}{\partial t}-W\frac{\partial}{\partial z}\right)^2\nabla^2 P+4\Omega^2\frac{\partial^2 P}{\partial z^2} = 0. \tag{2.4}$$

In discussing the motion in $z > 0$ let us assume that P and as many of its derivatives as necessary are given at $z = 0$ for all $t \geqslant 0$ and that they tend to zero as $x^2+y^2 \to \infty$. Further define P_1, the Laplace transform of P with respect to t, by

$$P_1(x, y, z, s) = \int_0^\infty e^{-st}P(x, y, z, t)\,dt, \tag{2.5}$$

so that

$$P = \frac{1}{2\pi i}\int_{c-i\infty}^{c+i\infty} P_1 e^{st}\,ds, \qquad c > 0, \tag{2.6}$$

the path of integration lying to the right of all singularities of P_1. If ultimately the flow is steady the value of P then is given by the residue of the pole of P_1 at $s = 0$. The equation satisfied by P_1 is, from (2.3) and (2.4),

$$\left(s-W\frac{\partial}{\partial z}\right)^2\nabla^2 P_1+4\Omega^2\frac{\partial^2 P_1}{\partial z^2} = 4\Omega^2\left\{\frac{\partial q_z}{\partial z}\right\}_{t=0}, \tag{2.7}$$

the right-hand side being the value of $\partial(\nabla^2 P)/\partial t$ when $t = 0$: the initial value of $\nabla^2 P$ is zero because the relative motion is initially irrotational with potential ϕ_0. On writing $P_2 = P_1-\phi_0$, P_2 satisfies

$$\left(s-W\frac{\partial}{\partial z}\right)^2\nabla^2 P_2+4\Omega^2\frac{\partial^2 P_2}{\partial z^2} = 0. \tag{2.8}$$

Since $P_2 \to 0$ as $x^2+y^2 \to \infty$ and is bounded in $z > 0$ we may write

$$P_2 = \int_{-\infty}^{\infty} e^{ilx}\, dl \int_{-\infty}^{\infty} e^{imy} Q(l, m, z, s)\, dm, \tag{2.9}$$

where l, m are real and Q satisfies

$$\left(s - W\frac{d}{dz}\right)^2\left(\frac{d^2Q}{dz^2} - \sigma^2 Q\right) + 4\Omega^2 \frac{d^2Q}{dz^2} = 0 \tag{2.10}$$

where $\sigma^2 = l^2+m^2$.

This equation is an ordinary linear equation of the fourth order and has four independent solutions, each of the form $\exp \alpha z$, where α is a root of the quartic

$$(s-\alpha W)^2(\alpha^2-\sigma^2)+4\Omega^2\alpha^2 = 0. \tag{2.11}$$

When s is large the four roots of (2.11) are

$$\pm\sigma, \qquad (s/W) \pm ik, \tag{2.12}$$

k being equal to $2\Omega/W$.

Hence there is only one acceptable root α_0 in $z > 0$ leading to

$$Q = F(s, l, m)e^{\alpha_0 z} \tag{2.13}$$

where F is an unknown function and α_0 is that root which tends to $-\sigma$ as $s \to \infty$. The other three roots can only be used to specify the solution in $z < 0$, and two of them correspond to waves carried along with the stream. To discuss the ultimate steady motion the behaviour of α_0 near $s = 0$ must be determined. Before doing this, however, we shall prove that if the real part of s is positive, the real part of α_0 is negative, and that the branch points of α_0, *qua* function of s, are either on the imaginary axis or on the negative part of the real axis.

First, α_0 is a continuous function of s and has a negative real part when s has a large positive real part. Further, if the real part of α_0 is zero, we may set $\alpha_0 = i\beta$, where β is real,

$$(s - iW\beta)^2 = -\frac{4\Omega^2\beta^2}{\beta^2+\sigma^2},$$

and so s is wholly imaginary. Hence α_0 can only cross the imaginary axis with s and, therefore, if the real part of s is positive, the real part of α_0 is negative. In addition, there cannot be any interchange between α_0 and the other roots in this domain of s.

Secondly, the branch points of α, *qua* function of s, occur when two of the roots of (2.11) are equal. It may be shown after some elimination that this occurs when

$$s = W(\sigma^{\frac{1}{3}} - k^{\frac{1}{3}})^{\frac{1}{2}}. \tag{2.14}$$

At this value of s the roots are

$$\sigma^{\frac{1}{3}}(\sigma^{\frac{1}{3}} - k^{\frac{1}{3}})^{\frac{1}{2}}, \qquad \sigma^{\frac{1}{3}}(\sigma^{\frac{1}{3}} - k^{\frac{1}{3}})^{\frac{1}{2}}$$

and

$$(\sigma^{\frac{1}{3}} - k^{\frac{1}{3}})^{\frac{1}{2}}\{-k^{\frac{1}{3}} \pm (\sigma^{\frac{1}{3}} - \sigma^{\frac{1}{3}}k^{\frac{1}{3}} + k^{\frac{1}{3}})^{\frac{1}{2}}\}. \tag{2.15}$$

We can make α_0 a single-valued function of s by requiring that $\alpha_0 \to -\sigma$ as $s \to \infty$ along the positive real axis and cutting the s-plane from the relevant branch points in (2.15) to infinity along straight lines parallel to the negative real axis of s. If $\sigma > k$ there are two branch points at real values of s, but from (2.15) the positive value of s corresponds to two of the roots with positive real parts being equal and is not a branch point of α_0. Therefore, if $\sigma > k$ the only branch point of α_0, *qua* function of s, is at

$$s = -W(\sigma^2 - k^2)^{\frac{1}{2}}. \tag{2.16}$$

If $\sigma < k$, however, there are two on the imaginary axis of s.

From these two results we deduce that it is permissible to determine the behaviour of α_0 as $s \to 0$ by considering positive real values of s only. Then the left-hand side of (2.11) is negative when $\alpha = 0$ and positive when $\alpha = -\infty$ so that there is always a negative real root which must be α_0. In particular when s is small but positive the root is

$$-(\sigma^2 - k^2)^{\frac{1}{2}} + O(s) \quad \text{if} \quad \sigma > k$$

and

$$-\frac{\sigma}{k-\sigma}\frac{s}{W} + O(s^2) \quad \text{if} \quad \sigma < k. \tag{2.17}$$

Hence in the limit $s \to 0$, $\alpha_0 \to -(\sigma^2 - k^2)^{\frac{1}{2}}$ if $\sigma > k$ and $\alpha_0 \to 0$ if $\sigma < k$. If in the solution for Q, the value of F in (2.13) with $l^2 + m^2 < k^2$ is not identically zero, then the ultimate steady motion must include a cylindrical component. Therefore it does not tend to the undisturbed state as $z \to +\infty$ and the premiss on which the hypothesis is based does not hold. On the other hand, if there is no cylindrical component,

$$F \equiv 0 \quad \text{if} \quad \sigma < k,$$

and in the special case of axial symmetry we have immediately the form of the hypothesis in (1.6).

The same argument may be applied to regions far downstream of the body by considering the three roots of (2.11) with positive real parts when s has a positive real part. It may be shown that as $s \to 0$ through positive values these roots tend to

$$0,\ 0,\ (\sigma^2 - k^2)^{\frac{1}{2}} \quad \text{if} \quad \sigma > k$$

and

$$0,\ \pm i(k^2 - \sigma^2)^{\frac{1}{2}} \quad \text{if} \quad \sigma < k. \tag{2.18}$$

Thus, even if ultimately there is no two-dimensional component at large distances downstream there are still wave-like components coming from the conjugate imaginary roots when $\sigma < k$.

Finally, it is noted that the branch points are an indication of any inherent tendency of the solution to become unstable for large t. A branch point with a positive real part will make a contribution to P which increases exponentially in amplitude while the contribution from a branch point

with a negative real part will tend to zero exponentially with time. Branch points which are wholly imaginary correspond to oscillatory motions which may increase or decrease algebraically in amplitude. The solution of the present problem when $k = \infty$ is already known (4): in it the branch points all occur on the imaginary axis in agreement with (2.16) and, further, the contributions to the solution from them are algebraically small when t is large. It is likely therefore that at finite values of k the imaginary branch points make small contributions to the solution at large times. The contribution from the real branch point is exponentially small. There is a possibility that F may have a pole or branch points at a different point from those discussed above but again arguing from the solution when $k = \infty$, this is not likely. It is concluded therefore that the solution ahead of the body is ultimately steady.

3. The stream functions which satisfy (1.6)

We have from (1.5)

$$\psi = r \int_k^\infty A(\sigma) J_1(\sigma r) \exp\{-z(\sigma^2 - k^2)^{\frac{1}{2}}\}\, d\sigma \quad \text{if} \quad z > 0 \tag{3.1}$$

to satisfy (1.6). When r is small

$$\psi = \tfrac{1}{2} r^2 \int_k^\infty \sigma A(\sigma) \exp\{-z(\sigma^2 - k^2)^{\frac{1}{2}}\}\, d\sigma = \tfrac{1}{2} r^2 \int_0^\infty B(\tau) e^{-\tau z}\, d\tau, \tag{3.2}$$

where $\tau^2 = \sigma^2 - k^2$ and $\tau A(\sigma) = B(\tau)$.

Finally, expanding B in a power series about $\tau = 0$ we have

$$\psi = k^2 r^2 \sum C_s z^{-s}$$

in which the s are arbitrary positive numbers and C_s arbitrary constants. Or, if (R, θ) is a point in the fluid ahead of the body where

$$R\cos\theta = z, \qquad R\sin\theta = r, \tag{3.3}$$

then $$\psi = \theta^2 \sum C_s R^{2-s} \text{ when } \theta \text{ is sufficiently small.} \tag{3.4}$$

It is required to find a solution of (1.2) such that (3.4) is satisfied and such that, as $\theta \to \pi$, $\psi \to 0$, so that the streamlines close up behind the body. Now the general solution of (1.2) which is bounded at both $\theta = 0$ and $\theta = \pi$ is a sum of terms of the form

$$(1-\mu^2) R^{\frac{1}{2}} J_{n+\frac{1}{2}}(kR) P_n'(\mu) \quad \text{and} \quad (1-\mu^2) R^{\frac{1}{2}} J_{-n-\frac{1}{2}}(kR) P_n'(\mu), \tag{3.5}$$

where $\mu = \cos\theta$, n is a positive integer, $J_{n+\frac{1}{2}}$ is a Bessel function, and $P_n(\mu)$ is a Legendre polynomial. The solution corresponding to $n = 0$ is

$$R^{\frac{1}{2}} J_{\pm\frac{1}{2}}(kR)(A + B\cos\theta), \tag{3.6}$$

where A and B are constants, and only vanishes at $\mu = \pm 1$ if $A = B = 0$.

We now express that term of (3.4) which is proportional to $R^{i+\frac{1}{2}}$, $i < \frac{3}{2}$, together with any other terms of (3.4), of smaller order as $R \to \infty$, as may be convenient, in terms of Bessel functions. The series of Bessel functions obtained may then be generalized into a solution of (1.2), which satisfies (1.6), on making use of (3.5). Consider

$$\phi_{i,t} = R^{i}(1-\mu^2) \sum_{s=0}^{t} \frac{(\frac{1}{2}kR)^{2s+i}(-1)^s}{s!(s+i)!}. \tag{3.7}$$

Provided only that $2t+i < \frac{3}{2}$, $\phi_{i,t}$ has the form of (3.4). Using the known identity

$$(\tfrac{1}{2}kR)^m = \sum_{u=0}^{\infty} \frac{(m+2u)(m+u-1)!}{u!} J_{m+2u}(kR) \tag{3.8}$$

and mathematical induction, it may be proved that

$$\phi_{i,t} = R^{i}(1-\mu^2)J_i(kR) + (1-\mu^2)R^{i} \sum_{u=t+1}^{\infty} \frac{(i+2u)(i+u+t)!(-1)^t J_{i+2u}(kR)}{u(i+u)(u-t-1)!(i+t)!\,t!}. \tag{3.9}$$

Hence the solution of (1.2), which behaves like $\phi_{i,t}$ when θ is small, is

$$\frac{R^{i}(1-\mu^2)J_i(kR)P'_{i-\frac{1}{2}}(\mu)}{(i+\frac{1}{2})(i-\frac{1}{2})} + \\ + R^{i}(1-\mu^2) \sum_{u=t+1}^{\infty} \frac{(i+2u)(i+u+t)!(-1)^t J_{i+2u}(kR)P'_{i+2u-\frac{1}{2}}(\mu)}{u(i+u)(u-t-1)!(i+t)!\,t!(i+2u+\frac{1}{2})(i+2u-\frac{1}{2})}. \tag{3.10}$$

From the properties of $P_n(\mu)$ we know that n must be an integer and from (3.6) $i+2u-\frac{1}{2}$ cannot vanish for any allowable i, u. Although $2t$ need only be less than $\frac{3}{2}-i$, it is convenient to take it as large as possible so that a Bessel function of negative order occurs only in the first term of the solution. First take therefore

$$i = -\tfrac{1}{2}-2m, \quad t = m \quad \text{and} \quad u = m+1+s$$

where m, $s+1$ are non-zero positive integers. Then (3.10) reduces, after multiplication by a numerical factor, to

$$\psi_{2m}(R,\theta) = R^{i}(1-\mu^2)P'_{2m}(\mu)J_{-\frac{1}{2}-2m}(kR) + \\ + R^{i}(1-\mu^2) \sum_{s=0}^{\infty} \frac{(4s+3)(2s)!(2m+1)!\,P'_{2s+1}(\mu)J_{2s+\frac{1}{2}}(kR)}{s!(s+1)!\,m!(m-1)!(m+s+1)(2s+1-2m)2^{2s+2m+1}}. \tag{3.11}$$

Secondly, take $\quad i = \frac{1}{2}-2m, \quad t = m, \quad u = m+1+s$

in (3.10). Then corresponding to (3.11) we have

$$\psi_{2m-1}(R,\theta) = R^{\frac{1}{2}}(1-\mu^2)P'_{2m-1}(\mu)J_{\frac{1}{2}-2m}(kR) -$$
$$- R^{\frac{1}{2}}(1-\mu^2)\sum_{s=0}^{\infty}\frac{(4s+5)(2s+1)!(2m)!\,P'_{2s}(\mu)J_{\frac{1}{2}+2s}(kR)}{s!(s+1)!\,m!(m-1)!(m+s+1)(2s-2m+3)2^{2s+2m+1}}. \tag{3.12}$$

The special case of (3.12) when $m = 1$ has also been obtained by Fraenkel (5) in a different way.

A partial check on these formulae may be made by evaluating (3.11) and (3.12) when R is large. It is then found, for example, that the leading term of the series in (3.12) is

$$(-)^m R^{\frac{1}{2}}(1-\mu^2)\operatorname{sgn}\mu P'_{2m-1}(\mu)\left(\frac{2}{\pi kR}\right)^{\frac{1}{2}}\sin kR$$

and cancels with the first term if $\mu > 0$. A similar result holds for (3.11).

4. Flow past a sphere

In this section we make use of the family of stream functions ψ_m satisfying (1.6) to determine the steady flow round a fixed sphere of radius a with its centre on the axis of rotation when at an infinite distance upstream the fluid has an axial component of velocity $-W$. Thus as $z \to \infty$

$$\Psi \to -\tfrac{1}{2}Wr^2. \tag{4.1}$$

From the previous section we know that the general solution of (1.2) satisfying (1.6) is

$$\Psi = -\tfrac{1}{2}Wr^2 + \frac{Wa^{\frac{1}{2}}}{2}\sum_{i=1}^{\infty}\psi_i(R,\theta)A_i \tag{4.2}$$

and the A_i have to be determined so that $\Psi = 0$ on $R = a$. Let us write (3.11) and (3.12) in the form

$$\psi_i = (1-\mu^2)P'_i(\mu)R^{\frac{1}{2}}J_{-i-\frac{1}{2}}(kR) + \sum_{j=0}^{\infty}\alpha_{ij}(1-\mu^2)P'_j(\mu)R^{\frac{1}{2}}J_{j+\frac{1}{2}}(kR), \tag{4.3}$$

where for convenience the numerical coefficients of the terms in the series have been replaced by α_{ij}, half of which are zero. We must choose the A_i so that

$$(1-\mu^2)\sum_{i=1}^{\infty}\sum_{j=1}^{\infty}\{A_i\delta_{ij}J_{-\frac{1}{2}-j}(ka) + A_i\alpha_{ij}J_{j+\frac{1}{2}}(ka)\}P'_j(\mu) = (1-\mu^2), \tag{4.4}$$

where $\delta_{ij} = 1$ if $i = j$ and vanishes otherwise. Inverting the order of summation, which may be justified *a posteriori*,

$$\sum_{j=1}^{\infty}(1-\mu^2)^{\frac{1}{2}}P'_j(\mu)\sum_{i=1}^{\infty}\{A_i\delta_{ij}J_{-\frac{1}{2}-j}(ka) + A_i\alpha_{ij}J_{j+\frac{1}{2}}(ka)\} = (1-\mu^2)^{\frac{1}{2}}. \tag{4.5}$$

Now the set of orthogonal functions $(1-\mu^2)P'_j(\mu)$, $j = 1, 2, 3, \ldots$ is complete

in the range $|\mu| \leqslant 1$ for all piecewise continuous functions which behave like $(1-\mu^2)^{\frac{1}{4}}$ near $\mu^2 = 1$. Hence in (4.5) the A_i must satisfy

$$\sum_{i=1}^{\infty} A_i\{\delta_{ij} J_{-\frac{1}{2}-j}(ka)+\alpha_{ij} J_{\frac{1}{2}+j}(ka)\} = \delta_{ij} \tag{4.6}$$

and the solution of this infinite set of linear equations determines Ψ. It has been solved numerically for $ka = 1, 2, 3, 4$, and the results are displayed in Table 1.

TABLE 1

ka	A_1	A_2	A_3	A_4	A_5	C_D
1	−0·903	−0·01				0·13
2	−2·08	−0·35	−0·01			1·4
3	−3·81	−2·48	−0·34	−0·15		14
4	−3·82	−10·92	−4·36	−1·09	−0·12	240

When $ka = 5$, $A_1 = -15$, but between $ka = 4$ and $ka = 5$ it changes sign twice since it is positive when $ka = 4{\cdot}49$ where $J_{\frac{1}{2}}(ka) = 0$. Thereafter it rapidly decreases, being -23 at $ka = 5{\cdot}2$, -83 at $ka = 5{\cdot}7$, infinitely close to $ka = 5{\cdot}76$, and $+31$ at $ka = 6$. At $ka = 5{\cdot}76$ the determinant of the coefficients of (4.6) when divided by the diagonal terms, which dominate it at sufficiently large values of i, j, vanishes without any of these terms being infinite. Although from a mathematical standpoint solutions can be obtained at higher values of ka it is physically inconceivable that this solution could occur when $ka \approx 5{\cdot}76$ and therefore also at higher values the mathematical solution must be rejected. It is concluded therefore that the problem is not properly posed if $ka \geqslant 5{\cdot}76$ and, indeed, it would be surprising if it did not cease to be properly posed at a lower value of ka. In the discussion of the drag given below we shall see that the drag on the sphere is out of all proportion even at values of ka as low as 3. It is interesting to note that according to Taylor's experiments (**1**) the character of the flow changed to include a cylindrical component when $ka \approx 2\pi$. Although this result was only obtained approximately so that it is not significantly different from 5·76 the agreement must be regarded as fortuitous since the physical breakdown may well occur before then.

From Squire's work (**6**) the pressure p in the fluid is given by

$$p = \text{const.} - \tfrac{1}{2}\rho(u^2+w^2) - \tfrac{1}{2}\rho\frac{k^2\psi^2}{r^2} + \tfrac{1}{2}\Omega^2\rho r^2, \tag{4.7}$$

where ρ is the density. Hence since $\psi = \frac{1}{4}Wa^2\sin^2\theta$ and $\Psi = 0$ on the sphere, the only part p_D of the pressure which contributes to the drag D is

$$p_D = -\frac{\rho}{2r^2}\left(\frac{\partial\Psi}{\partial R}\right)^2 \tag{4.8}$$

which comes from the longitudinal component of velocity. Hence

$$D = \int_0^{\pi} p_D \cos\theta \, 2\pi a^2 \sin\theta \, d\theta = -\int_{-1}^{+1} \frac{\pi\mu\rho}{1-\mu^2}\left(\frac{\partial\Psi}{\partial R}\right)^2 d\mu. \tag{4.9}$$

Now from (4.2), using (4.3) and (4.6),

$$\frac{1}{1-\mu^2}\frac{\partial\Psi}{\partial R} = -Wa\left(\frac{3}{4} - \frac{ka}{2}\frac{J_{\frac{3}{2}}'(ka)}{J_{\frac{1}{2}}(ka)}\right)P_1'(\mu) + \frac{Wa}{\pi}\sum_{i=1}^{\infty}\frac{(-)^{i+1}A_i}{J_{i-\frac{1}{2}}(ka)}P_i'(\mu)$$

$$= \frac{Wa}{\pi}\sum_{i=1}^{\infty}(-)^{i+1}B_i P_i'(\mu) \text{ say.} \tag{4.10}$$

Hence, substituting in (4.9) and writing

$$D = \rho\pi a^2 W^2 C_D(ka),$$

where C_D is the drag coefficient, we have

$$C_D = -\frac{1}{\pi^2}\sum_{i=1}^{\infty}\sum_{j=1}^{\infty}\int_{-1}^{+1} B_i B_j(-)^{i+j}\mu(1-\mu^2)P_i'(\mu)P_j'(\mu)\,d\mu$$

$$= \frac{2}{\pi^2}\sum_{i=1}^{\infty} B_i B_{i+1}\int_{-1}^{+1}\mu(1-\mu^2)P_i'P_{i+1}'\,d\mu$$

$$= \frac{4}{\pi^2}\sum_{i=1}^{\infty}\frac{i(i+1)(i+2)}{(2i+1)(2i+3)}B_i B_{i+1}. \tag{4.11}$$

If ka is so small that terms $O(ka)^{12}$ may be neglected, C_D may be calculated from A_1 and A_2 only. It is then found that

$$A_1 = [J_{-\frac{1}{2}}(ka)]^{-1}, \quad B_1 = \pi ka A_1 J_{-\frac{1}{2}}(ka) \quad \text{and} \quad B_2 = \tfrac{5}{8}A_1[J_{-\frac{1}{2}}(ka)]^{-1} \tag{4.12}$$

so that

$$C_D = \frac{(ka)^4}{4}\left[1-(ka)^2+(ka)^4-\tfrac{8}{9}(ka)^6\right]+O(ka)^{12}. \tag{4.13}$$

For larger values of ka, the values of C_D are given in Table 1 and may be compared with the value

$$C_D = 8ka/3\pi, \tag{4.14}$$

valid when ka is large, obtained in (4). In that solution (1.6) is inapplicable and the flow is wholly cylindrical. From a comparison between Table 1 and (4.14) it is inferred that the values of C_D obtained when $ka = 3$ and $ka = 4$ are too large and that in practice there would probably be a cylindrical component to the flow.

The author is grateful to Mr. L. E. Fraenkel for his constructive criticism of the first draft of this paper.

REFERENCES

1. G. I. Taylor, *Proc. Roy. Soc.* **A, 102** (1922) 180.
2. —— ibid. **104** (1923) 213.
3. R. R. Long, *J. Met.* **10** (1953) 197.
4. K. Stewartson, *Proc. Camb. Phil. Soc.* **48** (1952) 168.
5. L. E. Fraenkel, *Proc. Roy. Soc.* **A, 233** (1956) 506.
6. H. B. Squire, *Surveys in Mechanics*, ed. G. K. Batchelor and R. M. Davies (Cambridge, 1956), p. 139.

HEAT TRANSFER THROUGH THE LAMINAR BOUNDARY LAYER ON A CIRCULAR CYLINDER IN AXIAL INCOMPRESSIBLE FLOW

By D. E. BOURNE *and* D. R. DAVIES (*University of Sheffield*)

[Received 24 January 1957]

SUMMARY

This paper presents a method of calculating the distribution of rate of heat transfer into a laminar incompressible boundary layer from the exterior surface of a long thin circular cylinder, when the surface of the cylinder is maintained at a constant temperature and the flow is parallel to the cylinder axis; the temperature difference between the surface and the main stream is taken to be small enough to neglect buoyancy effects. A series solution, valid for small downstream distances from the nose, has been obtained already by Seban, Bond, and Kelly. This is now extended by deriving an asymptotic series solution, valid at large downstream distances, and bridging the gap between these two series solutions by an approximate solution, based on the method used recently by Davies and Bourne to calculate heat transfer from a flat plate. The calculation is used to demonstrate the effect of curvature and of Prandtl number on the local rate of heat transfer at various downstream distances by comparing with the corresponding flat plate results.

1. Introduction

In order to estimate the influence of curvature on the calculated values of local rate of heat transfer from heated surfaces into a given flow, the problem of forced convection from a heated circular cylinder into the surrounding axisymmetric, incompressible, laminar, boundary layer produced by a uniform stream was considered first by Seban and Bond (**1**). The front of the cylinder is supposed to be smooth enough to prevent boundary layer separation, and the variation with downstream distance of the local rate of heat transfer Q from the external surface of the cylinder is investigated. Seban and Bond give an exact solution of the appropriate temperature equation in the form of a series, valid for small values of $\nu x/Ua^2$ where U is the uniform mainstream velocity, x is downstream distance, ν kinematic viscosity, and a the cylinder radius. Important numerical corrections of this work by Seban and Bond were later given by Kelly (**2**), and we shall refer to their solution as the Seban–Bond–Kelly solution. The leading term of this series solution is equivalent to the flat plate solution, while the succeeding terms represent corrections for the effect of curvature which becomes increasingly important at large downstream distances. The Seban–Bond–Kelly solution extends the flat plate

solution, which is valid for values of $\nu x/Ua^2$ of less than about 0·0001, up to approximately $\nu x/Ua^2 = 0{\cdot}04$.

We first obtain an alternative solution for the region $\nu x/Ua^2 \leqslant 0{\cdot}0001$ by utilizing the Pohlhausen type of velocity profile given by Glauert and Lighthill (3) and extending a method of treating the heated flat plate problem described by Davies and Bourne (4). In the case of constant surface temperature the numerical result is within 2 per cent of the exact flat plate value and suggests that the Glauert–Lighthill profile is a suitable approximation to the basic flow distribution in this context.

We next obtain an asymptotic series solution, which is valid at large values of $\nu x/Ua^2$, based on the analysis described by Glauert and Lighthill (3). The series is expressed in terms of inverse powers of $\beta = \ln(4\nu x/Ua^2)$ up to the term involving $1/\beta^3$. As in the skin friction problem (3) this is sufficient to calculate Q for $\nu x/Ua^2 \geqslant 100$, although the results given by Glauert and Lighthill suggest that the series can be used, provided the Prandtl number is approximately equal to one, up to about $\nu x/Ua^2 = 10$.

In order to bridge the gap between the Seban–Bond–Kelly solution and the asymptotic solution an approximate method is required. A Kármán–Pohlhausen approximation could be employed, following the method given by Glauert and Lighthill, and the distribution of Q computed by numerical integration of a first-order linear differential equation for each prescribed Prandtl number. However, this method of approach is only applicable in the case of constant cylinder temperature. We use instead an alternative method which is applicable to an *arbitrary* distribution of cylinder temperature, and, in the case of constant cylinder temperature, it leads to a fairly simple computation, involving the numerical evaluation of quadratures at appropriate positions on the bridge. We begin with power law approximations of similar type to those used by Davies and Bourne, involving deviations from the Pohlhausen profile of similar magnitude to those experienced in the flat plate problem (4). The ensuing temperature equation is transformed into a von Mises form and the appropriate boundary conditions specified by regarding the heated cylinder as an assembly of continuous uniform circular sources, each source being positioned normally to the cylinder axis and of radius a. A solution of the temperature equation is then obtained for one circular source and the distribution of source strength (or local rate of heat transfer) is determined by solving an appropriate integral equation, so that the prescribed cylinder temperature is achieved. We find that the calculated value of Q at $\nu x/Ua^2 = 0{\cdot}04$ is within about 3 per cent of the value given by the exact Seban–Bond–Kelly solution, and the values of Q for $0{\cdot}04 < \nu x/Ua^2 < 10$ continue into those computed from the asymptotic solution. For reasons discussed in section 5

it is probable that the values of Q based on this approximate method are in error by no more than about 5 per cent.

The influence of curvature is displayed by comparing the calculated numerical values of Q, for air, with those given by the flat plate solution, and the dependence of Q on σ, the Prandtl number, is also discussed. The thickness of the boundary layer, at small values of $\nu x/Ua^2$, is very small compared with the cylinder radius, and consequently Q varies with $\sigma^{\frac{1}{3}}$ as in the flat plate case, but as $\nu x/Ua^2$ increases the value of the index of σ decreases from $\frac{1}{3}$, and at very large values of $\nu x/Ua^2$, Q is independent of σ. When the numerical value of σ is about 1·0, the variation with $\nu x/Ua^2$ of the quantities given by (*a*) [local skin-friction on the cylinder/local skin-friction on the flat plate], and (*b*) [local rate of heat transfer on the cylinder/local rate of heat transfer on the flat plate] are similar, but when σ differs markedly from 1·0 this is not true. Thus at very large x-values, the asymptotic solution shows that the ratio of (*a*) to (*b*), at a prescribed x, is given by $\sigma^{-\frac{1}{3}}$, while at small values of $\nu x/Ua^2$ it is 1·0.

2. Solutions for small downstream distances

The boundary layer equations are

$$u\frac{\partial u}{\partial x}+v\frac{\partial u}{\partial r}=\frac{\nu}{r}\frac{\partial}{\partial r}\left(r\frac{\partial u}{\partial r}\right) \tag{1}$$

for the velocity distribution,

$$u\frac{\partial T}{\partial x}+v\frac{\partial T}{\partial r}=\frac{\kappa}{r}\frac{\partial}{\partial r}\left(r\frac{\partial T}{\partial r}\right) \tag{2}$$

for the temperature distribution (neglecting frictional heating), and the continuity equation is

$$\frac{\partial}{\partial r}(rv)+\frac{\partial}{\partial x}(ru)=0, \tag{3}$$

where x denotes downstream distance, r the radial distance from the axis, u and v the downstream and radial velocity components respectively, T the temperature, and κ the thermal diffusivity.

The Seban–Bond–Kelly series solution for heat transfer, referred to in the Introduction, is valid for $\nu x/Ua^2 < 0{\cdot}04$ and is given, in the case of constant cylinder temperature, in the form

$$\frac{Q}{k(T_1-T_0)}=0{\cdot}664\pi\sigma^{\frac{1}{3}}\left(\frac{Ua^2}{\nu x}\right)^{\frac{1}{2}}\left\{1+2{\cdot}30\left(\frac{\nu x}{Ua^2}\right)^{\frac{1}{2}}-\ldots\right\}, \tag{4}$$

where Q is the local rate of heat transfer (per unit length of the cylinder), σ is the Prandtl number, k the thermal conductivity, T_1 the cylinder

temperature, and T_0 the air stream temperature. The leading term in (4) represents the flat plate solution for a Blasius layer.

We now consider an alternative method of approach which *suggests* the approximate treatment used for larger values of $\nu x/Ua^2$. We adopt the Pohlhausen profile used successfully by Glauert and Lighthill (**3**). The order of magnitude of the error involved, due to the use of this profile, in the heat problem can also be estimated from this by comparing the ensuing solution with the exact solution (**4**). The Pohlhausen profile is

$$\frac{u}{U} = \frac{1}{\alpha(x)}\ln(1+y/a), \quad \text{for } y \leqslant \delta = a(e^{\alpha}-1), \tag{5}$$

and

$$\frac{u}{U} = 1, \quad \text{for } y \geqslant \delta, \tag{6}$$

where δ is the 'boundary layer thickness' which appears in Pohlhausen treatments and y denotes distance from the cylinder surface. The parameter α is given numerically as a function of x by Glauert and Lighthill. We define the stream function ψ, to satisfy (3), by the relations

$$\frac{\partial\psi}{\partial r} = ru \quad \text{and} \quad \frac{\partial\psi}{\partial x} = -rv. \tag{7}$$

Expanding the logarithmic form in (5) and retaining only the first term, the velocity profile, at very small $\nu x/Ua^2$ values, is given by

$$\frac{u}{U} = \frac{\zeta}{\alpha}, \quad \text{where } \zeta = \frac{y}{a}, \tag{8}$$

and, using (7), the stream function ψ becomes

$$\psi = \frac{Ua^2}{2\alpha}\zeta^2. \tag{9}$$

The von Mises method (**5**, p. 126), used in the case of the flat plate (**4**), is easily extended to the cylinder problem, and the basic equation (2) simplifies to the form

$$\frac{\partial T}{\partial x} = \kappa\frac{\partial}{\partial\psi}\left\{(r^2u)\frac{\partial T}{\partial\psi}\right\}. \tag{10}$$

Neglecting squares and higher powers of ζ we have, using (8),

$$r^2u = a^2U\alpha^{-1}\zeta, \tag{11}$$

and hence, using (9) and (11), equation (10) now becomes

$$\frac{\partial T}{\partial x} = (2^{\frac{1}{2}}U^{\frac{1}{2}}\alpha^{-\frac{1}{2}}\kappa a)\frac{\partial}{\partial\psi}\left\{\psi^{\frac{1}{2}}\frac{\partial T}{\partial\psi}\right\}. \tag{12}$$

Using the Seban–Bond–Kelly solution, it can be shown that, when $\nu x/Ua^2 \to 0$,

$$\frac{1}{\alpha} \sim 0{\cdot}332\left(\frac{\nu x}{Ua^2}\right)^{-\frac{1}{2}}, \tag{13}$$

and on substituting $X = x^{\frac{1}{2}}$, (12) reduces to

$$\frac{\partial T}{\partial X} = c\frac{\partial}{\partial \psi}\left(\psi^{\frac{1}{2}}\frac{\partial T}{\partial \psi}\right), \tag{14}$$

where $$c = 2^{\frac{1}{2}}3^{-1}(0{\cdot}332)^{\frac{1}{2}}U^{\frac{1}{2}}a^{\frac{1}{2}}\kappa\nu^{-\frac{1}{2}}.$$

Equation (14) is identical in form with basic equation (11) discussed by Davies and Bourne (**4**), and their analysis applies with $Q/2\pi a$ replacing Q, the rate of heat transfer per unit length of a line source. We obtain

$$\frac{Q}{k(T_1-T_0)} = 0{\cdot}678\pi\sigma^{\frac{1}{2}}\left(\frac{Ua^2}{\nu x}\right)^{\frac{1}{2}}. \tag{15}$$

This result is within about 2 per cent of the exact flat plate solution. The small error is due to the logarithmic approximation of the Pohlhausen profile but, as discussed by Glauert and Lighthill, the error on this account is likely to decrease as $\nu x/Ua^2$ increases; for this reason the logarithmic profile (5) is used in the following sections, for all values of $\nu x/Ua^2$. Solution (15) is only valid down to $\nu x/Ua^2 = 0{\cdot}0001$, when higher terms in ζ become significant, so that an alternative method must be used.

3. The asymptotic series solution for large downstream distances

Following the method of treating the velocity boundary layer equation (1) given by Glauert and Lighthill (**3**),† we now obtain a solution of the temperature equation (2), which will be valid at large downstream distances where the boundary layer thickness is much larger than the cylinder radius a. Glauert and Lighthill consider a series expansion for the stream function

$$\psi = \nu x f(\xi, x) \sim \nu x\left\{f_0(\xi)+\frac{f_1(\xi)}{\beta}+\frac{f_2(\xi)}{\beta^2}+\ldots\right\}, \tag{16}$$

where $$\xi = \frac{Ur^2}{4\nu x} \quad \text{and} \quad \beta = \ln\left(\frac{4\nu x}{Ua^2}\right), \tag{17}$$

so that $$u = \tfrac{1}{2}Uf' \quad \text{and} \quad v = \frac{\nu}{r}(\xi f'-f-xf_x); \tag{18}$$

primes and x suffixes denote partial differentiation with respect to ξ and x respectively. They show that

$$f_0 = 2\xi, \tag{19}$$

$$f_1 = 2\xi\,\mathrm{Ei}(-\xi)+2e^{-\xi}-2, \tag{20}$$

$$f_2' = 2e^{-\xi}\,\mathrm{Ei}(-\xi)-4\,\mathrm{Ei}(-2\xi)-\{\mathrm{Ei}(-\xi)\}^2+4\,\mathrm{Ei}(-\xi)\ln\xi+ \\ +6\,\mathrm{Ei}(-\xi)-6\,\mathrm{El}(-\xi), \tag{21}$$

where $$\mathrm{Ei}(-\xi) = \int_{\infty}^{\xi} e^{-t}t^{-1}\,dt \quad \text{and} \quad \mathrm{El}(-\xi) = \int_{\infty}^{\xi} \mathrm{Ei}(-t)t^{-1}\,dt.$$

† An asymptotic series solution for skin-friction has also been obtained by Stewartson (**6**).

The similarity in form of the velocity and temperature equations immediately suggests that an asymptotic series solution, of the same nature as the Glauert–Lighthill solution for the velocity profile, exists for the temperature profile. Accordingly we consider the series expansion

$$\frac{T-T_1}{T_0-T_1} = g(\xi, x) = g_0(\xi)+\frac{g_1(\xi)}{\beta}+\frac{g_2(\xi)}{\beta^2}+\ldots, \tag{22}$$

the temperature boundary conditions being expressed in the form

$$g \to 1 \quad \text{as } \xi \to \infty, \tag{23}$$

and

$$g \to 0 \quad \text{as } \xi \to e^{-\beta}. \tag{24}$$

Using (18) and (22) the temperature equation (2) becomes

$$xf'g_x - fg' - xf_x g' = 2\sigma^{-1}g' + 2\sigma^{-1}\xi g''. \tag{25}$$

Substituting the series (16) and (22) and equating inverse powers of β we obtain the equations

$$\xi g_0'' + g_0' + \tfrac{1}{2}\sigma f_0 g_0' = 0, \tag{26}$$

$$\xi g_1'' + g_1' + \tfrac{1}{2}\sigma(g_0' f_1 + g_1' f_0) = 0, \tag{27}$$

$$\xi g_2'' + g_2' + \tfrac{1}{2}\sigma(f_2 g_0' - f_1 g_0' + f_0' g_1 + f_1 g_1' + f_0 g_2') = 0, \tag{28}$$

and in general

$$\xi g_n'' + g_n' + \tfrac{1}{2}\sigma\Big\{\sum_{m=0}^{n} f_m g_{n-m}' - \sum_{m=1}^{n-1} m(f_m g_{n-m-1}' - g_m f_{n-m-1}')\Big\} = 0. \tag{29}$$

Following closely the analysis of Glauert and Lighthill for the velocity profile, we now transfer the inner boundary condition (24) to $\xi = 0$, since $g_0, g_1, \ldots,$ are independent of β. Now it is easily seen that near $\xi = 0$ equation (25) has the form

$$\xi g'' + g' = 0,$$

with solution

$$g = C + D\ln\xi.$$

Hence, near $\xi = 0$, each separate term in the series (22) must have the form

$$g \sim c_n + d_n \ln\xi, \tag{30}$$

where c_n and d_n are constants. Using these forms in (22) with the condition (24) we obtain

$$\sum_{n=0}^{\infty} \frac{c_n - \beta d_n}{\beta^n} = 0, \tag{31}$$

so that

$$d_0 = 0,\ d_1 = c_0,\ d_2 = c_1, \ldots,\ d_n = c_{n-1}. \tag{32}$$

The inner boundary condition is thus expressed by (30) and (32) as $\xi \to 0$. The condition at infinity (23) becomes

$$g_0 \to 1, \qquad g_n \to 0 \ (n > 0), \quad \text{as } \xi \to \infty. \tag{33}$$

Substituting (19) into (26), we find the equation for g_0 is

$$\xi g_0'' + g_0' + \sigma\xi g_0' = 0,$$

the solution of which, under the conditions $g_0 \to c_0$ as $\xi \to 0$ and $g_0 \to 1$ as $\xi \to \infty$, is seen by inspection to be

$$g_0 = 1. \tag{34}$$

This represents an isothermal solution $T = T_0$ and corresponds, as we would expect, to the solution $f_0 = 2\xi$ which represents a uniform stream of velocity U in the velocity case.

Equation (27) now becomes

$$\xi g_1'' + g_1' + \sigma\xi g_1' = 0, \tag{35}$$

with associated boundary conditions

$$g_1 \sim c_1 + \ln\xi \text{ as } \xi \to 0, \quad \text{and} \quad g_1 \to 0 \text{ as } \xi \to \infty. \tag{36}$$

The appropriate solution of (35) is

$$g_1 = G\,\mathrm{Ei}(-\sigma\xi),$$

where G is an arbitrary constant. As $\xi \to 0$, it may be shown that

$$\mathrm{Ei}(-\sigma\xi) \sim \ln\xi + (\gamma + \ln\sigma).$$

Hence, using (36), we find that

$$G = 1,$$

$$c_1 = \gamma + \ln\sigma, \tag{37}$$

and

$$g_1 = \mathrm{Ei}(-\sigma\xi). \tag{38}$$

Using (19)–(21), (34), and (38), equation (28) becomes

$$\xi g_2'' + g_2' + \sigma\xi g_2' + \{\sigma\,\mathrm{Ei}(-\xi)e^{-\sigma\xi} + \sigma\xi^{-1}e^{-(1+\sigma)\xi} + \sigma\,\mathrm{Ei}(-\sigma\xi) - \sigma\xi^{-1}e^{-\sigma\xi}\} = 0, \tag{39}$$

with the boundary conditions

$$g_2 \sim c_2 + (\gamma + \ln\sigma)\ln\xi \text{ as } \xi \to 0, \quad \text{and} \quad g_2 \to 0 \text{ as } \xi \to \infty. \tag{40}$$

Integration of (39) yields

$$g_2 = e^{-\sigma\xi}\,\mathrm{Ei}(-\xi) - (1+\sigma)\,\mathrm{Ei}\{-(1+\sigma)\xi\} + (1+\sigma)\,\mathrm{Ei}(-\sigma\xi)\ln\xi - \\ -(2+\sigma)\,\mathrm{El}(-\sigma\xi) + H\,\mathrm{Ei}(-\sigma\xi) - \sigma\int_{\infty}^{\xi} e^{-\sigma t}\,\mathrm{Ei}(-t)t^{-1}\,dt, \tag{41}$$

where H is an arbitrary constant. It is easily shown that each member of (41) tends to zero as ξ tends to infinity, and the boundary condition as $\xi \to \infty$ is satisfied. In order to apply the inner boundary condition we use the result, quoted by Glauert and Lighthill (**3**), that as $\xi \to 0$

$$\mathrm{El}(-\xi) \sim \tfrac{1}{2}(\gamma + \ln\xi)^2 + \tfrac{1}{12}\pi^2 \tag{42}$$

and the result, obtained in the Appendix of this paper that, as $\xi \to 0$,

$$\int_{\infty}^{\xi} e^{-\sigma t}\,\mathrm{Ei}(-t)t^{-1}\,dt \sim \tfrac{1}{2}(\gamma + \ln\xi)^2 + \tfrac{1}{12}\pi^2 - S_\sigma, \tag{43}$$

where

$$S_\sigma = \frac{\sigma}{1^2} - \frac{\sigma^2}{2^2} + \frac{\sigma^3}{3^2} - \ldots. \tag{44}$$

The series S_σ is convergent and therefore directly summable for $|\sigma| \leqslant 1$, which is the case considered in section 5 of this paper (for air $\sigma = 0{\cdot}72$). If $\sigma > 1$, the series diverges but is nevertheless summable by Euler's method (see, for example, Hardy (7)).† It follows that, as $\xi \to 0$,

$$g_2 \sim \{H(\gamma+\ln\sigma)-\gamma\sigma-\gamma^2(1+\sigma)-\tfrac{1}{6}(1+\sigma)\pi^2-(1+\sigma)\ln(1+\sigma)- \\ -\tfrac{1}{2}(2+\sigma)(2\gamma+\ln\sigma)\ln\sigma+\sigma S_\sigma\}+\{H-\sigma-(1+\sigma)\gamma-\ln\sigma\}\ln\xi, \quad (45)$$

and applying the inner boundary condition (40) we find

$$H = \sigma(1+\gamma)+2(\gamma+\ln\sigma), \quad (46)$$

and

$$c_2 = d_3 = \gamma^2+(\sigma+2\gamma)\ln\sigma+(1-\tfrac{1}{2}\sigma)(\ln\sigma)^2- \\ -(1+\sigma)\ln(1+\sigma)-\tfrac{1}{6}(1+\sigma)\pi^2+\sigma S_\sigma. \quad (47)$$

When $\sigma = 1$, these reduce to the equivalent results obtained by Glauert and Lighthill (3).

Proceeding in this way accuracy to any inverse power of β can be achieved but the integrations clearly become extremely complicated. In the case of air we find, following Glauert and Lighthill, that the results obtained up to this stage are sufficient to compute the rate of heat transfer for $\nu x/Ua^2 \geqslant 100$. In the skin friction case the frictional drag τ, calculated with three terms in the series for f, was still in agreement at $\nu x/Ua^2 = 10$ with the result suggested by the Pohlhausen method. It therefore appears probable that these first three terms are sufficient to estimate Q for $\nu x/Ua^2 \geqslant 10$ for the flow of air past a heated cylinder.

The local rate of heat transfer, per unit length of the cylinder, is now given by

$$\frac{Q}{k(T_1-T_0)} = 2\pi a\left(\frac{\partial g}{\partial r}\right)_{r=a} = 4\pi(\xi g')_{\xi=e^{-\beta}} \sim 4\pi\xi\left\{\sum_{n=0}^{\infty}\frac{g_n'}{\beta^n}\right\}_{\xi=e^{-\beta}}. \quad (48)$$

As $\xi \to 0$, $\xi g_n' \to d_n$, and hence

$$\frac{Q}{k(T_1-T_0)} \sim 4\pi\sum_{n=0}^{\infty}\frac{d_n}{\beta^n}. \quad (49)$$

The calculated values of d_1, d_2, d_3 show finally that

$$\frac{Q}{k(T_1-T_0)} = 4\pi\left[\frac{1}{\beta}+\frac{(\gamma+\ln\sigma)}{\beta^2}+ \right. \\ \left. +\frac{\{\gamma^2+(\sigma+2\gamma)\ln\sigma+(1-\tfrac{1}{2}\sigma)(\ln\sigma)^2-(1+\sigma)\ln(1+\sigma)-\tfrac{1}{6}(1+\sigma)\pi^2+\sigma S_\sigma\}}{\beta^3}\right]+ \\ +O\left(\frac{1}{\beta^4}\right). \quad (50)$$

† S_σ is tabulated in the range $-1 \leqslant \sigma \leqslant 5$ (see E. O. Powell, *Phil. Mag.* **34** (1943), 600).

It is also of considerable interest to note that at sufficiently large values of x (or β), Q is independent of σ, so that, using (50) and (4), the value of the ratio

$$R_H = \frac{Q \text{ at downstream distance } x \text{ for a cylinder}}{Q \text{ at downstream distance } x \text{ for a flat plate}} \sim \frac{4\pi\beta^{-1}}{0{\cdot}664\pi\sigma^{\frac{1}{2}}(Ua^2/\nu x)^{\frac{1}{2}}};$$

the value of the corresponding quantity of skin-friction, using the Glauert–Lighthill asymptotic solution and the Blasius flat plate solution, is

$$R_D = \frac{\tau \text{ at downstream distance } x \text{ for a cylinder}}{\tau \text{ at downstream distance } x \text{ for a flat plate}} \sim \frac{4\pi\beta^{-1}}{0{\cdot}664\pi(Ua^2/\nu x)^{\frac{1}{2}}}.$$

Hence, for large values of $\nu x/Ua^2$,

$$R_H/R_D = \sigma^{-\frac{1}{2}}, \tag{51}$$

while at very small values of $\nu x/Ua^2$, this is, of course, unity. These results are of importance in calculating particular cases, as discussed in section 5.

4. An approximate solution for intermediate downstream distances

Lighthill (**8**), in treating the heated flat plate problem, found that a linear approximation to the exact velocity profile in the neighbourhood of the surface led to a reasonably accurate result for local rate of heat transfer Q in certain cases of the velocity form $U = cx^m$, but in other cases, when the exact velocity curves deviate considerably from the tangent at the origin, a considerable degree of error ensued in the calculated values of Q. However, this error was reduced to very small proportions by Davies and Bourne (**4**), using power law representations of the exact profiles. This suggests that an approximate method based on similar premisses is likely to yield sufficiently accurate results here and we show in section 5 that this is so.

Using the continuity equation (7) and the Pohlhausen velocity profile (5) we first write

$$\frac{\partial\psi}{\partial\eta} = \frac{a^2U}{\alpha}\eta\ln\eta, \tag{52}$$

where $\eta = r/a$. Integration yields

$$\psi = \frac{a^2U}{4\alpha}\{(2\ln\eta - 1)\eta^2 + 1\}, \tag{53}$$

so that $\psi = 0$ when $\eta = 1$. The temperature equation (10) in von Mises form then becomes

$$\frac{\partial T}{\partial x} = \frac{\kappa a^2U}{\alpha}\frac{\partial}{\partial\psi}\left\{(\eta^2\ln\eta)\frac{\partial T}{\partial\psi}\right\}. \tag{54}$$

In order to proceed further and apply the method of sources, used

successfully in the heated flat plate problem by Davies and Bourne (4), we write

$$(2\ln\eta-1)\eta^2+1 = X(\eta), \qquad \eta^2\ln\eta = Y(\eta), \tag{55}$$

and suppose that a good power law representation of the variation of Y with X can be constructed in the form

$$Y = BX^t, \tag{56}$$

where B and t are constants. In calculating Q at a given downstream distance x_1 the numerical values of B and t are chosen to give a good fit over the range of η corresponding to the thickness of the boundary layer at this x_1 value. This procedure is then repeated for other values of x_1; the numerical details and implications in the case of air flow over the cylinder are discussed in section 5. Substitution of (55) and (56) into (54) now gives

$$\frac{\partial T}{\partial x} = (4^t Ba^{2(1-t)}U^{(1-t)}\kappa)\alpha^{(t-1)}\frac{\partial}{\partial\psi}\left(\psi^t\frac{\partial T}{\partial\psi}\right). \tag{57}$$

Equation (57) next reduces to the form of the basic equation (11) of (4), if we write

$$\int_0^x \{\alpha(x)\}^{(t-1)}\,dx = X', \tag{58}$$

where $\alpha(x)$ is given numerically by the Glauert–Lighthill results. We now have

$$\frac{\partial T}{\partial X'} = c\frac{\partial}{\partial\psi}\left(\psi^t\frac{\partial T}{\partial\psi}\right), \tag{59}$$

where

$$c = 4^t Ba^{2(1-t)}U^{(1-t)}\kappa.$$

Suppose now that a continuous uniform circular source, of radius a, normal to the generators of the cylinder, is stationed on the surface of the cylinder, $\psi = 0$, at $x = x_0$, and emits Q units of heat per unit of time. The analysis of the flat plate approximate solution (4) follows with Q replaced by $Q/2\pi a$ and the distribution of local rate of heat transfer may be calculated for *any prescribed* downstream distribution of surface temperature. The result, when the surface temperature of the cylinder is independent of x, is

$$\frac{Q}{k(T_1-T_0)} = 2^{(2+t)/(2-t)}\sin\left(\frac{\pi}{2-t}\right)\Gamma\left(\frac{1}{2-t}\right)(2-t)^{t/(2-t)}B^{1/(2-t)}\times$$

$$\times\left\{\alpha\left(\frac{\nu x}{Ua^2}\right)\right\}^{(t-1)}\left\{\int_0^{\nu x/Ua^2}\alpha^{(t-1)}\,dx'\right\}^{(t-1)/(2-t)}\sigma^{(1-t)/(2-t)}, \tag{60}$$

where

$$x' = \nu x/Ua^2.$$

5. Calculated distribution of local rate of heat transfer in air

To illustrate numerically the formal results obtained in the previous sections, we now consider the case of air flow over the cylinder, for which

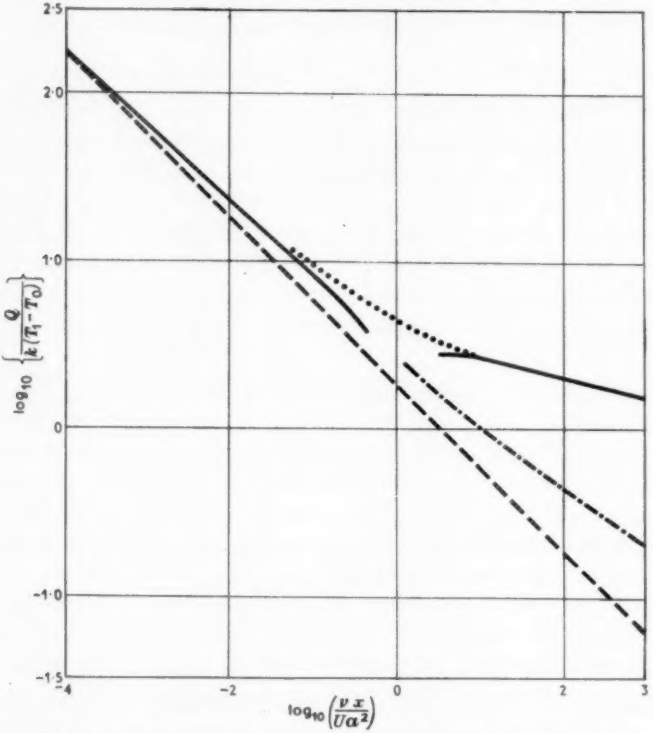

FIG. 1. Distribution of Q, local rate of heat transfer, along the surface of a circular cylinder, heated to a constant temperature and positioned with its axis parallel to a uniform stream of air. Q, rate of heat transfer per unit length of cylinder; k, thermal conductivity; (T_1-T_0), temperature difference between cylinder and main stream; ν, kinematic viscosity; x, downstream distance; U, main stream velocity; a, radius of cylinder; — — — — values of Q based on flat plate solution; —·—·— values of Q based on an exact representation of conditions of flow near the surface; ——— values of Q based on the Seban–Bond–Kelly solution (on the left) and the asymptotic solution (on the right); ..... values of Q based on the power law approximate solution

we take $\sigma = 0{\cdot}72$. All the results discussed in this section are exhibited graphically in Fig. 1, together with the corresponding results for a flat plate.

As in the skin-friction problem, the probable limit of reliability of the Seban–Bond–Kelly temperature solution is at a value of $\nu x/Ua^2$ of about

0·04. The limit of reliability of the asymptotic series solution is probably at about $\nu x/Ua^2 = 100$, where the third term in the series is about 9 per cent of the first two terms together (taking $\sigma = 0{\cdot}72$). At $\nu x/Ua^2 = 10$, it is about 28 per cent of the first two taken together; these results are similar to those discussed by Glauert and Lighthill. However, since σ is of the order of one for air and, since the Glauert–Lighthill asymptotic solution appears to be a good approximation to the true skin-friction variation up to about $\nu x/Ua^2 = 10$, it is probable that the asymptotic series solution (50) for the temperature problem is a good approximation to the true values of Q up to about $\nu x/Ua^2 = 10$.

The approximate solution described in section 4 is now used to bridge the gap, $0{\cdot}04 < \nu x/Ua^2 < 10$, between the results computed from the Seban–Bond–Kelly series and the asymptotic series. The computation of $Q(x)$ by this approximate method involves (i) the evaluation of the parameters B and t, and (ii) the numerical evaluation of $\int_0^{\nu x/Ua^2} \alpha^{(t-1)}\,dx'$, using the distribution of α given numerically by Glauert and Lighthill (**3**), and Q has been evaluated at several points on this 'bridge', the same procedure of power law fitting being used in each case. At a given intermediate value of $\nu x/Ua^2$, the appropriate α value is noted from the Glauert–Lighthill results, and the thickness of the momentum boundary layer δ evaluated using (5). The thickness of the temperature boundary layer δ_H, for $\sigma = 0{\cdot}72$, is then given approximately by the boundary layer equations (1) and (2) to be $\delta/(0{\cdot}72)^{\frac{1}{3}}$. The values of $X(\eta)$ and $Y(\eta)$, introduced in section 4, are computed at intervals up to $\eta_T = 1+\delta/a$, and in the uniform stream region above η_T the values of $X(\eta_T)+2\alpha(\eta^2-\eta_T^2)$ and $\eta^2\alpha$, which correspond to X and Y respectively when $y \geqslant \delta$, are computed from $\eta = 1+\delta/a$ to $\eta = 1+\delta_H/a$. Values of B and t in the power law $Y = BX^t$ are now chosen to obtain zero deviation from the exact $Y = f(X)$ relation at the mid-point of δ_H and to minimize the deviations elsewhere. In this way the best fit is obtained over the central bulk of the boundary layer (where most of the flux of heat takes place). The deviations are small, being 4 per cent at most over 95 per cent of the range at the smaller intermediate values and 10 per cent at the larger values. Numerical values of B and t appropriate to a given $\nu x/Ua^2$ in the intermediate range do not of course yield a good approximate description of $Y = f(X)$ at points far upstream. However, the calculated value of Q at a chosen distance x is likely to depend critically on the distribution of flow properties in the neighbourhood of x and is not so dependent on conditions far upstream, the main contribution to the temperature near the surface coming from the sources in the immediate upstream neighbourhood of x. The discontinuity in the slope, $\partial u/\partial y$,

associated with the profile (5) at $y = \delta$ may also be considered an objectionable feature, but, as noted by Glauert and Lighthill, this does not necessarily lead to serious error in Pohlhausen treatments. The error is likely to be small for values of σ only slightly less than 1·0 (as in the case of air, considered in this section), since most of the heat flux across a plane normal to the surface will take place in the region $y < \delta$. In the case of fluids, whose Prandtl numbers are in excess of unity, this difficulty does not enter at all, as $\delta_H < \delta$.

We note that this approximate treatment, which has the advantage of involving fairly simple computation, is shown to lead to reasonable numerical results (probably to within 5 per cent of the true values) for the following reasons:

(i) the computed values of Q, based on this power law method, are found to be within 3 per cent of the Seban–Bond–Kelly results for the smaller values of $\nu x/Ua^2$;

(ii) these values of Q run smoothly into the numerical results given by the asymptotic series solution at very large values of $\nu x/Ua^2$;

(iii) all the values computed in the intermediate range of $\nu x/Ua^2$ are found to be within 5 per cent of the results suggested by considering the ratio R_H/R_D defined in section 3. The analysis described in section 3 shows that the numerical results for the ratio R_H/R_D are likely to vary between 1·0, at small $\nu x/Ua^2$ values, up to 1·12 (for $\sigma = 0{\cdot}72$), at very large $\nu x/Ua^2$ values. At $\nu x/Ua^2 = 100$ the asymptotic series solution for heat and skin friction shows that $R_H/R_D = 1{\cdot}06$, so that over the intermediate range of $\nu x/Ua^2$ the computed values of R_H/R_D should lie between about 1·01 and 1·05. This serves as a useful check on the numerical results given by our approximate method for R_H/R_D and we find that they are all within about 5 per cent of this small range of probable values. Consideration of (iii) above could, of course, be used to deduce approximate values of the interpolation function needed. The power law analysis, however, is capable of application to any prescribed downstream distribution of surface temperature, and by its use formulae describing the temperature distribution in the airflow can easily be derived; the dependence of Q on σ is also conveniently deduced by its use.

In the case of the flat plate problem Q depends on $\sigma^{\frac{1}{3}}$ at all values of $\nu x/Ua^2$. The effect of curvature, however, on this dependence is found to be considerable. At small $\nu x/Ua^2$ values Q on the cylinder is, of course, proportional to $\sigma^{\frac{1}{3}}$ as in the flat plate problem, but the index of σ decreases as downstream distance increases. This index is given by $(1-t)/(2-t)$ in the analysis of section 4 (equation (60)); e.g. at $\nu x/Ua^2 = 0{\cdot}003$, 0·06, 0·3, and 1·6, $(1-t)/(2-t)$ is given by the power law results, for air, to be 0·31,

0·27, 0·21, and 0·18, while at $\nu x/Ua^2 = \infty$ it is zero. These numerical results are likely to be approximately true for fluids whose Prandtl numbers are near 0·72.

Finally, it is of some interest to calculate $Q(x)$ over the whole range of $\nu x/Ua^2$ by the method of section 4, using values of the parameters B and t which ensure an exact representation of conditions near the surface, as in Lighthill's linear approximation for the flat plate problem. The increasingly logarithmic behaviour of the velocity profile in the cylinder case, as x increases, results in a rapid divergence from the tangent linear approximation to the profile near the surface and very good results cannot be expected in this context. As $r \to a$ ($\eta \to 1$), it is easily seen, using (55) and (56), that $t \to \frac{1}{2}$ and $B \to 1/\sqrt{2}$. When $\nu x/Ua^2 = 0{\cdot}0001$, the value of Q calculated in this way is 2 per cent greater than that given by the exact flat plate solution and is in agreement with our approximate solution. At $\nu x/Ua^2 = 0{\cdot}001$, Q is in excess by 4 per cent of the exact flat plate value, whereas the Seban–Bond–Kelly solution (and also our approximate solution at this stage) leads to an excess of 7 per cent; this is also the result obtained in the skin friction case. The results based on this approximation are seen from Fig. 1 to be seriously in error at larger downstream distances. At $\nu x/Ua^2 = 100$, the result, though an improvement on the flat plate solution, is nevertheless still considerably below the true value calculated from the asymptotic solution.

The effect of curvature on Q is clearly seen in Fig. 1 and shows, for instance, that the numerical value of Q calculated from the asymptotic solution, at $\nu x/Ua^2 = 100$, is ten times the flat plate value.

Acknowledgement

One of the authors, D. E. Bourne, gratefully acknowledges the receipt of a maintenance grant from the Department of Scientific and Industrial Research during the course of this work.

APPENDIX

In section 3 we made use of the result that, as $\xi \to 0$,

$$\int_{\infty}^{\xi} e^{-\sigma t}\,\mathrm{Ei}(-t)t^{-1}\,dt \sim \tfrac{1}{2}(\gamma+\ln\xi)^2+\tfrac{1}{24}\pi^2-S_\sigma, \qquad (61)$$

where $S_\sigma = \dfrac{\sigma}{1^2}-\dfrac{\sigma^2}{2^2}+\dfrac{\sigma^3}{3^2}-\ldots$. To derive (61) we first integrate the left-hand side by parts,

$$\int_{\infty}^{\xi} e^{-\sigma t}\,\mathrm{Ei}(-t)t^{-1}\,dt = \tfrac{1}{2}\{\mathrm{Ei}(-\xi)\}^2 e^{(1-\sigma)\xi}-\tfrac{1}{2}(1-\sigma)\int_{\infty}^{\xi}\{\mathrm{Ei}(-t)\}^2 e^{(1-\sigma)t}\,dt. \qquad (62)$$

Hence as $\xi \to 0$,
$$\int_{\infty}^{\xi} e^{-\sigma t}\,\mathrm{Ei}(-t)t^{-1}\,dt \sim \tfrac{1}{2}(\gamma+\ln\xi)^2+I, \tag{63}$$

where $I = \frac{1}{2}(1-\sigma)\int_0^{\infty}\{\mathrm{Ei}(-t)\}^2 e^{(1-\sigma)t}\,dt$ and may be shown to be convergent for $\sigma \geqslant -1$. Expanding the exponential term in I and integrating by parts yields

$$I = \tfrac{1}{2}(1-\sigma)\int_0^{\infty}\sum_{r=0}^{\infty}\frac{(1-\sigma)^r}{r!}t^r\{\mathrm{Ei}(-t)\}^2\,dt = -\int_0^{\infty}\sum_{r=0}^{\infty}\frac{(1-\sigma)^{r+1}t^{r+1}e^{-t}\,\mathrm{Ei}(-t)\,dt}{(r+1)!\,t}.$$

Hence

$$\begin{aligned} I &= -\int_0^{\infty}\{e^{(1-\sigma)t}-1\}t^{-1}e^{-t}\,\mathrm{Ei}(-t)\,dt \\ &= -\lim_{\substack{X\to\infty\\ x\to 0}}\int_x^X\{e^{-\sigma t}t^{-1}\,\mathrm{Ei}(-t)-e^{-t}t^{-1}\,\mathrm{Ei}(-t)\}\,dt \\ &= -\lim_{\substack{X\to\infty\\ x\to 0}}\int_x^X\sum_{r=0}^{\infty}\left\{\frac{(-\sigma)^{r+1}t^r\,\mathrm{Ei}(-t)}{(r+1)!}-\frac{(-1)^{r+1}t^r\,\mathrm{Ei}(-t)}{(r+1)!}\right\}dt. \end{aligned}$$

Now
$$\int_0^{\infty}\frac{(-\sigma)^{r+1}t^r\,\mathrm{Ei}(-t)\,dt}{(r+1)!} = -\frac{(-\sigma)^{(r+1)}}{(r+1)^2},$$

by repeated integration by parts. Hence we find that

$$I = \sum_{r=0}^{\infty}\left\{-\frac{(-1)^{r+1}}{(r+1)^2}+\frac{(-\sigma)^{r+1}}{(r+1)^2}\right\} = \frac{\pi^2}{12}-S_\sigma, \tag{64}$$

and the required result (61) follows. We note that the result (42), quoted by Glauert and Lighthill, follows from (61) as the special case $\sigma = 0$.

REFERENCES

1. R. A. Seban and R. Bond, *J. Aero. Sci.* **18** (1951) 671.
2. H. R. Kelly, ibid. **21** (1954) 634.
3. M. B. Glauert and M. J. Lighthill, *Proc. Roy. Soc.* A, **230** (1955) 188.
4. D. R. Davies and D. E. Bourne, *Quart. J. Mech. App. Math.* **9** (1956) 457.
5. S. Goldstein (Ed.), *Modern Developments in Fluid Dynamics* (Oxford, 1938).
6. K. Stewartson, *Quart. Appl. Math.* **13** (1955) 113.
7. G. H. Hardy, *Divergent Series* (Oxford, 1949).
8. M. J. Lighthill, *Proc. Roy. Soc.* A, **202** (1950) 359.

HYPO-ELASTIC POTENTIALS

By J. L. ERICKSEN

(*Applied Mathematics Branch, Mechanics Division, U.S. Naval Research Laboratory, Washington 25, D.C.*)

[Received 17 January 1957]

SUMMARY

For some hypo-elastic materials it is possible to introduce a scalar potential analogous to the elastic potential or strain energy function of elasticity theory. Conditions necessary and sufficient for the existence of such a potential are derived.

1. HYPO-ELASTICITY, as defined by Truesdell (**1, 2, 3**), is the theory of materials with constitutive equations given by relations of the form

$$\mathring{t}_{ij} \equiv \dot{t}_{ij} - t_{ik} v_{j,k} - t_{jk} v_{i,k} + t_{ij} v_{k,k} = A_{ijkm} d_{km}$$

in cartesian tensor notation. Here t_{ij} is the stress tensor, v_k the velocity vector, $2d_{km} = v_{k,m} + v_{m,k}$, A_{ijkm} is a tensor invariant of t_{ij} such that $A_{ijkm} = A_{jikm} = A_{ijmk}$, and the 'dot' denotes the material derivative. For our purposes, it is slightly more convenient to use an equivalent formulation which has been emphasized by Noll (**4**, section 14) and Thomas (**5**, **6**), namely

$$\frac{Dt_{ij}}{dt} \equiv \dot{t}_{ij} - t_{ik}\omega_{jk} - t_{jk}\omega_{ik} = B_{ijkm} d_{km}, \tag{1}$$

where $2\omega_{ij} = v_{i,j} - v_{j,i}$ and B_{ijkm} is a tensor invariant of t_{ij} with the same symmetry as A_{ijkm}. We assume that B_{ijkm} is a continuously differentiable function of t_{pq} in some region R of stress values. Also, in R, B_{ijkm} is required to possess an inverse C_{ijkm}, which is a tensor invariant of stress with the same symmetry as B_{ijkm} such that

$$2C_{ijkm} B_{kmrs} = 2B_{ijkm} C_{kmrs} = \delta_{ir}\delta_{js} + \delta_{is}\delta_{jr}. \tag{2}$$

It exists if and only if $Dt_{ij}/dt = 0$ implies $d_{ij} = 0$. It is to be understood that values of t_{ij} not in R are henceforth excluded.

Our purpose is to characterize the class of hypo-elastic materials for which there exist scalar invariants ϕ and ψ of t_{ij} such that the equations

$$t_{ij} d_{ij} = \phi\dot{\psi} \tag{3}$$

hold whenever t_{ij} and $v_{i,j}$ satisfy (1). When ϕ and ψ exist, we call ψ a *hypo-elastic potential*. Thomas (**7**, **8**) has considered equations similar to but not identical with (3).

Noll (**4**, section 15) has shown that hypo-elasticity includes as a special case the more familiar theory of elasticity for isotropic materials which

assumes that stress is a function of strain, derivable from a scalar strain energy function. For the materials described by both theories, (3) holds; ϕ can be taken to be the mass density and ψ the strain energy per unit mass, these being expressed as functions of stress.

2. Any scalar invariant of t_{ij} is expressible as a function of the three invariants $\qquad I_1 \equiv t_{ii}, \qquad I_2 \equiv t_{ij}t_{ij}, \qquad I_3 \equiv t_{ij}t_{jk}t_{ki}.$

It is easily verified that

$$\dot{I}_N = \frac{\partial I_N}{\partial t_{ij}}\dot{t}_{ij} = \frac{\partial I_N}{\partial t_{ij}}\frac{Dt_{ij}}{dt} \quad (N = 1, 2, 3),$$

from which it follows that (3) can be written in the form

$$t_{km}\,d_{km} = \phi\dot{\psi} = \phi\,\frac{\partial\psi}{\partial t_{ij}}\,\dot{t}_{ij} = \phi\,\frac{\partial\psi}{\partial t_{ij}}\,\frac{Dt_{ij}}{dt} = \phi\,\frac{\partial\psi}{\partial t_{ij}}\,B_{ijkm}\,d_{km}. \tag{4}$$

In order that† $(4)_4$ holds for all t_{ij} and d_{ij} consistent with (1), it is necessary and sufficient that

$$t_{km} = \phi\,\frac{\partial\psi}{\partial t_{ij}}\,B_{ijkm}. \tag{5}$$

To see this, we note that when the velocity gradients are specified arbitrarily as continuous functions of the time t, (1) becomes a system of first order ordinary differential equations for determining $t_{ij}(t)$. There will exist a unique solution taking on arbitrarily prescribed values at any given time t_0. The velocity gradients can be chosen so that the symmetric tensor d_{ij} takes on any desired value at t_0, so t_{ij} and d_{ij} can be assigned arbitrarily at t_0. Thus $(4)_4$ must be an identity in t_{km} and d_{km}.

From (2) and (5), we have‡

$$\phi\,\frac{\partial\psi}{\partial t_{ij}} = D_{ij}, \tag{6}$$

where $$D_{ij} \equiv t_{km}C_{kmij} \tag{7}$$

is a tensor invariant of the stress. As such, it is expressible in the form§

$$D_{ij} = A_0\delta_{ij} + A_1 t_{ij} + A_2 t_{ik}t_{kj}, \tag{8}$$

where the A's are scalar invariants of t_{ij}. Equation (8) follows from (7) whether or not a hypo-elastic potential exists.

3. We first obtain formal conditions which are necessary and sufficient for

† $(4)_4$ means the fourth equation in (4).

‡ In forming derivatives with respect to t_{ij}, we replace t_{ij} by its equivalent $\frac{1}{2}(t_{ij}+t_{ji})$ in the function differentiated, so that $\partial/\partial t_{ij} = \partial/\partial t_{ji}$.

§ For the case where D_{ij} is a polynomial in the stress, this follows as a special case of a result due to Weitzenböck (**9**). The A's are then polynomials in I_1, I_2, and I_3. For more general functions, it follows as a special case of the result given in (**10**, section 40), which is derived assuming no continuity. References to other proofs are given in (**11**, section 6).

the existence of a hypo-elastic potential. In N dimensions, the equations

$$\left(\frac{\partial v_\alpha}{\partial y^\beta}-\frac{\partial v_\beta}{\partial y^\alpha}\right)v_\gamma+\left(\frac{\partial v_\beta}{\partial y^\gamma}-\frac{\partial v_\gamma}{\partial y^\beta}\right)v_\alpha+\left(\frac{\partial v_\gamma}{\partial y^\alpha}-\frac{\partial v_\alpha}{\partial y^\gamma}\right)v_\beta=0 \quad (\alpha,\beta,\gamma=1,\ldots,N) \quad (9)$$

are satisfied if and only if the vector field $v_\alpha(y^\beta)$ is proportional to a gradient, $v_\alpha=\phi\,\partial\psi/\partial y^\beta$, (9) being the integrability conditions for the latter system. Regarding D_{ij} as a vector in six-dimensional stress space, we obtain from (9)

$$\left(\frac{\partial D_{ij}}{\partial t_{km}}-\frac{\partial D_{km}}{\partial t_{ij}}\right)D_{rs}+\left(\frac{\partial D_{km}}{\partial t_{rs}}-\frac{\partial D_{rs}}{\partial t_{km}}\right)D_{ij}+\left(\frac{\partial D_{rs}}{\partial t_{ij}}-\frac{\partial D_{ij}}{\partial t_{rs}}\right)D_{km}=0, \quad (10)$$

as necessary and sufficient conditions for the existence of functions ϕ and ψ satisfying (6). To conclude that a hypo-elastic potential exists if and only if (10) is satisfied, we must show that the solutions ϕ and ψ of (6) are scalar invariants of t_{ij}. Formally, we must show that, for arbitrary t_{ij},

$$\phi(t^*_{ij})=\phi(t_{ij}), \qquad \psi(t^*_{ij})=\psi(t_{ij})$$

whenever t^*_{ij} is related to t_{ij} by an orthogonal transformation:

$$t^*_{ij}=t_{km}A_{ki}A_{mj}, \qquad A_{ki}A_{kj}=\delta_{ij}.$$

We first consider ψ. For infinitesimal transformations, we may set $A_{ij}=\delta_{ij}+\Omega_{ij}=\delta_{ij}-\Omega_{ji}$ and linearize $\psi(t^*_{ij})-\psi(t_{ij})$ with respect to Ω_{ij}, obtaining

$$\begin{aligned}\psi(t^*_{ij})-\psi(t_{ij})&=\frac{\partial\psi}{\partial t_{ij}}(t^*_{ij}-t_{ij})\\&=\frac{\partial\psi}{\partial t_{ij}}(t_{im}\Omega_{mj}+t_{jm}\Omega_{mi})=2\,\frac{\partial\psi}{\partial t_{ij}}t_{im}\Omega_{mj}\\&=E_{mj}\Omega_{mj},\end{aligned}$$

where

$$E_{ij}=\frac{\partial\psi}{\partial t_{kj}}t_{ki}-\frac{\partial\psi}{\partial t_{ki}}t_{kj}.$$

Using (8), one can easily show that $E_{ij}\equiv 0$ when ψ is a solution of (6). The equations $E_{ij}=0$ constitute a system of three independent linear first order partial differential equations for ψ. A routine calculation shows that a general solution is an arbitrary function of the functions I_N introduced earlier, from which it follows that ψ is a scalar invariant of t_{ij}. As a consequence, $\partial\psi/\partial t_{ij}$ is a tensor invariant of t_{ij}. From (6),

$$\dot{\phi}=\left(\frac{\partial\psi}{\partial t_{ij}}\frac{\partial\psi}{\partial t_{ij}}\right)^{-1}\frac{\partial\psi}{\partial t_{km}}D_{km},$$

from which it is clear that ϕ is also a scalar invariant of t_{ij}. *Thus a hypo-elastic potential exists if and only if D_{ij} satisfies* (10).

It should be noted that D_{ij} does not determine ϕ and ψ uniquely. We have

$$\phi \frac{\partial \psi}{\partial t_{ij}} = \phi' \frac{\partial \psi'}{\partial t^{ij}}$$

if and only if $$\phi = \phi' \left(\frac{dF}{d\psi'}\right)^{-1}, \qquad \psi = F(\psi'),$$

where $F(\psi')$ is any continuously differentiable function of ψ' such that

$$dF/d\psi' \neq 0.$$

4. We now obtain a characterization which seems to have greater intuitive appeal. Consider any material for which a hypo-elastic potential exists, so that (3) and (5) hold. Suppose a particle P is, at some time t', subject to a non-zero stress t'_{ij} and that the neighbouring material is deformed in such a way that $t_{ij}\, d_{ij} = 0$ at P. From (3), either $\phi = 0$ or ψ remains constant at P. From (5), $\phi \neq 0$ in the neighbourhood of the non-zero stress t'_{ij}. Furthermore, from (5), not all the derivatives $\partial\psi/\partial t_{ij}$ vanish at t'_{ij}, so the equation $\psi(t_{ij}) = \psi(t'_{ij})$ cannot hold for all t_{ij} in the neighbourhood of t'_{ij}. Thus, when (3) holds, there exist, in the neighbourhood of every non-zero stress, stresses which cannot be attained by continuously deforming the material in such a way that $t_{ij}\, d_{ij} = 0$.

Whenever (1) holds, we have

$$t_{ij}\, d_{ij} = D_{ij} \frac{Dt_{ij}}{dt}, \tag{11}$$

where D_{ij} is given by (7). Using (8) and (11), we obtain

$$t_{ij}\, d_{ij} = D_{ij}\, \dot{t}_{ij}.$$

If we choose the t_{ij} to be functions of the time satisfying the Pfaffian equation

$$D_{ij}\, \dot{t}_{ij} = 0, \tag{12}$$

we may assign the quantities $\omega_{ij} = -\omega_{ij}$ arbitrarily as functions of time and use (1) to calculate d_{ij}. Whatever be the choice of ω_{ij}, we have, from (12), $t_{ij}\, d_{ij} = 0$. In (12), the D_{ij} are continuously differentiable functions of t_{ij} which, by (2) and (7), all vanish if and only if $t_{ij} = 0$. In some neighbourhood of an arbitrarily prescribed non-zero stress, we can choose coordinates so that $D_{11} \neq 0$. Then (12) becomes

$$\dot{t}_{11} + F_{12}\dot{t}_{12} + F_{13}\dot{t}_{13} + F_{23}\dot{t}_{23} + F_{22}\dot{t}_{22} + F_{33}\dot{t}_{33} = 0, \tag{13}$$

where the F's, given by

$$\begin{aligned} F_{ij} &\equiv D_{ij}/D_{11} \quad \text{when} \quad i = j \\ &\equiv 2D_{ij}/D_{11} \quad \text{when} \quad i \neq j, \end{aligned}$$

are continuously differentiable functions of stress in the region considered. In this region, we assume that, in every neighbourhood of each non-zero

stress t'_{ij}, there exists a stress which cannot be joined to t_{ij} by a solution of (13). Then, by a theorem due to Carathéodory (**12**), there exist, at least locally, functions $\alpha(t_{11}, t_{12}, t_{13}, t_{23}, t_{22}, t_{33})$ and $\beta(t_{11}, t_{12}, t_{13}, t_{23}, t_{22}, t_{33})$, where α is continuous and β continuously differentiable, such that

$$1 \equiv \alpha \frac{\partial \beta}{\partial t_{11}}, \qquad F_{ij} \equiv \alpha \frac{\partial \beta}{\partial t_{ij}} \quad (i \leqslant j,\ i+j > 2).$$

Setting $\phi = D_{11}\alpha$, $\psi = \beta\{t_{11}, \frac{1}{2}(t_{12}+t_{21}), \frac{1}{2}(t_{13}+t_{31}), \frac{1}{2}(t_{23}+t_{32}), t_{22}, t_{33}\}$, we obtain

$$D_{ij} \equiv \phi \frac{\partial \psi}{\partial t_{ij}}.$$

Our assumption thus implies the existence of solutions to (6). As noted above, a hypo-elastic potential exists when solutions to (6) exist.

To sum up, we have shown that, *for a hypo-elastic potential to exist, it is necessary and sufficient that, in every neighbourhood of each non-zero stress, there exist stresses which cannot be attained by continuously deforming the material in such a way that* $t_{ij}\, d_{ij} = 0$.

5. Results analogous to those derived here can be deduced for the situation obtained by replacing $t_{ij}\, d_{ij}$ by $M \equiv (t_{ij} - \frac{1}{3}t_{kk}\,\delta_{ij})\, d_{ij}$ in (3). These may be of interest in plasticity theories of the type discussed by Green (**13**, **14**), which involve different equations of the type (1) for loading ($M \geqslant 0$) and unloading ($M \leqslant 0$).

An analysis due to Caprioli (**15**) leads us to conjecture that if the constitutive equations imply that the work done by the stress in deforming any initially unstressed material volume is non-negative, whatever be the deformation, then a hypo-elastic potential exists and ϕ can be taken to be the mass density.

The constitutive equations (1) are not appropriate for incompressible materials, so our results are not directly applicable to them. It should be a simple matter to work out similar results for these, using the constitutive equations proposed by Noll (**4**, section 14).

REFERENCES

1. C. Truesdell, *Comm. Pure Appl. Math.* **8** (1955) 123–32.
2. —— *J. Rat. Mech. Anal.* **4** (1955) 83–133.
3. —— *J. Appl. Phys.* **27** (1956) 441–7.
4. W. Noll, *J. Rat. Mech. Anal.* **4** (1956) 3–81.
5. T. Y. Thomas, *Proc. Nat. Acad. Sci.* **41** (1955) 716–20.
6. —— ibid. 762–70.
7. —— ibid. **42** (1956) 603–8.
8. —— to appear in *J. Math. Phys.*

9. R. Weitzenböck, *Math. Z.* **10** (1921) 80–87.
10. R. S. Rivlin and J. L. Ericksen, *J. Rat. Mech. Anal.* **4** (1955) 323–425.
11. C. Truesdell, ibid. **1** (1952) 125–300.
12. C. Carathéodory, *Math. Annalen*, **67** (1909) 355–86.
13. A. E. Green, *Proc. Roy. Soc.* A, **234** (1956) 46–59.
14. —— *J. Rat. Mech. Anal.* **5** (1956) 725–34.
15. L. Caprioli, *Boll. Un. Mat. Ital.* (3) **10** (1955) 481–3.

DIFFUSION OF LOAD FROM A BOOM INTO A RECTANGULAR SHEET

By J. B. CALDWELL (*Admiralty Offices, Bath*)

[Received 13 December 1956]

SUMMARY

A solution is obtained for an elastic plane-stress problem in which load is applied to a finite rectangular sheet through a boom riveted to one of its longer edges. The other edges of the sheet are stiffened, and resistance to bending in the plane of the sheet is provided by an elastic restraint along the loaded edge. Using a stress function in Fourier series form, both the efficiency of the sheet under load and the maximum shear stress in the structure are obtained as the sums of infinite series from which the relative importance of the principal parameters of the problem can be deduced. It is shown that the flexibility of the elastic restraint and of the riveted connexion have significant effects on the efficiency of the sheet and on the magnitude of the maximum shear stress respectively.

1. Introduction

A SHIP'S superstructure, although it may extend over only part of the length of the vessel, must contribute in some measure to the flexural strength of the hull, by virtue of its attachment to the upper deck. The determination of the additional hull strength in way of the superstructure involves essentially the problem of diffusion into a finite rectangular sheet of load applied to one of its longer edges.

Fig. 1 illustrates the problem to be considered. A load P is applied at each end of a 'boom' (representing the upper deck) of constant cross-sectional area A, to which is attached a rectangular sheet (the vertical sides of the superstructure) of length l and breadth b. The boom and sheet may be of different materials, and are connected by a single line of rivets of known shear stiffness having constant diameter and spacing. Coordinate axes of x and y originate at the centre of the loaded edge of the sheet, and the edge $y = b$ is reinforced by a 'stringer' (the top of the superstructure) of constant cross-sectional area a. It is assumed that the shear and flexural stiffnesses of boom and stringer are negligible by comparison with those of the sheet in its own plane. At the edges $x = \pm\frac{1}{2}l$ transverse displacements of the sheet in the y-direction are prevented by 'stiffeners' (the end bulkheads of the superstructure) having infinite extensional stiffness but zero flexural stiffness. Lateral displacement of the structure is resisted by an 'elastic foundation' (representing transverse stiffening of the upper

deck) assumed to be continuous and of constant flexibility along the length of the sheet.

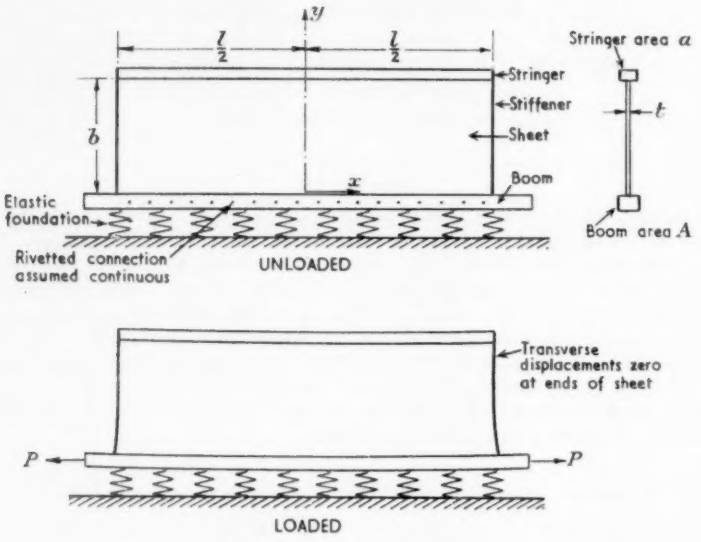

FIG. 1. Structure and loading

It is required to find firstly the proportion of the applied load carried by the sheet and stringer, and, secondly, the maximum stress in the structure. Of the various methods of analysis which have been developed for similar diffusion problems, neither the 'finite-stringer' method (**1**, **2**) nor the 'stringer-sheet' method (**3**, **4**, **5**) is applicable to this case; since the former assumes the sheet to be incapable of sustaining direct stress, and the latter implies that the sheet is infinitely stiff in the transverse direction and therefore cannot be used if the boundary conditions involve transverse stresses. Goodey (**5**) and Mitchell (**6**) have given more rigorous solutions using Fourier integrals to solve the equation governing plane stress distribution in semi-infinite sheets. These solutions, and most approximate methods, concern the diffusion problems where, unlike the present case, both structure and loading are symmetrical. Furthermore, since the dimensions of superstructures vary widely according to the type of ship, we require a solution that is applicable to sheets of finite dimensions.

In this paper a Fourier series form for the stress function is obtained which satisfies the plane stress equation and the conditions at the edges of the sheet. It is shown that the efficiency of sheet and stringer in carrying

applied load can readily be determined from a series involving explicit forms of the principal parameters of the problem. A simple relationship between the efficiency series and the magnitude of the peak shear stress in the structure is established, from which the conditions for a theoretically infinite shear stress are derived. Some general conclusions concerning the effects of flexibility of the elastic foundation and the boom-sheet connexion are given.

2. Notation

a	cross-sectional area of stringer.
A	cross-sectional area of boom.
b	breadth of sheet.
c	$= \cosh \alpha b$; $c_y = \cosh \alpha y$.
C	constant of integration.
E_b	elastic modulus of boom.
E_s	elastic modulus of sheet.
f	stress.
F	force in sheet and stringer.
k	flexibility of 'elastic foundation'.
l	length of sheet.
n	harmonic number (odd values).
p_x	force in stringer.
P_x	force in boom.
P	applied load.
Q, R, S	functions of β and λ. $U = Q/R$; $V = S/R$.
s	$= \sinh \alpha b$; $s_y = \sinh \alpha y$.
t	thickness of sheet.
T	function of β, λ and σ. $W = T/R$.
u, v	displacements in x, y directions.
x, y	coordinate directions.
α	$= n\pi/l$.
β	$= \alpha b = n\pi b/l$.
γ	$= \dfrac{1+\Lambda+\lambda}{1+\lambda}$.
Δ	determinant involving β, θ, λ, Λ, σ, and ψ.
η	efficiency.
θ	$= \dfrac{E_s}{b}\left(\dfrac{u-u_B}{f_{xy}}\right)_{x,0}$, rivet shear flexibility factor.
λ	$= a/bt$. $\lambda' = 1+2\lambda$.
Λ	$= A\mu/bt$.
μ	$= E_b/E_s$.

σ Poisson's ratio. $\sigma' = 1+\sigma$; $\sigma'' = \sigma-1$.
ϕ stress function.
ψ $= E_s kt/b$, foundation flexibility factor.

3. Stress function, stresses, and displacements

The stress function ϕ defining the stress distribution in the sheet must satisfy the plane stress equation

$$\nabla^4\phi = 0.$$

A suitable expression for ϕ is

$$\phi = \sum_{n=1}^{\infty} \left\{C_1 b^2\cosh\left(\frac{n\pi y}{l}\right)+C_2 b^2\sinh\left(\frac{n\pi y}{l}\right)+ \right. \\ \left. +C_3 by\cosh\left(\frac{n\pi y}{l}\right)+C_4 by\sinh\left(\frac{n\pi y}{l}\right)\right\}\cos\left(\frac{n\pi x}{l}\right), \quad (1)$$

in which b and l are breadth and length of the sheet respectively, $C_{1\ldots4}$ are constants to be determined, and n has odd values only. In what follows we will consider only the nth term of this series. Putting

$$\alpha = \frac{n\pi}{l}; \qquad \beta = \alpha b, \qquad \cosh\alpha y = c_y, \qquad \sinh\alpha y = s_y,$$

then the stresses and displacements at a point (x, y) in the sheet are

$$\left.\begin{aligned} f_x &= [C_1\beta^2 c_y+C_2\beta^2 s_y+C_3\beta(2s_y+\alpha y c_y)+C_4\beta(2c_y+\alpha y s_y)]\cos\alpha x \\ f_y &= -[C_1\beta^2 c_y+C_2\beta^2 s_y+C_3\alpha\beta y c_y+C_4\alpha\beta y s_y]\cos\alpha x \\ f_{xy} &= [C_1\beta^2 s_y+C_2\beta^2 c_y+C_3(\beta c_y+\alpha\beta y s_y)+C_4(\beta s_y+\alpha\beta y c_y)]\sin\alpha x \\ u &= E_s^{-1}[C_1\sigma'\beta b c_y+C_2\sigma'\beta b s_y+C_3(2bs_y+\sigma'\beta y c_y)+ \\ &\qquad +C_4(2bc_y+\sigma'\beta y s_y)]\sin\alpha x \\ v &= -E_s^{-1}[C_1\sigma'\beta b s_y+C_2\sigma'\beta b c_y+C_3(\sigma'\beta y s_y+\sigma'' b c_y)+ \\ &\qquad +C_4(\sigma'\beta y c_y+\sigma'' b s_y)]\cos\alpha x \end{aligned}\right\}. \quad (2)$$

The presence of edge stiffeners of infinite extensional but zero flexural stiffness requires that

$$f_x = v = 0, \quad \text{when} \quad x = \pm\tfrac{1}{2}l.$$

These conditions are satisfied by equations (2).

4. Derivation of the boundary conditions

The load P applied to the structure can be expressed in the form

$$P = \sum P_n\cos\left(\frac{n\pi x}{l}\right) = \sum_{n\,\text{odd}}^{\infty}\frac{4P}{\pi n}\sin(\tfrac{1}{2}n\pi)\cos\left(\frac{n\pi x}{l}\right), \quad (3)$$

and we shall deal with the nth term of this series. The first boundary condition is that the rate of increase of load P_x in the boom plus the load transferred to the sheet by shear in the connexion must equal the rate at which the applied load increases. That is, if t is the thickness of the sheet

$$\frac{dP_x}{dx}+t(f_{xy})_{x,0}=\frac{d}{dx}(P_n\cos\alpha x). \tag{4}$$

A relationship between the boom load P_x and the stresses in the sheet at $y=0$ is obtained by considering relative displacements of boom and sheet. If u_B and u are displacements of corresponding points in boom and sheet respectively, then due to the shear flexibility of the connexion, u_B will differ from u by an amount depending on the shear stress $(f_{xy})_{x,0}$ at that point. We assume that the rivet line may be replaced by an equivalent continuous connexion of constant shear flexibility. It is convenient to introduce a shear flexibility parameter θ, such that

$$\theta=\frac{E_s}{b}\left(\frac{u-u_B}{f_{xy}}\right)_{x,0}. \tag{5}$$

After rearrangement and differentiation equation (5) becomes

$$E_s\frac{du_B}{dx}=\left[E_s\frac{du}{dx}-\theta b\frac{df_{xy}}{dx}\right]_{x,0}$$

since θ is independent of x. If the elastic modulus of the boom is E_b, the load in the boom is

$$P_x=AE_b\frac{du_B}{dx};$$

and since for the sheet

$$E_s\left(\frac{du}{dx}\right)_{x,0}=(f_x-\sigma f_y)_{x,0},$$

the relationship between boom load and stresses in the sheet may be written

$$P_x=A\mu\left[f_x-\sigma f_y-\theta b\frac{df_{xy}}{dx}\right]_{x,0} \tag{6}$$

in which $\mu=E_b/E_s$. Substituting equation (6) in equation (4) the first boundary condition becomes

$$A\mu\frac{d}{dx}\left[f_x-\sigma f_y-\theta b\frac{df_{xy}}{dx}\right]_{x,0}+t(f_{xy})_{x,0}=-P_n\alpha\sin\alpha x. \tag{7}$$

The second boundary condition concerns transverse displacements of the structure under load. If the displacement of a unit length of the 'elastic foundation' (see Fig. 1) due to a unit load is k, then the transverse displacement $(v)_{x,0}$ of the structure is related to the transverse stress $(f_y)_{x,0}$ by the equation

$$(v)_{x,0}=kt(f_y)_{x,0}, \tag{8}$$

since the boom is assumed to have zero shear stiffness. We now introduce a dimensionless parameter ψ, termed the 'foundation flexibility factor' such that

$$\psi = \frac{E_s kt}{b}. \tag{9}$$

Equation (8) can then be written

$$(E_s v - \psi b f_y)_{x,0} = 0, \tag{10}$$

which is the second boundary condition.

At the edge $y = b$ of the sheet the transverse stress in the sheet must be zero since the flexural stiffness of the stringer is zero. The third boundary condition is therefore

$$(f_y)_{x,b} = 0. \tag{11}$$

The fourth condition is obtained by considering the equilibrium of an element of the stringer. If the direct force in the stringer is p_x, then

$$\frac{dp_x}{dx} - t(f_{xy})_{x,b} = 0. \tag{12}$$

The longitudinal strains in sheet and stringer at their connexion are equal (because of equation (11)) and hence if the materials of sheet and stringer have the same elastic modulus E_s, then

$$p_x = a(f_x)_{x,b}$$

where a is the cross-sectional area of the stringer. Using this relationship in equation (12), the fourth boundary condition is

$$a\frac{d}{dx}(f_x)_{x,b} - t(f_{xy})_{x,b} = 0. \tag{13}$$

It can be shown that the first and fourth conditions taken together satisfy the requirement that the total load in boom, sheet, and stringer at any section is equal to the applied load at that section.

5. Solution of the boundary equations

Equations (7), (10), (11), and (13) define the conditions to be satisfied by the stress function (1). By substituting equations (2) into these equations, the following are obtained

$$\left.\begin{aligned} C_1 A\mu\sigma'\beta^2 - C_2(A\mu\theta\beta^3 + bt\beta) - C_3(A\mu\theta\beta^2 + bt) + 2C_4 A\mu\beta &= P_x \\ C_1\psi\beta^2 - C_2\sigma'\beta - C_3\sigma'' &= 0 \\ C_1 c + C_2 s + C_3 c + C_4 s &= 0 \\ C_1\beta s + C_2\beta c + C_3\left[c + \beta s\left(1 + \frac{2a}{bt}\right)\right] + C_4\left[s + \beta c\left(1 + \frac{2a}{bt}\right)\right] &= 0 \end{aligned}\right\}, \tag{14}$$

in which $\quad c = \cosh\alpha b = \cosh\beta, \qquad s = \sinh\alpha b = \sinh\beta.$

We now introduce ratios Λ and λ defining the relative 'effective' areas of boom and stringer to that of the sheet by the equations

$$\Lambda = \frac{AE_b}{btE_s} = \frac{A\mu}{bt} \quad \text{and} \quad \lambda = \frac{a}{bt}.$$

Then, putting $\lambda' = 1+2\lambda$, equations (14) may be written

$$\begin{vmatrix} \Lambda\sigma'\beta^2 & -\beta(\Lambda\theta\beta^2+1) & -(\Lambda\theta\beta^2+1) & 2\Lambda\beta \\ \psi & -\sigma'/\beta & -\sigma''/\beta^2 & 0 \\ 1 & \tanh\beta & 1 & \tanh\beta \\ \beta\tanh\beta & \beta & 1+\lambda'\beta\tanh\beta & \tanh\beta+\lambda'\beta \end{vmatrix} \begin{vmatrix} C_1 \\ C_2 \\ C_3 \\ C_4 \end{vmatrix} = \begin{vmatrix} P_n/bt \\ 0 \\ 0 \\ 0 \end{vmatrix}$$

or

$$|\Delta||C| = |D|. \tag{15}$$

It can be shown that

$$\left.\begin{aligned} C_1 &= \frac{P_n}{\Delta bt}\left[\sigma'\lambda'\operatorname{sech}^2\beta - \sigma''\left(\frac{\tanh^2\beta}{\beta^2} + 2\lambda\frac{\tanh\beta}{\beta}\right)\right] \\ C_2 &= \frac{P_n}{\Delta bt}\left[\psi\lambda'\beta\operatorname{sech}^2\beta + \sigma''\left(\frac{\tanh\beta}{\beta^2} + \frac{\lambda'}{\beta} - \frac{\tanh^2\beta}{\beta}\right)\right] \\ C_3 &= \frac{P_n}{\Delta bt}\left[\sigma'\left(\tanh^2\beta - \lambda' - \frac{\tanh\beta}{\beta}\right) - \psi(\tanh^2\beta + 2\lambda\beta\tanh\beta)\right] \\ C_4 &= \frac{P_n}{\Delta bt}\left[\sigma'\left(2\lambda\tanh\beta + \frac{1}{\beta}\right) - \frac{\sigma''\operatorname{sech}^2\beta}{\beta} + \psi(\tanh\beta + \lambda'\beta\tanh^2\beta - \beta)\right] \end{aligned}\right\} \tag{16}$$

in which

$$\Delta = \psi[(\Lambda\theta\beta^2+1)Q + \Lambda S] + (\Lambda\theta\beta^2+1)R + \Lambda T \tag{17}$$

and

$$\left.\begin{aligned} Q &= \tanh^2\beta + 2\lambda\beta\tanh\beta - \lambda'\beta^2\operatorname{sech}^2\beta \\ R &= 2\left(\frac{\tanh\beta}{\beta} + \lambda' - \tanh^2\beta\right) \\ S &= 2(\beta\tanh\beta + \lambda'\beta^2\tanh^2\beta - \beta^2) \\ T &= \sigma'^2\lambda'\beta^2\operatorname{sech}^2\beta + 2\sigma'(3-\sigma)\lambda\beta\tanh\beta + 4 - \sigma''^2\tanh^2\beta \end{aligned}\right\}. \tag{18}$$

From equations (2), (16), (17), and (18) the stresses and displacements in the sheet due to the load $P_n\cos\alpha x$ can be calculated. By summing the effects of each component of the load series the resultant effect of a load P acting on the structure may be found.

The solution indicates that the stress distribution is dependent on the dimensionless parameters β, λ, Λ, θ, and ψ, and to a very small extent on Poisson's ratio σ. Particular cases of the general problem can easily be derived. Putting $\psi = 0$ corresponds to an inflexible 'elastic foundation' which prevents transverse displacements of the boom. This solution therefore applies to the symmetrical counterpart of the structure of Fig. 1, that is, where the sheet extends equally on each side of the boom. If $\psi = \infty$,

there is no restraint against lateral displacement. Both limiting cases are at present being studied experimentally. A further simplification follows from putting $\theta = 0$. This case corresponds to a continuous infinitely stiff connexion between boom and sheet, a condition more appropriate to a welded than a riveted connexion. Some consequences of this simplification are discussed in section 8.

6. Efficiency of sheet and stringer

If the sheet and stringer were fully effective under the load component $P_n \cos \alpha x$, then since the longitudinal strain in boom, sheet, and stringer would be equal, it follows that the longitudinal stress in sheet and stringer would be $(P_n \cos \alpha x)/(A\mu + bt + a)$. Hence the total load in sheet and stringer at a section distant x from the centre-line of the structure would be, in the fully effective condition:

$$F'_x = \frac{(bt+a)P_n \cos \alpha x}{A\mu + bt + a} = \frac{(1+\lambda)P_n \cos \alpha x}{1+\Lambda+\lambda} \tag{19}$$

in which Λ and λ are the area ratios previously defined. In general, however, the load is not distributed uniformly across the width of the sheet. The total load F_x in sheet and stringer can be obtained by integrating the shear flow at the junction of boom and sheet, viz.

$$F_x = -t \int_x^{\frac{1}{2}l} (f_{xy})_{x,0}\, dx, \tag{20}$$

and from equations (2) and (16) it follows that

$$\begin{aligned}(f_{xy})_{x,0} &= (C_2\beta^2 + C_3\beta)\sin \alpha x \\ &= \frac{-P_n\beta}{\Delta bt}\Big[\psi(\tanh^2\beta + 2\lambda\beta \tanh\beta - \lambda'\beta^2 \operatorname{sech}^2\beta) + \\ &\qquad + 2\left(\frac{\tanh\beta}{\beta} + \lambda' - \tanh^2\beta\right)\Big]\sin \alpha x.\end{aligned}$$

Using the functions Q and R defined by equations (18),

$$(f_{xy})_{x,0} = -\frac{P_n\beta}{bt}\left(\frac{\psi Q + R}{\Delta}\right)\sin \alpha x. \tag{21}$$

Then if the efficiency η_n of sheet and stringer under a load component $P_n \cos \alpha x$ is expressed as the ratio of the load F_x to the 'fully effective' load F'_x, we find that

$$\eta_n = \frac{F_x}{F'_x} = \frac{(P_n\beta/bt)(\psi Q + R)t \int_x^{\frac{1}{2}l} \sin \alpha x\, dx}{\Delta(1+\lambda)(1+\Lambda+\lambda)^{-1}P_n \cos \alpha x} = \gamma\eta'_n \tag{22}$$

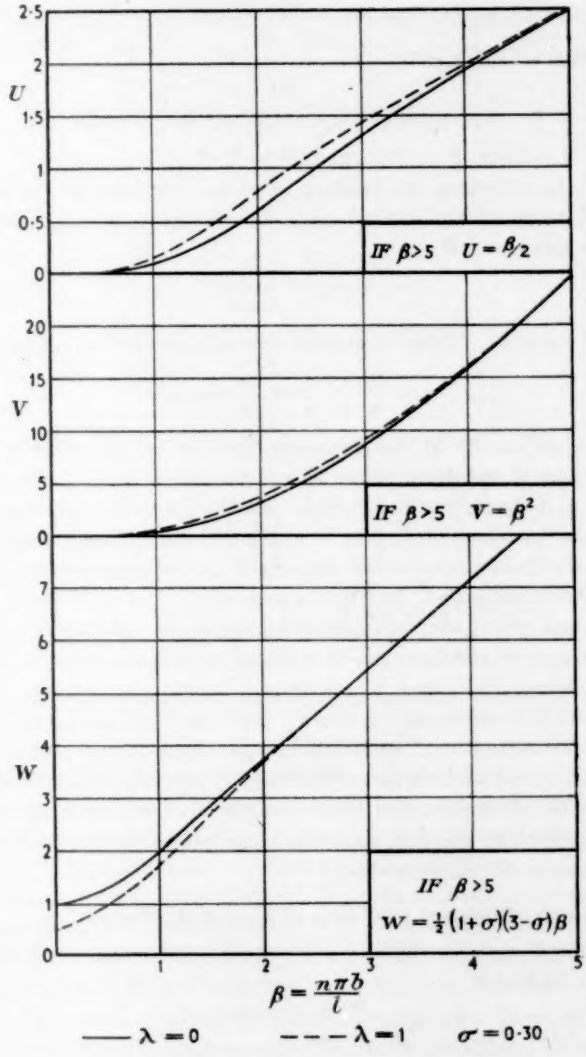

FIG. 2. Values of U, V, and W

in which $$\gamma = \frac{1+\Lambda+\lambda}{1+\lambda}$$

and $$\eta_n' = \frac{\psi Q + R}{\Delta}. \tag{23}$$

Hence, from equation (17),

$$\eta_n' = \frac{\psi U + 1}{\psi[(\Lambda\theta\beta^2+1)U+\Lambda V]+\Lambda\theta\beta^2+1+\Lambda W} \tag{24}$$

in which $U = Q/R$, $V = S/R$, and $W = T/R$.

Finally, by summing the loads in sheet and stringer due to each component $P_n \cos \alpha x$ of the applied load, the efficiency of sheet and stringer under the total load P is

$$\eta = \frac{\sum \eta_n P_n \cos \alpha x}{\sum P_n \cos \alpha x}, \tag{25}$$

and using equation (22) for η_n and equation (3) for the load series

$$\eta = \frac{4\gamma}{\pi} \sum \frac{\eta_n'}{n} \sin \frac{n\pi}{2} \cos \alpha x. \tag{26}$$

Thus the efficiency of the structure depends on the ratio γ of cross-sectional area of the structure to that of the sheet and stringer and upon the terms η_n' defined by equation (24). Each term in this 'efficiency series' involves the functions U, V, and W which contain λ, β, and σ only. These functions are fundamental to the solution of the diffusion problem and have therefore been computed. In Fig. 2 values of U, V, and W for $0 \leqslant \beta \leqslant 5$ are given, and corresponding expressions which are valid for $\beta > 5$.

Some general conclusions can be deduced by inspection of the efficiency term η_n'. Since U, V, and W are always positive, as are the flexibility factors θ and ψ, it can be shown that η_n' decreases with increasing values of ψ; that is, the efficiency of sheet and stringer decreases as the flexibility of the 'elastic foundation' increases. Similarly, it is evident that efficiency will decrease as the rivet shear flexibility factor θ increases, although as will be shown in section 8, this will lead to a reduction in the magnitude of the maximum shear stress in the sheet.

7. Maximum efficiency and rate of load diffusion

The efficiency η of the sheet and stringer is a maximum at the centre of length $x = 0$. Hence

$$\eta_{\max} = \frac{4\gamma}{\pi} \sum \frac{\eta_n'}{n} (-1)^{\frac{1}{2}(n-1)}. \tag{27}$$

Values of $\eta_{\max}$ have been computed from equation (27) for structures in which both rivet shear flexibility θ and foundation flexibility ψ are zero (Fig. 3), and in which $\theta = 0$, $\psi = \infty$ (Fig. 4). In each case three values

of the boom/sheet area ratio Λ, and two values of the stringer/sheet area ratio λ have been taken.

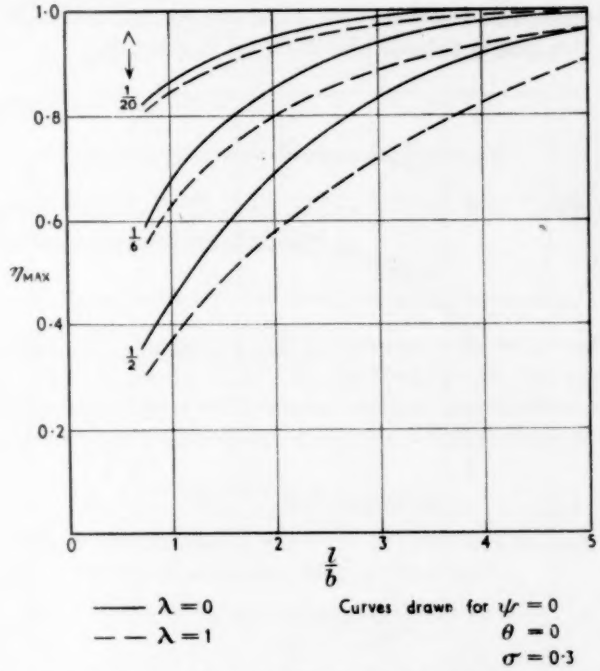

FIG. 3. Maximum efficiency of sheet and stringer. Zero foundation flexibility

Comparison of Figs. 3 and 4 indicates that if $\psi = 0$, i.e. lateral displacement is prevented, the applied load will ultimately diffuse fully into the structure provided the length of the sheet is large compared with its breadth; but if $\psi = \infty$, i.e. lateral displacement is unrestrained, the maximum proportion of the load taken by sheet and stringer is largely dependent on the relative areas of boom and sheet. The influence of λ and Poisson's ratio σ is generally small; the results for $\psi = \infty$ are independent of σ.

Since the maximum efficiency in a particular case is a measure of the degree to which the load diffuses from boom to sheet, then the distance from the end of the sheet at which diffusion is complete is b times half the value of l/b at which the efficiency reaches its maximum value. Here the effect of foundation flexibility is most marked. For example, when $\theta = 0$, $\Lambda = \frac{1}{6}$, and $\lambda = 0$, Fig. 3 indicates that if $\psi = 0$ diffusion is virtually complete within a distance of about $3b$ from the end of the sheet; whereas if

$\psi = \infty$ (Fig. 4) diffusion is complete at a distance from the end of the sheet approximately equal to its breadth b. Thus the effect of bending of the structure in the xy-plane due to eccentricity of the applied load is to decrease the proportion of load carried by sheet and stringer, but to increase the rate at which this load is diffused into the sheet and stringer.

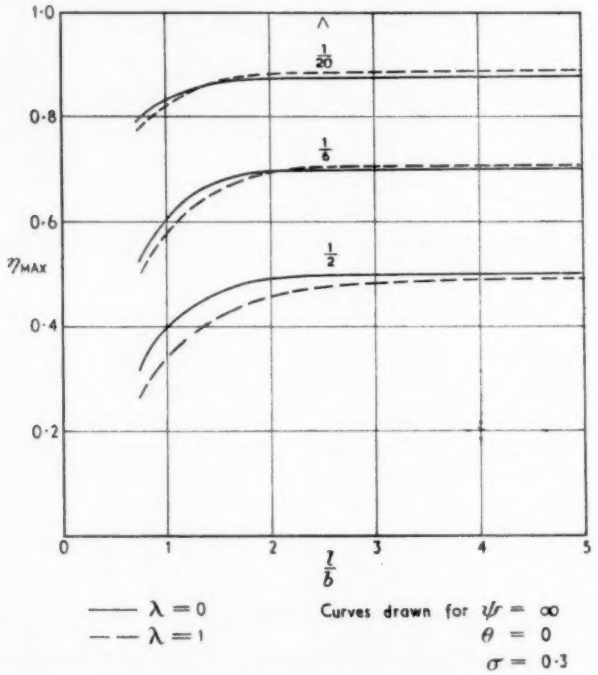

FIG. 4. Maximum efficiency of sheet and stringer. Infinite foundation flexibility

If lateral displacements are unrestrained, $\psi = \infty$, then as $l/b \to \infty$ the results of the foregoing theory should approach those of the conventional theory for tie bars under eccentric end tension. The latter indicates a non-linear response to applied load, arising from the term $\operatorname{sech}\sqrt{(Pl^2/4B)}$, in which B is the flexural stiffness of the structure referred to bending in the xy-plane. The present theory, on the other hand, is linear with respect to P. It can be shown that if $l/b = \infty$, the maximum efficiencies predicted by the two theories are identical if $\operatorname{sech}\sqrt{(Pl^2/4B)} = 1$, and since for the type of structure under consideration $\sqrt{(Pl^2/4B)}$ is unlikely to exceed 0·3, the discrepancy between the theories will always be less than 5 per cent., so that the linearity of the present solution does not invalidate the results obtained.

8. Maximum shear stress in the sheet

It follows from equations (3) and (21) that the shear stress at the junction of boom and sheet is

$$(f_{xy})_{x,0} = -\sum \frac{4P}{\pi n}\left(\frac{n\pi b}{l}\right)\left(\frac{1}{bt}\right)\frac{\psi Q + R}{\Delta}\sin(n\pi/2)\sin(\alpha x),$$

and therefore, using equation (23),

$$(f_{xy})_{x,0} = -\frac{4P}{tl}\sum \eta'_n \sin(n\pi/2)\sin(\alpha x).$$

In particular when $x = \frac{1}{2}l$, since $\sin^2\frac{1}{2}n\pi = 1$ for odd values of n, the maximum shear stress in the structure is

$$(f_{xy})_{\frac{1}{2}l,0} = (f_{xy})_{\max} = -\frac{4P}{tl}\sum \eta'_n. \tag{28}$$

This relationship enables the peak shear stress to be calculated from the efficiency series—equation (24); and furthermore the condition for a theoretically infinite shear stress is obtained by examining the convergence of the η'_n series. Using equations (17) and (18), it can be shown that

$$(\eta'_n)_{\beta\to\infty} \to \frac{\psi/\Lambda}{\psi\theta\beta^2 + (\psi + 2\theta)\beta}.$$

Then if θ is non-zero, since ψ, θ, and β are all positive, each term in the η'_n series is less than the corresponding term of the series

$$\eta'_n = \frac{\psi/\Lambda}{\psi\theta\beta^2} = \frac{1}{\Lambda\theta\beta^2}.$$

But since this latter series is known to be convergent $\left(\text{for } n \text{ odd } \sum 1/n^2 = \frac{1}{8}\pi^2\right)$ then the series for η'_n, equation (24), is convergent. Therefore for non-zero values of the rivet shear flexibility factor θ, the maximum shear stress is finite.

If, on the other hand, the connexion is infinitely stiff in shear, then $\theta = 0$, and the series for η'_n leads to

$$(\eta'_n)_{\beta\to\infty} \to \frac{1}{\Lambda\beta},$$

which represents a non-convergent series. In this case the peak shear stress is theoretically infinite.

The effect of rivet shear flexibility on the maximum shear stress is illustrated in Fig. 5, where for $\psi = 0$, $\lambda = 1$, and $l/b = \pi$, the ratio of maximum shear stress to maximum direct stress f_0 in the boom clear of the sheet is given for three values of Λ and $0{\cdot}01 \leqslant \theta \leqslant 100$. Tests on single riveted lap joints by Flint (7) indicate that in ship structural connexions

$0{\cdot}01 < \theta < 0{\cdot}1$. Within this range the maximum shear stress is unlikely to be excessive unless the boom area ratio Λ is large, or the modular ratio $\mu = E_b/E_s$ is small.

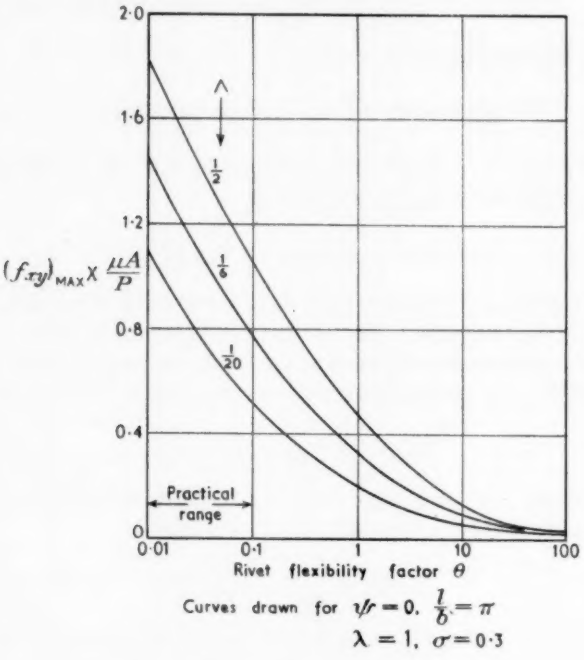

FIG. 5. Maximum shear stress in sheet

9. Conclusions

A Fourier series form for the stress function can be used in the two-dimensional elastic problem of diffusion into a finite rectangular sheet of load applied to a boom riveted to one of its longer edges. It is shown that lateral resistance to bending of the structure in its own plane has a significant effect on the rate at which load is diffused into the structure, and upon the efficiency of the sheet in carrying direct load. A relationship between this efficiency and the maximum shear stress in the sheet has been established, from which it has been shown that the peak shear stress varies with the shear flexibility of the connexion between boom and sheet, and is infinite when the rivet flexibility is zero. The effect of variations in the geometry and elastic properties of the structure can be determined without difficulty.

Acknowledgement

This work forms part of an investigation into the strength of ships' superstructures and deckhouses and has been carried out for the Aluminium Development Association, whose co-operation is gratefully acknowledged.

REFERENCES

1. H. L. Cox, H. E. Smith, and C. G. Conway, *Diffusion of Concentrated Loads into Monocoque Structures*, A.R.C. R. & M. 1780 (1937).
2. W. J. Duncan, *Diffusion of Load in Certain Stringer Sheet Combinations*, ibid. 1825 (1938).
3. D. Williams, R. D. Starkey, and R. H. Taylor, *Distribution of Stress between Spar Flanges and Stringers for a Wing under Distributed Loading*, ibid. 2098 (1939).
4. E. H. Mansfield, 'Rivet flexibility and load diffusion', *Aircraft Engineering*, **21** (1949) 96.
5. W. J. Goodey, 'Stress diffusion problems', ibid. **18** (1946) 195.
6. L. H. Mitchell, 'A Fourier integral solution for the stresses in a semi-infinite strip', *Quart. J. Mech. App. Math.* **7** (1954) 51.
7. A. R. Flint, 'Tests on riveted joints in aluminium alloy plating', British Shipbuilding Research Association Report (unpublished) (1952).

A THREE-DIMENSIONAL PROBLEM FOR HIGHLY ELASTIC MATERIALS SUBJECT TO CONSTRAINTS

By J. E. ADKINS

(*British Rubber Producers' Research Association, Welwyn Garden City, Herts.*†)

[Received 27 September 1956]

SUMMARY

Consideration is given to highly elastic materials which may deform subject to a three-dimensional system of constraints, such as would be produced by three sets of ideally thin, flexible inextensible cords whose paths are defined by the coordinate curves of a general curvilinear reference frame related to points in the undeformed body. When the cords of each set lie initially in parallel straight lines, the equations governing the deformation may be solved in terms of arbitrary functions. The nature of the solution for the general case is also examined.

1. Introduction

In the theory of finite elastic deformations, some consideration has recently been given to materials which may deform subject to certain types of geometrical constraint (**1**, **2**, **3**, **4**). Examples of this feature are provided by incompressible materials, where there are no volume changes during deformation, and by bodies reinforced by systems of ideally thin, flexible, inextensible cords, which prohibit extension in certain directions in each element containing them. Each such constraint thus implies a geometrical relationship between the variables defining the deformation and introduces an arbitrary parameter into the stress system.

A case of special interest arises when a uniform plane thin sheet of elastic material is reinforced with a network consisting of two sets of thin, inextensible cords lying in its middle plane. This problem has been considered by the writer (**2**), and the very similar problem, of a network of cords, without elastic material, by Rivlin (**8**). In both cases a pair of differential equations is obtained for the determination of the deformation, and if the cords lie initially in parallel straight lines, these equations may be solved in terms of arbitrary functions. It may be shown quite generally that the system of differential equations for the determination of the stress and displacement functions is hyperbolic in character.

In the present paper the analogous three-dimensional problem is examined

† Now at the University of Nottingham.

briefly, it being assumed that any deformation is subject to the restriction that there shall be no extension along the coordinate lines of a curvilinear reference frame related to points in the undeformed body. The equations for the determination of the stress and displacement functions are again seen to be hyperbolic, the characteristic surfaces being those defining the system of constraints; when these surfaces are planes, the general solution can be given in terms of arbitrary functions.

2. Notation and formulae

The notation employed is that originated by Green and Zerna (**5**, **6**) and extended by the writer (**2**). The points of an unstressed and unstrained body at rest at time $t = 0$ are defined by a system of rectangular cartesian coordinates x^i, or by a general curvilinear system of coordinates θ^i. The latter reference frame moves with the material as it is deformed and forms a curvilinear system in the strained body at time t. Points of the deformed body may also be defined by a set of rectangular cartesian coordinates y^i, and in the present paper we shall take the x^i-axes and y^i-axes to coincide. With the coordinate system θ^i in the unstrained body we may associate covariant and contravariant metric tensors g_{ij}, g^{ij}, the corresponding quantities for this coordinate system in the strained body at time t being G_{ij}, G^{ij}. The covariant strain tensor γ_{ij}, referred to the coordinates θ^i, may then be defined by

$$\gamma_{ij} = \tfrac{1}{2}(G_{ij} - g_{ij}). \tag{2.1}$$

For a second system of curvilinear coordinates $\bar{\theta}^i$, metric and strain tensors $\bar{g}_{ij}$, $\bar{g}^{ij}$, $\bar{G}_{ij}$, $\bar{G}^{ij}$, and $\bar{\gamma}_{ij}$ may be similarly defined and may be derived from the corresponding unbarred quantities in the usual manner by tensor transformations.

We consider here elastic materials subject to constraints which may be described by means of functional relationships

$$f_m(\bar{\gamma}_{ij}) = 0 \quad (m = 1, 2, \ldots, n,\ n < 6) \tag{2.2}$$

between the strain components $\bar{\gamma}_{ij}$, the restriction upon the value of n resulting from the consideration that more than five such constraints would permit only rigid-body motions. For such materials it has been shown by the writer that the stress tensor τ^{ij} referred to the convected coordinates θ^i in the deformed body, may be written in the form

$$\tau^{ij} = \tau_e^{ij} + \tfrac{1}{2} \sum_{m=1}^{n} q_m \frac{\partial f_m}{\partial \bar{\gamma}_{rs}} \left(\frac{\partial \theta^i}{\partial \bar{\theta}^r} \frac{\partial \theta^j}{\partial \bar{\theta}^s} + \frac{\partial \theta^i}{\partial \bar{\theta}^s} \frac{\partial \theta^j}{\partial \bar{\theta}^r} \right) \quad (n < 6), \tag{2.3}$$

where q_m are arbitrary scalar functions of θ^i, and τ_e^{ij} is a function depending upon the constraints only to the extent to which the relations (2.2) introduce

simplifications in the form of the strain-energy function W. The exact form of τ_e^{ij} is unimportant for the purpose of the present paper; the general expression is (**2**, **6**)

$$\tau_e^{ij} = \frac{1}{2\sqrt{\left(\frac{g}{G}\right)}}\left(\frac{\partial W}{\partial \gamma_{ij}} + \frac{\partial W}{\partial \gamma_{ji}}\right),$$

where

$$g = |g_{ij}|, \qquad G = |G_{ij}|.$$

In the absence of body forces the equations of equilibrium may be written

$$\tau^{ij}{}_{\|i} = 0, \tag{2.4}$$

where the double line signifies covariant differentiation with respect to the deformed body, that is, with respect to θ^i and the metric tensor components G_{ij}, G^{ij}.

3. The constraint conditions

The two-dimensional problem in which a plane uniform elastic sheet is reinforced in its middle plane by means of two sets of thin, flexible, inextensible cords following the coordinate lines of a plane curvilinear reference frame, and is subjected to a plane deformation has been examined by Adkins (**2**). The analogous problem for a plane network of initially straight cords, without elastic material, has been considered by Rivlin (**8**). For the case of an elastic sheet, it is assumed that the cords restrict the deformation so that there is no extension along any member of the families of curves in which they lie.

A natural extension of this problem to three dimensions is obtained by postulating a material which is such that in any deformation there can be no extension along any of the coordinate curves of the reference frame $\bar{\theta}^i$. If corresponding elements of length in the body before and after deformation are denoted by ds_0 and ds respectively, we have

$$ds_0^2 = g_{ij}\, d\theta^i d\theta^j = \bar{g}_{ij}\, d\bar{\theta}^i d\bar{\theta}^j,$$

$$ds^2 = G_{ij}\, d\theta^i d\theta^j = \bar{G}_{ij}\, d\bar{\theta}^i d\bar{\theta}^j,$$

and since $ds_0 = ds$ along the curves $\bar{\theta}^i = \text{const}$, $\bar{\theta}^j = \text{const}$ $(i \neq j)$, these expressions lead to the constraint conditions

$$\bar{g}_{ii} = \bar{G}_{ii} \quad \text{or} \quad \bar{\gamma}_{ii} = 0 \quad (i \text{ not summed}), \tag{3.1}$$

which may also be written

$$\bar{G}_{ii} = \frac{\partial y^r}{\partial \bar{\theta}^i}\frac{\partial y^r}{\partial \bar{\theta}^i} = \bar{g}_{ii} = \frac{\partial x^r}{\partial \bar{\theta}^i}\frac{\partial x^r}{\partial \bar{\theta}^i} \quad (i \text{ not summed}). \tag{3.2}$$

If the coordinate surfaces $\bar{\theta}^i = \text{constant}$ in the undeformed body are

planes, so that the components of the metric tensor $\bar{g}_{ii}$ are constants, equations (3.2) may evidently be integrated to yield

$$\left.\begin{aligned} y^1 &= f_1(\bar{\theta}^1)+f_2(\bar{\theta}^2)+f_3(\bar{\theta}^3) \\ y^2 &= g_1(\bar{\theta}^1)+g_2(\bar{\theta}^2)+g_3(\bar{\theta}^3) \\ y^3 &= h_1(\bar{\theta}^1)+h_2(\bar{\theta}^2)+h_3(\bar{\theta}^3) \end{aligned}\right\}, \tag{3.3}$$

where $f_r(\bar{\theta}^r)$, $g_r(\bar{\theta}^r)$, and $h_r(\bar{\theta}^r)$ are functions whose first derivatives, denoted by primes, satisfy the relations

$$f_r'^2+g_r'^2+h_r'^2 = \bar{g}_{rr}, \tag{3.4}$$

but which are otherwise arbitrary.

4. Equations of equilibrium; stress strain relations

For the purpose of this paper, it is convenient to introduce a symmetric covariant tensor ϕ_{ij} which is such that

$$\tau^{ij} = \epsilon^{ikm}\epsilon^{jln}\phi_{kl}\|_{mn}, \tag{4.1}$$

where ϵ^{ijk} takes the value $1/\sqrt{G}$ or $-1/\sqrt{G}$ according as i, j, k is an even or odd permutation of the numbers 1, 2, 3, and is zero if any two indices are equal. It is easily verified that when τ^{ij} is expressed in this manner, the equations of equilibrium (2.4) are identically satisfied. Moreover, this remains true even if the off-diagonal components ϕ_{ij} $(i \neq j)$ are zero. We therefore choose ϕ_{ij} so that the components $\bar{\phi}_{ij}$ for $i \neq j$ are zero in the reference frame $\bar{\theta}^i$ defining the system of constraints. From (4.1) we then obtain

$$\bar{\tau}^{ij} = \bar{\epsilon}^{ikm}\bar{\epsilon}^{jkn}\bar{\phi}_{kk}\|_{mn}, \tag{4.2}$$

where the double line now denotes covariant differentiation with respect to $\bar{\theta}^i$ and the metric tensor components $\bar{G}_{ij}$, $\bar{G}^{ij}$. The components $\bar{\phi}_{kk}$ correspond to the stress functions of the classical theory of elasticity, given, for example, by Love (7).

The constraint conditions (3.1), when combined with (2.3), yield for τ^{ij} the formulae

$$\tau^{ij} = \tau_e^{ij} + \sum_{r=1}^{3} q_r \frac{\partial\theta^i}{\partial\bar{\theta}^r}\frac{\partial\theta^j}{\partial\bar{\theta}^r}, \tag{4.3}$$

or, if the coordinate systems θ^i and $\bar{\theta}^i$ are allowed to coincide,

$$\bar{\tau}^{ij} = \bar{\tau}_e^{ij} + \sum_{r=1}^{3} q_r \delta_r^i \delta_r^j, \tag{4.4}$$

δ_r^i being the Kronecker delta. Combining (4.4) and (4.2) then gives

$$\bar{\tau}^{ii} = \bar{\tau}_e^{ii}+q_i = \bar{\epsilon}^{ikm}\bar{\epsilon}^{ikm}\bar{\phi}_{kk}\|_{mm} \quad (i \text{ not summed}), \tag{4.5}$$

$$\bar{\tau}^{ij} = \bar{\tau}_e^{ij} = \bar{\epsilon}^{ikm}\bar{\epsilon}^{jkn}\bar{\phi}_{kk}\|_{mn} \quad (i \neq j). \tag{4.6}$$

If the deformation has been determined from the constraint conditions

(3.2), the components $\bar{\tau}_e^{ij}$ may be regarded as known functions of $\bar{\theta}^i$ and (4.6) furnishes three equations for the determination of the functions $\bar{\phi}_{kk}$. The parameters q_i are then given by (4.5); if the constraints arise from systems of thin flexible inextensible cords, these parameters may be expressed in terms of the tensions in the individual cords and the spacing of the adjacent cords of each system.

When the coordinate surfaces $\bar{\theta}^i$ in the undeformed body are planes, we see, from (3.3), that the metric tensor components $\bar{G}_{ik}$ are given by

$$\bar{G}_{ik} = f'_i f'_k + g'_i g'_k + h'_i h'_k, \tag{4.7}$$

so that the derivatives $\partial \bar{G}_{ij}/\partial \bar{\theta}^k$ are zero if i, j, and k are all different; it follows that the Christoffel symbols $\bar{\Gamma}^i_{rs}$ formed with the barred quantities $\bar{G}_{ij}$, $\bar{G}^{ij}$ vanish if $r \neq s$. Equations (4.6) then yield

$$\bar{\tau}_e^{23} = -\frac{1}{\bar{G}} \frac{\partial^2 \bar{\phi}_{11}}{\partial \bar{\theta}^2 \partial \bar{\theta}^3}, \quad \bar{\tau}_e^{13} = -\frac{1}{\bar{G}} \frac{\partial^2 \bar{\phi}_{22}}{\partial \bar{\theta}^1 \partial \bar{\theta}^3}, \quad \bar{\tau}_e^{12} = -\frac{1}{\bar{G}} \frac{\partial^2 \bar{\phi}_{33}}{\partial \bar{\theta}^1 \partial \bar{\theta}^2}. \tag{4.8}$$

Since the components $\bar{\tau}_e^{ij}$ are, for a given type of material, known functions of f_r, g_r, h_r and their derivatives, we may obtain from (4.8) by integration

$$\left.\begin{aligned} \bar{\phi}_{11} &= \chi_{23} + \Theta_1(\bar{\theta}^1, \bar{\theta}^2) + \Theta_2(\bar{\theta}^1, \bar{\theta}^3) \\ \bar{\phi}_{22} &= \chi_{13} + \Phi_1(\bar{\theta}^1, \bar{\theta}^2) + \Phi_2(\bar{\theta}^2, \bar{\theta}^3) \\ \bar{\phi}_{33} &= \chi_{12} + \Psi_1(\bar{\theta}^1, \bar{\theta}^3) + \Psi_2(\bar{\theta}^2, \bar{\theta}^3) \end{aligned}\right\}, \tag{4.9}$$

where

$$\chi_{rs} = -\int^{\bar{\theta}^s} d\bar{\theta}^s \int^{\bar{\theta}^r} \bar{G} \bar{\tau}_e^{rs} \, d\bar{\theta}^r \tag{4.10}$$

are known functions of $\bar{\theta}^i$, and Θ_α, Φ_α, and Ψ_α are arbitrary functions of the arguments indicated.

The remaining components $\bar{\tau}^{rr}$ of the stress tensor are obtained by combining (4.9) with (4.5) and evaluating the covariant derivatives. Since

$$\sqrt{\bar{G}} = \begin{vmatrix} f'_1 & f'_2 & f'_3 \\ g'_1 & g'_2 & g'_3 \\ h'_1 & h'_2 & h'_3 \end{vmatrix}, \tag{4.11}$$

it follows that

$$\bar{G}^{ij} = \frac{1}{\bar{G}} \left(\frac{\partial \sqrt{\bar{G}}}{\partial f'_i} \frac{\partial \sqrt{\bar{G}}}{\partial f'_j} + \frac{\partial \sqrt{\bar{G}}}{\partial g'_i} \frac{\partial \sqrt{\bar{G}}}{\partial g'_j} + \frac{\partial \sqrt{\bar{G}}}{\partial h'_i} \frac{\partial \sqrt{\bar{G}}}{\partial h'_j} \right), \tag{4.12}$$

and the non-zero components of the Christoffel symbols $\bar{\Gamma}^i_{jk}$ take the forms

$$\bar{\Gamma}^i_{11} = \bar{G}^{i2} \bar{G}_{12,1} + \bar{G}^{i3} \bar{G}_{13,1}, \qquad \bar{\Gamma}^1_{11} = \frac{1}{2\bar{G}} \frac{\partial \bar{G}}{\partial \bar{\theta}^1}, \tag{4.13}$$

analogous formulae holding for $\bar{\Gamma}^i_{22}$ and $\bar{\Gamma}^i_{33}$. Combination of these results with (4.7), (4.11), and (4.12) yields

$$\bar{\Gamma}^i_{rr} = \left(f''_r \frac{\partial \sqrt{\bar{G}}}{\partial f'_i} + g''_r \frac{\partial \sqrt{\bar{G}}}{\partial g'_i} + h''_r \frac{\partial \sqrt{\bar{G}}}{\partial h'_i} \right) \Big/ \sqrt{\bar{G}}. \tag{4.14}$$

From (4.5) we may now obtain

$$\bar{\tau}^{11} = \frac{1}{\sqrt{\bar{G}}}\frac{\partial}{\partial\bar{\theta}^3}\left(\frac{1}{\sqrt{\bar{G}}}\frac{\partial\bar{\phi}_{22}}{\partial\bar{\theta}^3}\right)+\frac{1}{\sqrt{\bar{G}}}\frac{\partial}{\partial\bar{\theta}^2}\left(\frac{1}{\sqrt{\bar{G}}}\frac{\partial\bar{\phi}_{33}}{\partial\bar{\theta}^2}\right)-$$

$$-\bar{\Gamma}^2_{33}\frac{\partial}{\partial\bar{\theta}^2}\left(\frac{\bar{\phi}_{22}}{\bar{G}}\right)-\bar{\Gamma}^3_{22}\frac{\partial}{\partial\bar{\theta}^3}\left(\frac{\bar{\phi}_{33}}{\bar{G}}\right)-\frac{1}{\bar{G}}\left(\bar{\Gamma}^1_{22}\frac{\partial\bar{\phi}_{33}}{\partial\bar{\theta}^1}+\bar{\Gamma}^1_{33}\frac{\partial\bar{\phi}_{22}}{\partial\bar{\theta}^1}\right),$$

with corresponding expressions for $\bar{\tau}^{22}$ and $\bar{\tau}^{33}$.

5. General nature of the equations

In the two-dimensional problem examined in the earlier work (**2**, **8**) the differential equations which enter into the analysis are found to be hyperbolic, and it is then possible to prove that specified distributions of stress and displacement along a plane arc are sufficient to determine the deformation and the stress system within a region bounded by the given arc and the characteristic curves through its ends. The general similarity of the basic assumptions and the resulting equations in the present instance suggests that analogous results may be obtained for the three-dimensional problem. A full analysis for all possible cases would evidently prove much more lengthy than the corresponding treatment for two dimensions. We shall therefore concentrate attention on proving the following proposition:

If the displacement components, and hence the quantities y^i, are given over any surface S, no part of which coincides with a characteristic surface, then the deformation is completely determined within a region V mapped out by S and the characteristic lines through its boundary C.

We may, without loss of generality, choose S to be the surface $\theta^3 =$ constant, the lines $\theta^\alpha =$ constant ($\alpha = 1, 2$) then forming a curvilinear system on this boundary. For brevity, we use the notation

$$y^p_{,\alpha} = \frac{\partial y^p}{\partial\theta^\alpha}, \qquad \bar{y}^p_{,j} = \frac{\partial y^p}{\partial\bar{\theta}^j}, \qquad \bar{\theta}^i_{,\alpha} = \frac{\partial\bar{\theta}^i}{\partial\theta^\alpha}, \tag{5.1}$$

it being understood that in the subsequent work Greek indices take the values 1, 2. Since the components y^i are given over the boundary S, their derivatives $y^i_{,\alpha}$ may be regarded as known quantities over this surface, whilst the quantities $\bar{\theta}^i_{,\alpha}$ are also known from geometrical considerations. It is then possible to show that the constraint conditions (3.2) enable the derivatives $\bar{y}^i_{,j}$ to be calculated over S.

From the relations $\qquad y^p_{,\alpha} = \bar{y}^p_{,k}\bar{\theta}^k_{,\alpha},$

which hold over S, we may obtain

$$A^{kj}\bar{y}^p_{,k} = B^{pj}, \tag{5.2}$$

where

$$\left.\begin{aligned} B^{pj} &= y^p_{,1}\bar{\theta}^j_{,2} - y^p_{,2}\bar{\theta}^j_{,1} \\ A^{kj} &= \bar{\theta}^k_{,1}\bar{\theta}^j_{,2} - \bar{\theta}^k_{,2}\bar{\theta}^j_{,1} \quad (A^{kk} = 0) \end{aligned}\right\}, \tag{5.3}$$

and A^{kj} transforms as an antisymmetric contravariant tensor with respect to transformations of coordinates $\bar{\theta}^i$. Equations (5.2) yield

$$B^{p1}-A^{31}\bar{y}^p_{,3}=A^{21}\bar{y}^p_{,2}, \qquad B^{p2}-A^{32}\bar{y}^p_{,3}=A^{12}\bar{y}^p_{,1},$$

from which, by squaring, summing over p, and making use of the constraint conditions (3.2) to eliminate $\sum_{p=1}^{3}(y^p_{,1})^2$ and $\sum_{p=1}^{3}(y^p_{,2})^2$, we obtain

$$\sum_{p=1}^{3}(B^{p1})^2-\sum_{p=1}^{3}C_{p1}\bar{y}^p_{,3}+(A^{31})^2\bar{g}_{33}=(A^{21})^2\bar{g}_{22},$$

$$\sum_{p=1}^{3}(B^{p2})^2-\sum_{p=1}^{3}C_{p2}\bar{y}^p_{,3}+(A^{32})^2\bar{g}_{33}=(A^{12})^2\bar{g}_{11},$$

or

$$\sum_{p=1}^{3}C_{p1}\bar{y}^p_{,3}=\chi_1, \qquad \sum_{p=1}^{3}C_{p2}\bar{y}^p_{,3}=\chi_2, \tag{5.4}$$

χ_1, χ_2 and $C_{p\alpha}$ being given by

$$\left.\begin{aligned}\chi_1&=\sum_{p=1}^{3}(B^{p1})^2+(A^{31})^2\bar{g}_{33}-(A^{21})^2\bar{g}_{22}\\ \chi_2&=\sum_{p=1}^{3}(B^{p2})^2+(A^{32})^2\bar{g}_{33}-(A^{12})^2\bar{g}_{11}\end{aligned}\right\}, \tag{5.5}$$

and

$$C_{p\alpha}=2B^{p\alpha}A^{3\alpha} \quad (\alpha \text{ not summed}). \tag{5.6}$$

Writing

$$C_{12}\chi_1-C_{11}\chi_2=\Psi_1, \qquad C_{22}\chi_1-C_{21}\chi_2=\Psi_2, \tag{5.7}$$

$$\left.\begin{aligned}\Delta_{12}&=C_{11}C_{22}-C_{12}C_{21}=4A^{31}A^{32}(B^{11}B^{22}-B^{12}B^{21})\\ \Delta_{13}&=C_{12}C_{31}-C_{11}C_{32}=4A^{31}A^{32}(B^{12}B^{31}-B^{11}B^{32})\\ \Delta_{23}&=C_{22}C_{31}-C_{21}C_{32}=4A^{31}A^{32}(B^{22}B^{31}-B^{21}B^{32})\end{aligned}\right\}, \tag{5.8}$$

we may obtain from (5.4)

$$\bar{y}^1_{,3}=(\Psi_2-\Delta_{23}\bar{y}^3_{,3})/\Delta_{12}, \qquad \bar{y}^2_{,3}=-(\Psi_1-\Delta_{13}\bar{y}^3_{,3})/\Delta_{12}, \tag{5.9}$$

and when these expressions are introduced into the third of the constraint conditions (3.2), we have

$$\bar{g}_{33}=\{(\Delta^2_{12}+\Delta^2_{13}+\Delta^2_{23})(\bar{y}^3_{,3})^2-2(\Delta_{13}\Psi_1+\Delta_{23}\Psi_2)\bar{y}^3_{,3}+\Psi^2_1+\Psi^2_2\}/\Delta^2_{12}.$$

Solving this equation we obtain

$$\bar{y}^3_{,3}=\{M\pm(M^2-LN)^{\frac{1}{2}}\}/L, \tag{5.10}$$

where

$$\left.\begin{aligned}L&=\Delta^2_{12}+\Delta^2_{13}+\Delta^2_{23}\\ M&=\Delta_{13}\Psi_1+\Delta_{23}\Psi_2\\ N&=\Psi^2_1+\Psi^2_2-\bar{g}_{33}\Delta^2_{12}\end{aligned}\right\} \tag{5.11}$$

are quantities whose values are known over S.

The sign occurring in the expression (5.10) is determined from the consideration that the functional determinant

$$\sqrt{\bar{G}}=\frac{\partial(y^1,y^2,y^3)}{\partial(\bar{\theta}^1,\bar{\theta}^2,\bar{\theta}^3)}$$

must be positive. For, when the relations (5.2) are used to eliminate the derivatives $\bar{y}^p_{,1}$, $\bar{y}^p_{,2}$ from the expression for $\sqrt{\bar{G}}$, and the resulting formula simplified by means of (5.8), we obtain

$$\sqrt{\bar{G}} = (\Delta_{23}\bar{y}^1_{,3} - \Delta_{13}\bar{y}^2_{,3} - \Delta_{12}\bar{y}^3_{,3})/(4A^{12}A^{21}A^{31}A^{32}).$$

Further reduction by means of (5.9) and (5.11) yields the result

$$\sqrt{\bar{G}} = -(L\bar{y}^3_{,3} - M)/(4A^{12}A^{21}A^{31}A^{32}\Delta_{12}),$$

or, by virtue of (5.10),

$$\sqrt{\bar{G}} = \mp(M^2 - LN)^{\frac{1}{2}}/(4A^{12}A^{21}A^{31}A^{32}\Delta_{12}), \tag{5.12}$$

the upper and lower signs in (5.10) and (5.12) corresponding. All of the quantities entering into this expression are determined uniquely by the boundary conditions over the surface S and the geometrical parameters of the undeformed body, and only one of the signs occurring in (5.12), and hence in (5.10), is therefore possible if the expression for $\sqrt{\bar{G}}$ is to be positive.

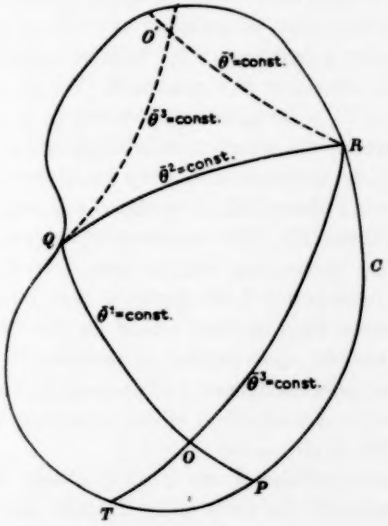

FIG. 1

When $\bar{y}^3_{,3}$ has been determined, unique values for the remaining first derivatives of y^i follow from the linear relations (5.9) and (5.2). Higher order derivatives of y^i with respect to the coordinates $\bar{\theta}^k$ may be obtained by differentiation of the expressions for those of the first order, the analysis following the lines indicated for the two-dimensional problem (**2**). By Taylor's theorem, an expansion for the coordinates y^k may then be obtained,

valid within a finite region V bounded by S, and satisfying the constraint conditions within V and the boundary conditions on S. By this means, the values of y^i may be determined over a surface S', close to but not coincident with S; the region throughout which the solution is known may then be extended by a repetition of the procedure, starting from S'.

The region throughout which a solution can be obtained by this method may be mapped out as follows. Let characteristic surfaces $\bar{\theta}^i$ = constant intersect the surface S in the curves PQ, QR, RT as shown in the accompanying diagram, the points P, Q, R, and T lying on the boundary curve C of S. If PQ, RT intersect in O, the curvilinear tetrahedron bounded by the portion OQR of S and the characteristic surfaces through OQ, QR, and RO represents a region V' throughout which the values of y^i, and hence the deformation, may be determined by the foregoing process. In crossing the surface $\bar{\theta}^1$ = constant from a point just inside this region, the quantities y^i, and hence their tangential derivatives $\bar{y}^i_{,2}$, $\bar{y}^i_{,3}$, must be continuous, but this consideration does not apply to the normal derivatives, and hence to $\bar{y}^i_{,1}$ which may be assigned any values consistent with the first of the constraint conditions (3.2). Similar considerations apply for each of the boundary surfaces $\bar{\theta}^i$ = constant. To determine the values of y^i outside the region V', it is therefore necessary to make use of boundary conditions on S outside the curvilinear triangle OQR. Regions adjacent to V throughout which the deformation may be determined may be mapped out by drawing further characteristic surfaces adjacent to the boundaries of V'. The dotted lines QO', RO' represent the intersection of two such surfaces with S. By continuing this procedure until the entire area S bounded by C has been covered, the region V may be defined throughout which the deformation may be determined by the boundary conditions on S. It follows from this analysis that the constraint equations (3.2) are hyperbolic, with the surfaces defined by the system of constraints forming characteristic surfaces; examination of the equations (4.6) for $\bar{\phi}_{kk}$ shows that these are similar in character.

If the characteristic surfaces $\bar{\theta}^i$ are initially planes, the constraint conditions have a solution of the form (3.3). In this solution, the functions f_r, g_r, h_r, are determined apart from arbitrary additive constants, by the boundary conditions, and consideration of the second and higher order derivatives of the coordinates y^i becomes unnecessary.

This work forms part of a programme of research undertaken by the board of the British Rubber Producers' Research Association.

REFERENCES

1. J. E. Adkins, *J. Rat. Mech. Anal.* **5** (1956) 189.
2. —— *Phil. Trans.* A, **249** (1956) 125.
3. —— and R. S. Rivlin, ibid. **248** (1955) 201.
4. J. L. Ericksen and R. S. Rivlin, *J. Rat. Mech. Anal.* **3** (1954) 281.
5. A. E. Green and W. Zerna, *Phil. Mag.* **41** (1950) 313.
6. —— —— *Theoretical Elasticity* (Oxford, 1954).
7. A. E. H. Love, *The Mathematical Theory of Elasticity*, 4th edn. (Cambridge, 1952).
8. R. S. Rivlin, *J. Rat. Mech. Anal.* **4** (1955) 951.

UNIFIED THEORY OF INTERNAL BALLISTICS

By J. N. KAPUR (*Hindu College, Delhi University, Delhi*)

[Received 27 September 1956.—Revise received 11 April 1957]

SUMMARY

In the present paper, a unified theory of internal ballistics of orthodox, leaking, recoilless, high-low pressure, recoilless high-low pressure guns, and of solid-fuel rockets has been presented. The internal ballistics of the most general weapon—R.C.L. H./L. gun—have been studied in detail.

1. Introduction

THE main problems of internal ballistics have been almost completely solved for the orthodox gun (Corner (**1**), H.M.S.O. (**2**)). For the newer and still unorthodox guns like the R.C.L. and the H./L. guns, solutions have also been given (Corner (**1**, **3**, **4**), H.M.S.O. (**2**)). A theory of the internal ballistics of solid-fuel rockets also exists (Crawford (**5**), Trubridge (**6**), Wimpress (**7**)). But most of these theories have so far been developed independently. A unified theory for all these is still awaited, though indication of its necessity was given as early as 1950 by Corner (**1**) when he predicted the union of gun and rocket theory covering in one style of treatment the many new weapons. It is obvious that such a theory cannot be a simple one; nor for that matter, it is likely to throw additional light on the understanding of the extreme cases—the orthodox gun and the solid-fuel rocket—which are already quite well understood. The attempt is worth while from the point of view of development of 'half and half' weapons, i.e. weapons which have partly the characteristics of guns and partly those of rockets.

In the present paper we have made an attempt to develop such a unified theory of internal ballistics. The most general weapon considered here is the recoilless high-low pressure gun, and we first write down the system of equations for this gun. From this we deduce as particular cases, the system of equations for R.C.L. gun, for H./L. gun, for orthodox gun, and for a solid-fuel rocket.

Before the charge is burnt, the isothermal model for R.C.L. H./L. gun has been studied, but since after burning, the gases cool off considerably due to expansion, the variation of temperature has been taken into account for this case.

2. Fundamental equations for a recoilless high-low pressure gun

The figure below gives the basic diagram for such a gun.

Let F, C, D, B, η, δ denote respectively the force-constant, mass, ballistic size, rate-of-burning constant, co-volume per unit mass, and density of the charge. Let K_1, K_2 be the capacities of the two chambers when the shot is in its initial position, and let A be the area of cross-section of the bore.

FIG. 1. A R.C.L. H./L. gun

At time t, let x, z, f denote respectively the shot-travel, the fraction of the charge mass burnt, the fraction of the web size remaining, and let p_1, T_1, ρ_1, CN_1; p_2, T_2, ρ_2, CN_2 denote respectively the pressures, temperatures, gas densities, and gas masses in the two chambers. Then we have the following basic equations for the R.C.L. H./L. gun:

Equation of state for the first chamber

$$p_1\left[K_1-\frac{C(1-z)}{\delta}-CN_1\eta\right]=CN_1RT_1. \tag{1}$$

Equation of state for the second chamber

$$p_2[K_2+Ax-CN_2\eta]=CN_2RT_2. \tag{2}$$

Equation of continuity for the first chamber

$$C\frac{dz}{dt}=C\frac{dN_1}{dt}+\frac{\psi S_1 p_1}{(RT_1)^{\frac{1}{2}}}+\frac{\psi S_2 p_1}{(RT_1)^{\frac{1}{2}}}. \tag{3}$$

Here S_1, S_2 are the throat areas of the two nozzles and

$$\psi=\gamma^{\frac{1}{2}}\left(\frac{2}{\gamma+1}\right)^{(\gamma+1)/2(\gamma-1)}. \tag{4}$$

Also we have assumed that

$$\frac{p_2}{p_1}\leqslant\left(\frac{2}{\gamma+1}\right)^{\gamma/(\gamma-1)}. \tag{5}$$

If p_2/p_1 is greater than this critical value, ψ has to be replaced by

$$\left(\frac{2\gamma}{\gamma-1}\right)^{\frac{1}{2}}\left(\frac{p_2}{p_1}\right)^{1/\gamma}\left\{1-\left(\frac{p_2}{p_1}\right)^{(\gamma-1)/\gamma}\right\}^{\frac{1}{2}}. \tag{4a}$$

In practice, however, (5) will be satisfied and we shall assume in the rest of the paper, unless stated otherwise explicitly, that ψ is constant. We then have

The equation of continuity for the second chamber

$$C\frac{dN_2}{dt}=\frac{\psi S_2 p_1}{(RT_1)^{\frac{1}{2}}}, \tag{6}$$

so that (3) can also be written as

$$C\frac{dz}{dt}=C\frac{dN_1}{dt}+C\frac{dN_2}{dt}+\frac{\psi S_1 p_1}{(RT_1)^{\frac{1}{2}}}. \tag{7}$$

The equation of motion of the shot

$$(1{\cdot}05W+\tfrac{1}{3}C)\frac{d^2x}{dt^2}=W_2\frac{d^2x}{dt^2}=Ap_2. \tag{8}$$

The rate-of-burning equation

$$D\frac{df}{dt}=-B(p_1). \tag{9}$$

The form-function

$$z=\phi(f). \tag{10}$$

Energy equation for the first chamber

(i) In time dt, a mass $C\,dz$ with internal energy $C\,dz\,C_v\,T_0$ enters the gas. Let δT_1 be the change in temperature of the first chamber due to this additional gas, then

$$C\,dz\,C_v\,T_0=CN_1C_v\,\delta T_1+C\,dz\,C_v\,T_1$$

or

$$\delta T_1=\frac{dz}{N_1}(T_0-T_1).$$

(ii) In time dt, a mass $C(dz-dN_1)$ escapes through the nozzles. Since the expansion is adiabatic, we have if ΔT_1 is the change in temperature due to this effect

$$\frac{\Delta T_1}{T_1}=\frac{\gamma-1}{1-\eta\rho_1}\frac{\Delta\rho_1}{\rho_1}=\frac{\gamma-1}{1-\eta\rho_1}\frac{dN_1-dz}{N_1}.$$

Hence,

$$\frac{\Delta T_1}{T_1}=(\gamma-1)(1+\epsilon)\frac{dN_1-dz}{N_1},$$

where

$$\epsilon=\frac{\eta\rho_1}{1-\eta\rho_1}.$$

The change dT_1 in temperature, due to both the factors, is

$$dT_1=\delta T_1+\Delta T_1=\frac{dz}{N_1}(T_0-T_1)+\frac{T_1}{N_1}(\gamma-1)(1+\epsilon)(dN_1-dz).$$

Hence

$$\frac{d}{dt}(N_1T_1)=T_0\frac{dz}{dt}-[\gamma+(\gamma-1)\epsilon]T_1\left(\frac{dz}{dt}-\frac{dN_1}{dt}\right).$$

Using (3),

$$\frac{d}{dt}(N_1T_1)=T_0\frac{dz}{dt}-[\gamma+(\gamma-1)\epsilon]\left[\frac{\psi S_1 p_1}{CR}(RT_1)^{\frac{1}{2}}+\frac{\psi S_2 p_1}{CR}(RT_1)^{\frac{1}{2}}\right]. \tag{11}$$

If we neglect the co-volume term, the energy equation for the first chamber becomes

$$\frac{d}{dt}(N_1 T_1) = T_0 \frac{dz}{dt} - \frac{\gamma \psi S_1 p_1}{CR}(RT_1)^{\frac{1}{2}} - \frac{\gamma \psi S_2 p_1}{CR}(RT_1)^{\frac{1}{2}}. \tag{12}$$

This derivation of the energy equation for a R.C.L. H./L. gun is based on Corner's (3) method of deducing the energy equation for a R.C.L. gun. Alternative derivations of the same equations are obtained by using the principles used in Kothari (8) or Kapur (9).

Energy equation for the second chamber

In time dt

(i) the addition of internal energy to the second chamber due to the energy brought by the mass $C\,dN_2$ entering from the first chamber is

$$C\,dN_2\left(\frac{R}{\gamma-1}\right)dT_1;$$

(ii) this gas, when it forces its way from the first chamber does work on the middle nozzle and this energy is also added to the energy of the second chamber. This is

$$C\,dN_2\,RT_1(1+\epsilon);$$

(iii) increase in internal energy of the second chamber is

$$\frac{CR}{\gamma-1}\,d(N_2 T_2);$$

(iv) work done on the shot is

$$Ap_2\,dx.$$

Hence the energy equation for the second chamber is

$$\frac{C\,dN_2\,RT_1}{\gamma-1} + C\,dN_2\,RT_1(1+\epsilon) = \frac{CR}{\gamma-1}\,d(N_2 T_2) + Ap_2\,dx,$$

or taking heat losses into account,

$$\frac{d}{dt}(N_2 T_2) = -\frac{Ap_2}{CR}(\tilde{\gamma}-1)\frac{dx}{dt} + [1+(\gamma-1)(1+\epsilon)]T_1\frac{dN_2}{dt}. \tag{13}$$

The equations (1), (2), (3), (6), (8), (9), (10), and (13) constitute the most general system of equations, from which the system of equations of all weapons will be deduced as particular cases. This we proceed to do in the next section.

3. Particular cases

3.1. *R.C.L. H./L. gun. Isothermal model. Before charge is burnt*

In this model we assume the temperatures of both the chambers to be constant and to be the same. These two assumptions replace equations (11)

and (13). In fact if γ and $\tilde{\gamma}$ are put equal to unity, (11) reduces to (3) and (13) becomes an identity. Denoting RT_1 and RT_2 by λ, equations (1), (2), (3), and (6) become

$$p_1\left[K_1-\frac{C(1-z)}{\delta}-CN_1\eta\right]=CN_1\lambda, \tag{14}$$

$$p_2[K_2+Ax-CN_2\eta]=CN_2\lambda, \tag{15}$$

$$C\frac{dz}{dt}=C\frac{dN_1}{dt}+\frac{\psi S_1 p_1}{\lambda^{\frac{1}{2}}}+\frac{\psi S_2 p_1}{\lambda^{\frac{1}{2}}}, \tag{16}$$

$$C\frac{dN_2}{dt}=\frac{\psi S_2 p_1}{\lambda^{\frac{1}{2}}}. \tag{17}$$

The seven equations (8), (9), (10), (14), (15), (16), and (17) constitute the system of equations for this model. The integration of this system will be discussed in section 4.

3.2. *R.C.L. H./L. gun. Non-isothermal model. After charge is burnt*

After all the charge is burnt $z=1, f=0$ and equations (1), (3), and (11) are modified to

$$p_1[K_1-CN_1\eta]=CN_1RT_1, \tag{18}$$

$$C\frac{dN_1}{dt}+\frac{\psi S_1 p_1}{(RT_1)^{\frac{1}{2}}}+\frac{\psi S_2 p_1}{(RT_1)^{\frac{1}{2}}}=0, \tag{19}$$

$$\frac{d}{dt}(N_1T_1)+[\gamma+(\gamma-1)\epsilon]\left[\frac{\psi S_1 p_1}{CR}(RT_1)^{\frac{1}{2}}+\frac{\psi S_2 p_1}{CR}(RT_1)^{\frac{1}{2}}\right]=0. \tag{20}$$

The seven equations (2), (6), (8), (13), (18), (19), and (20) constitute the system of equations for this model. The integration of this model for the case $\eta=0$, $\epsilon=0$ will be discussed in section 5.

3.3. *H./L. gun. Non-isothermal model. Before charge is burnt*

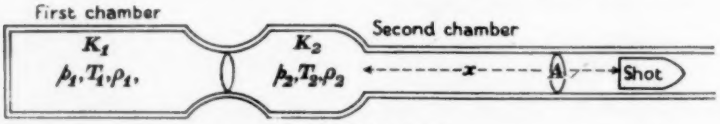

FIG. 2. H./L. gun

This case is obtained by putting in the general system of equations

$$S_1=0, \qquad N_2=z-N_1,$$

so that (3) and (6) become identical and equations (2), (3), (11), and (13) are modified to

$$p_2[K_2+Ax-C(z-N_1)\eta]=C(z-N_1)RT_2, \tag{21}$$

$$C\frac{dz}{dt} = C\frac{dN_1}{dt} + \frac{\psi S_2 p_1}{(RT_1)^{\frac{1}{2}}}, \tag{22}$$

$$\frac{d}{dt}(N_1 T_1) = T_0\frac{dz}{dt} - [\gamma+(\gamma-1)\epsilon]\frac{\psi S_2 p_1}{CR}(RT_1)^{\frac{1}{2}}, \tag{23}$$

$$\frac{d}{dt}[(z-N_1)T_2] = -\frac{Ap_2}{CR}(\bar{\gamma}-1)\frac{dx}{dt} + [\gamma+(\gamma-1)\epsilon]T_1\frac{d}{dt}(z-N_1). \tag{24}$$

The eight equations (1), (8), (9), (10), (21), (22), (23), (24) constitute the system of equations for the model. Its integration for a tubular charge with a linear law of burning has been discussed by Kapur (**10**).

3.4. *H./L. gun. Semi-non-isothermal model. Before charge is burnt*

In this model, the temperature T_1 in the first chamber is assumed constant, while temperature T_2 is assumed to vary. The first assumption replaces (23). Denoting the constant RT_1 by λ (24) is replaced by

$$\frac{d}{dt}[(z-N_1)(RT_2-\lambda)] = -\frac{Ap_2}{CR}(\bar{\gamma}-1)\frac{dx}{dt}. \tag{25}$$

The seven equations (8), (9), (10), (14), (21), (22), and (25) constitute the system of equations for the model. From (8) and (25)

$$\frac{d}{dt}[C(z-N_1)(RT_2-\lambda)] = -(\bar{\gamma}-1)W_2\frac{dx}{dt}\frac{d^2x}{dt^2}. \tag{26}$$

This is similar to the form of the energy equation derived by Aggarwal (**11**). He also discusses the integrations of the system for the linear law of burning.

3.5. *H./L. gun. Isothermal model. Before charge is burnt*

In the model T_1 and T_2 are assumed constant and to be the same. These two assumptions replace (23) and (24). Denoting RT_1 and RT_2 by λ, (21) is modified to

$$p_2[K_2+Ax-C(z-N_1)\eta] = C(z-N_1)\lambda. \tag{27}$$

The six equations (8), (9), (10), (14), (22), and (27) constitute the system of equations for the model. These are identical with the equations first deduced by Corner (**1**, **4**). Corner discussed the integration for this system for the linear law for a tubular charge. The integration for the more general form-function (10) has been studied by Aggarwal (**12**, **13**) and Kapur (**14**). Its integration for the general linear law has also been discussed by Kapur (**14**).

3.6. *H./L. gun. Non-isothermal model. After charge is burnt*

In this case $z = 1, f = 0$, and (21), (22), (23), and (24) are modified to

$$p_2[K_2+Ax-C(1-N_1)\eta] = C(1-N_1)RT_2, \tag{28}$$

$$\frac{dN_1}{dt} = -\frac{\psi S_1 p_1}{C(RT_1)^{\frac{1}{2}}}, \tag{29}$$

$$\frac{d}{dt}(N_1T_1) = -[\gamma+(\gamma-1)\epsilon]\frac{\psi S_1 p_1}{CR}(RT_1)^{\frac{1}{2}}, \tag{30}$$

$$\frac{d}{dt}[(1-N_1)T_2] = -\frac{Ap_2}{CR}(\bar{\gamma}-1)\frac{dx}{dt} - [\gamma+(\gamma-1)\epsilon]T_1\frac{dN_1}{dt}. \tag{31}$$

The six equations (8), (18), (28), (29), (30), and (31) constitute the system of equations for this model. This model was first discussed by Corner (**4**), but he overlooked the energy entering from the first chamber into the second. Consequently his energy equation corresponding to (31) did not contain the last term in the right-hand side of (31). The corrected equation was used in the discussion of the same problem in Kapur (**10**).

3.7. *Recoilless gun*

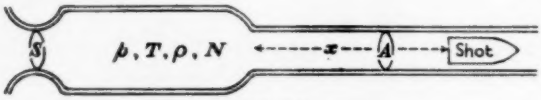

FIG. 3. R.C.L. gun

In this case

$$S_1 = S, \quad p_1 = p_2 = p, \quad T_1 = T_2 = T, \quad \rho_1 = \rho_2 = \rho, \quad N_1+N_2 = N.$$

We note that since $p_1 = p_2$ from (4a), the rate of mass flow from one chamber to the other vanishes and the term corresponding to this vanishes from (3). From (1) and (2) we get

$$p\left[K+Ax-\frac{C(1-z)}{\delta}-CN\eta\right] = CNRT, \tag{32}$$

from (7),

$$C\frac{dz}{dt} = C\frac{dN}{dt}+\frac{\psi Sp}{(RT)^{\frac{1}{2}}}, \tag{33}$$

and from (11) and (13),

$$\frac{d}{dt}(NT) = T_0\frac{dz}{dt}-\frac{\gamma\psi Sp}{CR}(RT)^{\frac{1}{2}}-\frac{Ap(\bar{\gamma}-1)}{CR}\frac{dx}{dt}. \tag{34}$$

The six equations (8), (9), (10), (32), (33), and (34) constitute the system of equations for a R.C.L. gun. These are the same as the equations for a leakirg gun obtained by Corner (**3**) except that instead of (32) Corner gives

$$p\left[K+Ax-\frac{C(1-z)}{\delta}-CN\eta\right] = CNRT\left(1+\frac{kCN}{6W}\right). \tag{33a}$$

The difference with this equation, as well as his definition of W_2, is due to his taking into account Lagrange's relation for the variations of pressure inside the chamber. The integration of this system of equations has been discussed by Corner (3).

3.8. *Orthodox gun*

FIG. 4. Orthodox gun

In this case

$$S_1 = 0, \quad p_1 = p_2 = p, \quad T_1 = T_2 = T, \quad \rho_1 = \rho_2 = \rho, \quad N_1 + N_2 = N = z.$$

Also since $p_1 = p_2$ from (4 a), the rate of mass flow from first chamber into the second vanishes and the corresponding term in (3) disappears. From the equations (1), (3), (11), and (13), we get

$$p\left[K + Ax - \frac{C}{\delta} + Cz\left(\frac{1}{\delta} - \eta\right)\right] = CzRT, \tag{35}$$

$$\frac{d}{dt}(zT) = T_0\frac{dz}{dt} - (\bar{\gamma}-1)\frac{Ap}{CR}\frac{dx}{dt}. \tag{36}$$

From (8), (35), and (36)

$$\frac{d}{dt}\left\{p\left[K + Ax - \frac{C}{\delta} + Cz\left(\frac{1}{\delta} - \eta\right)\right]\right\} = CF\frac{dz}{dt} - (\bar{\gamma}-1)W_2\frac{dx}{dt}\frac{d^2x}{dt^2},$$

which on integration gives

$$CFz = p\left[A(x+l) - Cz\left(\eta - \frac{1}{\delta}\right)\right] + \tfrac{1}{2}(\bar{\gamma}-1)W_2 v^2, \tag{37}$$

where

$$Al = K - \frac{c}{\delta},$$

and v denotes the velocity of the projectile. The four equations (8), (9), (10), and (37) give the standard equations for internal ballistics for an orthodox gun.

3.9. *Solid-fuel rocket*

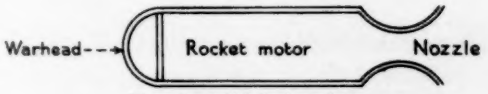

FIG. 5. Solid-fuel rocket

Here

$$S_1 = S, \quad S_2 = 0, \quad p_1 = p_2 = p, \quad T_1 = T_2 = T,$$
$$\rho_1 = \rho_2 = \rho, \quad N_1 + N_2 = N, \quad x = 0.$$

Except for $x = 0$ the conditions are the same as those for a R.C.L. gun. Thus the equations for a solid-fuel rocket can be deduced from those of section 3.7 by putting $x = 0$ in (32) and (34) so that

$$p\left[K - \frac{C(1-z)}{\delta} - CN\eta\right] = CNRT, \tag{38}$$

$$\frac{d}{dt}(NT) = T_0\frac{dz}{dt} - \frac{\gamma\psi Sp}{CR}(RT)^{\frac{1}{2}}. \tag{39}$$

The five equations (9), (10), (33), (38), and (39) constitute the system of equations for a solid-fuel rocket. The connexion between the theory of recoilless guns and solid-fuel rockets was first noticed in Kapur (**15**). The system was also integrated, both before and after the charge is burnt, with special reference to obtaining the equation of the pressure-time curve.

4. R.C.L. H./L. gun. Isothermal model before charge is burnt

Equations (8), (9), (10), (14), (15), (16), and (17) constitute the system of equations for the model. We consider their integration for the usual linear law of burning, so that (9) becomes

$$D\frac{df}{dt} = -\beta p_1. \tag{9a}$$

4.1. *Integration of the equations. Maximum pressure in the first chamber*

From (9a) and (16),

$$\frac{dz}{dt} = \frac{dN_1}{dt} - \Psi_1\frac{df}{dt} - \Psi_2\frac{df}{dt}, \tag{40}$$

where

$$\Psi_1 = \frac{\psi S_1 D}{C\beta\lambda^{\frac{1}{2}}}, \qquad \Psi_2 = \frac{\psi S_2 D}{C\beta\lambda^{\frac{1}{2}}}, \tag{41}$$

are the two dimensionless leakage parameters. Integrating, remembering that initially $z = 0$, $N_1 = 0$, $f = 1$, we have

$$N_1 = z - (\Psi_1 + \Psi_2)(1-f). \tag{42}$$

Similarly from (9a) and (17)

$$N_2 = \Psi_2(1-f). \tag{43}$$

From (42) and (43),

$$z = N_1 + N_2 + \Psi_1(1-f) \tag{44}$$

and from (10), (14), and (42),

$$p_1 = \frac{C\lambda[\phi(f) - (\Psi_1+\Psi_2)(1-f)]}{[K_1 - C/\delta + (C/\delta)\phi(f) - C\eta\phi(f) + C\eta(\Psi_1+\Psi_2)(1-f)]}. \tag{45}$$

Hence

$$\frac{1}{\lambda C}\frac{dp_1}{df} = \frac{\begin{array}{r}(K_1 - C/\delta)(\phi'(f) + \Psi_1 + \Psi_2) + \\ + C/\delta(\Psi_1+\Psi_2)\{\phi(f) + (1-f)\phi'(f)\}\end{array}}{\begin{array}{r}\{K_1 - C/\delta + (C/\delta)\phi(f) - C\eta\phi(f) + \\ + C\eta(\Psi_1+\Psi_2)(1-f)\}^2\end{array}}. \tag{46a}$$

For the form $z = (1-f)(1+\theta f)$

$$\frac{1}{\lambda C}\left[\frac{dp_1}{df}\right]_{\substack{z=1\\f=0}} = \frac{(K_1-C/\delta)(-1+\theta+\Psi_1+\Psi_2)+(C/\delta)\theta(\Psi_1+\Psi_2)}{\{K_1-C\eta+C\eta(\Psi_1+\Psi_2)\}^2}. \quad (46\,b)$$

For a tubular charge [$\theta = 0$], when all the charge is burnt, dp_1/df has same sign as $-1+\Psi_1+\Psi_2$. Thus if

$$\Psi_1+\Psi_2 > 1, \quad (47\,a)$$

the maximum pressure occurs before all the charge is burnt, and if

$$\Psi_1+\Psi_2 \leqslant 1, \quad (47\,b)$$

it occurs at all-burnt stage.

However, from (42), for a tubular charge

$$N_1 = (1-f)(1-\Psi_1-\Psi_2).$$

Thus if our equations are to remain valid (47 b) must be satisfied and for a tubular charge in a R.C.L. H./L. gun, the maximum pressure would definitely have to occur at the all-burnt stage.

If (47 a) were satisfied, it would imply, using (40), that the rate of escape of the gases from the first chamber is greater than the rate of production of gases, which is physically impossible. From (41), $\Psi_1+\Psi_2$ is proportional to S_1+S_2, so that in this case the nozzle throat areas would be too big to allow any accumulation of gases in the first chamber.

For an ordinary H./L. gun $\Psi_1 = 0$ and Ψ_2 is of the order of 0·5 and (47 b) is satisfied. Thus there also the maximum pressure in the first chamber occurs at the all-burnt stage.

For a cord charge ($\theta = 1$), dp_1/df is essentially positive at all-burnt and therefore maximum pressure occurs definitely before all-burnt. This result is also the same as for orthodox and for ordinary H./L. gun.

For the quadratic form-function, the condition that maximum pressure occurs before the all-burnt stage is

$$\Theta > \frac{(K_1-C/\delta)(1-\Psi_1-\Psi_2)}{(K_1-C/\delta)+(C/\delta)(\Psi_1+\Psi_2)}. \quad (48)$$

For a general form-function, the corresponding condition, from (46 a), is

$$K_1[\Psi_1+\Psi_2]+\left[K_1-\frac{C}{\delta}+\frac{C}{\delta}(\Psi_1+\Psi_2)\right]\phi'(0) > 0. \quad (49)$$

If $\Psi_1 = 0$, $\Psi_2 = \Psi$, (48) and (49) reduce to the corresponding conditions for ordinary H./L. guns (Kapur (**10**)). If (49) is satisfied, the maximum pressure occurs when

$$\left[K_1-\frac{C}{\delta}\right][\phi'(f)+\Psi_1+\Psi_2]+\frac{C}{\delta}[\Psi_1+\Psi_2][\phi(f)+(1-f)\phi'(f)] = 0. \quad (50)$$

The root between 0 and 1 determines the value of f at which maximum pressure occurs in the first chamber and then, substituting this value in (45), we get the value of the maximum pressure.

4.2. *Second chamber. Fundamental differential equation*

From (8) and (9),

$$\frac{d}{df}\left[p_1\frac{dx}{df}\right]=\frac{AD^2}{W_2\beta^2}\left(\frac{p_2}{p_1}\right).$$

Substituting for p_1, p_2 from (15), (43), and (45), we get

$$\frac{d}{df}\left\{\frac{\phi(f)-(1-f)(\Psi_1+\Psi_2)}{K_1-C/\delta-C(\eta-1/\delta)\phi(f)+C\eta(\Psi_1+\Psi_2)(1-f)}\frac{dx}{df}\right\}$$
$$=\left[\frac{AD^2}{W_2\beta^2}\frac{1}{C\lambda}\frac{\Psi_2(1-f)}{K_2+Ax-C\eta\Psi_2(1-f)}\right]\times$$
$$\times\left[\frac{K_1-C/\delta-C(\eta-1/\delta)\phi(f)+C\eta(\Psi_1+\Psi_2)(1-f)}{\phi(f)-(1-f)(\Psi_1+\Psi_2)}\right]. \quad (51)$$

For a tubular charge $\phi(f)=1-f=z$, this becomes

$$\frac{d}{dz}\left[\frac{z}{1+bz}\frac{dX}{dz}\right]=\frac{1+bz}{X-\nu z}, \quad (52)$$

where

$$\left.\begin{aligned} b&=\frac{C[1/\delta-\eta(1-\Psi_1-\Psi_2)]}{K_1-C/\delta}\\ \mu X&=K_2+Ax\\ \mu\nu&=C\eta\Psi_2\\ \mu^2&=\frac{A^2D^2}{\beta^2}\frac{(K_1-C/\delta)^2\Psi_2}{C\lambda W_2(1-\Psi_1-\Psi_2)^2}\end{aligned}\right\}. \quad (53)$$

(52) is the same as the corresponding equation of Corner (**4**) for H./ L. gun, only h and ν have to be adjusted. Corner's series solution for (52) as well as his numerical solution in powers of b and ν can be used here.

For a cord charge $\phi(f)=1-f^2$ and (51) can be integrated in series. Solutions given by Aggarwal (**12**) as modified by Kapur (**14**) can be easily adapted for this case.

Once we know X (or x) and dX/dz (or dx/df) as functions of f, we can find N_1 from (42), N_2 from (43), p_1 from (45), p_2 from (15), and

$$v=\frac{dx}{df}\frac{df}{dt}=-\frac{\beta}{D}p_1\frac{dx}{df}$$

from the knowledge of p_1 and dx/df. Also, from (9) and (45),

$$-\frac{\beta}{D}=\int_f^1\frac{[K_1-C/\delta+C/\delta\phi(f)-C\eta\phi(f)+C\eta(\Psi_1+\Psi_2)(1-f)]}{C\lambda[\phi(f)-(\Psi_1+\Psi_2)(1-f)]}df. \quad (54)$$

When $\phi(f) = 1-f$ or $(1-f)(1+\theta f)$, we easily get explicit relations between f and t, on evaluating the integral on the right-hand side of (54).

5. R.C.L. H./L. gun. Non-isothermal model after charge is burnt

While the isothermal model gives a more or less satisfactory solution before the charge is burnt, it breaks down completely after the charge is burnt as gases cool off considerably due to expansion.

Neglecting co-volume terms, the system of equation is given by (6), (8), (19), and the following:

$$p_1 K_1 = CN_1 RT_1, \tag{55}$$

$$p_2[K_2+Ax] = CN_2 RT_2, \tag{56}$$

$$\frac{d}{dt}(N_1 T_1) = -\gamma\left[\frac{\psi S_1 p_1}{CR}+\frac{\psi S_2 p_1}{CR}\right](RT_1)^{\frac{1}{2}}, \tag{57}$$

$$\frac{d}{dt}(N_2 T_2) = -\frac{Ap_2}{CR}(\bar{\gamma}-1)\frac{dx}{dt}+\gamma T_1\frac{dN_2}{dt}. \tag{58}$$

From (19) and (57), we get on integration

$$\left(\frac{N_1}{N_{1,B}}\right)^{\gamma-1} = \frac{T_1}{T_{1,B}}. \tag{59}$$

Again from (6) and (19), we get an integration

$$N_2-N_{2,B} = -\frac{S_2}{S_1+S_2}(N_1-N_{1,B}). \tag{60}$$

From (19), (55), and (59),

$$\frac{dT_1}{dt} = -mT_1^{\frac{1}{2}}, \tag{61}$$

where $$m = \frac{R^{\frac{1}{2}}\psi(S_1+S_2)}{K_1}\left(\frac{\gamma-1}{C}\right).$$

Integrating, $$T_1 = T_{1,B}\left[1+\frac{t-t_B}{\Theta_1}\right]^{-2}, \tag{62}$$

where $$\Theta_1 = \frac{2}{mT_{1,B}^{\frac{1}{2}}}.$$

From (55), (59), and (60),

$$\frac{p_1}{p_{1,B}} = \left[1+\frac{t-t_B}{\Theta_1}\right]^{-2\gamma/(\gamma-1)}, \tag{63}$$

$$\frac{N_1}{N_{1,B}} = \left[1+\frac{t-t_B}{\Theta_1}\right]^{-2/(\gamma-1)}. \tag{64}$$

From (8) and (58), we get an integration

$$N_2 T_2 - N_{2,B} T_{2,B} = -\frac{\tilde{\gamma}-1}{2CR} W_2 \left\{ \left(\frac{dx}{dt}\right)^2 - \left(\frac{dx}{dt}\right)_B^2 \right\} - \\ - \frac{\psi S_2}{C\sqrt{R}} \gamma p_{1,B} T_{1,B}^{\frac{1}{2}} \frac{\gamma-1}{2\gamma} \Theta_1 \left\{ \left(1+\frac{t-t_B}{\Theta_1}\right)^{-2\gamma/(\gamma-1)} - 1 \right\}. \quad (65)$$

If we use the isothermal model before the charge is burnt, (42), (43) give

$$N_{1,B} = 1 - \Psi_1 - \Psi_2, \qquad N_{2,B} = \Psi_2. \quad (66)$$

Also denoting $RT_{1,B}$ and $RT_{2,B}$ by λ (65) can be written as

$$\frac{C\lambda}{\gamma-1}[\Psi_2 - N_2 T_2'] = \tfrac{1}{2} W_2 \left[\left(\frac{dx}{dt}\right)^2 - \left(\frac{dx}{dt}\right)_B^2 \right] + \\ + \frac{\lambda^{\frac{1}{2}} p_{1,B} \psi S_2 \Theta_1}{2} \left\{ \left(1+\frac{t-t_B}{\Theta_1}\right)^{2\gamma/(\gamma-1)} - 1 \right\} \quad (67)$$

where T_2' is the ratio of the gas temperature to the mean value it had during burning.

When $\Psi_1 = 0$, $\Psi_2 = \Psi$ we expect (67) to reduce to an energy equation after the charge is burnt for a H./L. gun. We find that the corresponding equation of Corner (**1**, **3**) differs from (67) inasmuch as it does not contain the last term on the right-hand side of (67), which shows that he has neglected there the contribution of elements of gas entering from the first chamber into the second.

Concluding remarks

We have in the present paper, written a very general system of equations of internal ballistics for the recoilless high-low pressure gun and deduced the equations for R.C.L., H./L., orthodox guns, and solid-fuel rockets as particular cases. Before the all-burnt stage, the isothermal model has been studied completely for the R.C.L. H./L. gun, and the solution for this model for other guns and rockets can be easily deduced. After the all-burnt stage the model breaks down and the non-isothermal model has been studied.

The isothermal model has been used in Kapur (**16**) to study the equivalent non-leaking ballistic problem. The integration of the non-isothermal model has also been studied there for the particular case of a tubular charge for the linear law and certain interesting results regarding the variation of T_1, N_1, $N_1 T_1$ have been obtained. Once we integrate the non-isothermal model for the general law of burning and for the general form-function, the main step towards a unified theory would have been taken. The difficulties are however obvious, as satisfactory solutions, even in particular cases, have yet to be discovered.

Other problems which are under investigation are (i) the effect of

Lagrange's corrections, and (ii) the effect of bore resistance in the present unified theory. The second problem is being attacked on the lines used by Corner (**17**) for the orthodox gun.

Acknowledgements

I am grateful to Professor D. S. Kothari, Scientific Adviser to Ministry of Defence, Government of India and to Dr. R. S. Varma, Chief Scientist, Defence Science Laboratories, New Delhi, for their interest, and to Professor P. L. Bhatnagar, Head of the Department of Applied Mathematics, Indian Institute of Sciences, Bangalore and to Dr. J. Corner for their valuable advice on many important points.

REFERENCES

1. J. Corner, *Theory of Interior Ballistics of Guns* (New York, 1950), chapters v, vii, viii.
2. H.M.S.O., *Internal Ballistics* (London, 1951), chapters viii, ix, x.
3. J. Corner, 'Internal ballistics of a leaking gun', *Proc. Roy. Soc.* A, **188** (1947), 237.
4. —— *A Theory of the Internal Ballistics of the High-Low Pressure Gun* (J. Frank. Inst., 1948), p. 246.
5. B. Crawford, *Rocket Fundamentals*, N.D.R.C. Division 3, Section H.O.S.R.D. No. 3711 (1944), chapter iii.
6. Trubridge, *Theory of Internal Ballistics of Rockets* (*Solid Propellants*) (Ministry of Supply, London, 1951), chapters i, ii, iii.
7. R. Wimpress, *Internal Ballistics of Solid-Fuel Rockets* (New York, 1951), chapters iv, v, vi.
8. D. S. Kothari, 'Internal ballistics of a leaking gun', *Def. Sci. J.* **3** (1953).
9. J. N. Kapur, 'Internal ballistics of a H./L. gun', ibid. (in press).
10. —— 'Internal ballistics of a H./L. gun. Non-isothermal model', *Proc. Ind. Soc. Th. App. Mech.* **2** (1956).
11. S. P. Aggarwal, 'Internal ballistics of a H./L. gun. Non-isothermal model, *Proc. Nat. Inst. Sci. Ind.* **23** A (1957).
12. —— 'Internal ballistics of a H./L. gun', ibid. **21** A (1955) 350.
13. —— 'Internal ballistics of a H./L. gun for general form-function', ibid. **23** A (1957).
14. J. N. Kapur, 'Internal ballistics of a H./L. gun', ibid. **23** A (1957).
15. —— 'Pressure-time curve in internal ballistics of solid-fuel rockets, ibid. **23** A (1957) 150.
16. —— 'Internal ballistics of R.C.L. H./L. gun', *Applied Scientific Research* Holland **6** A (1957) 445.
17. J. Corner, 'The ballistic effects of bore resistance', *Quart. J. Mech. App. Math.* **2** (1949), 232.

ON THE THEORY OF ANISOTROPIC OBSTACLES IN CAVITIES†

By WALTER HAUSER

(*Staff Member, Lincoln Laboratory, M.I.T. Lexington, Massachusetts*)

[Received 7 February 1957.—Revise received 6 June 1957]

SUMMARY

Variational expressions for the resonant frequencies of a cavity containing a material with tensor electromagnetic properties are derived. The relationship of the variational expressions to the Bethe–Schwinger perturbation formula is shown. The advantage of this method over the Bethe–Schwinger perturbation method is discussed.

1. Introduction

MICROWAVE measurements of the electromagnetic properties of materials usually involve the effect of a perturbation of a microwave cavity or waveguide by a small sample of the material. Needless to say, the assumption that the material possesses a tensor electric permittivity and (or) magnetic permeability further complicates an already difficult problem. With the increased interest in recent years in the properties and application of ferrites in microwave work, one is confronted with the problem of obtaining at least approximate solutions to the problem of a cavity or waveguide perturbed by an anisotropic obstacle. Perturbation formulae (**1**) into which one substitutes the approximation that the fields equal the unperturbed solution or some other suitably chosen fields, have been partially successful in obtaining first order results. Perturbation theory however, is not completely satisfactory since higher order results are in general tedious to obtain, and first order results alone may not be sufficiently accurate.

This paper is the second (**2**) of a group of papers in which we concern ourselves with the development and application of a general method for obtaining approximate solutions to the problems of waveguides and cavities containing materials with tensor electromagnetic properties. The method is an extension of the work of Julian Schwinger (**3**) on the theory of obstacles in waveguides and cavities to anisotropic media. In each case with the introduction of an appropriate dyadic Green's function we are able to obtain a formal solution to the problem in terms of integrals involving the field vectors in the perturbing medium. While the resulting integral equations are by no means easier to solve, there exists the advantage of being able to construct stationary expressions for the quantities of interest

† The research reported in this document was supported jointly by the Army, Navy, and Air Force under contract with Massachusetts Institute of Technology.

from which the integral equations for the fields within the perturbing medium are derivable. Consequently, we have a very powerful method for obtaining approximate solutions for these quantities.

In this paper, for example, we concern ourselves with the problem of a cavity perturbed by an anisotropic material. We show that in this case the first order variation of $(\omega_0^2-\omega^2)$, the difference between the square of the resonant frequencies of the empty and loaded cavity, is zero with respect to similar variations of the fields in the perturbing medium. Berk (4) has treated this problem, obtaining variational principles which yield the differential equations satisfied by the electromagnetic field. His expressions, however, are not applicable to dissipative media, and furthermore require a knowledge of the fields over the entire cavity or guide.

While the full use of the variational method consists of the substitution of trial functions with unknown variational parameters followed by the calculation of the stationary quantity, we may at times obtain good first-order results by simply substituting completely determined trial functions. In such cases we show how the variational expression reduces to the Bethe–Schwinger perturbation formula (5) with the additional advantage of yielding the best amplitude for the trial field.

2. Integral equations and first variational principle for the electromagnetic field

We consider the problem of an anisotropic obstacle within a cavity free of charges and currents. The fields within the cavity satisfy the differential equations

$$\nabla\wedge\mathbf{E} = -j\omega\mu_0\mathbf{H}-j\omega\boldsymbol{\mu}'.\mathbf{H},$$
$$\nabla\wedge\mathbf{H} = j\omega\epsilon_0\mathbf{E}+j\omega\boldsymbol{\epsilon}'.\mathbf{E} \qquad (1)$$

where ϵ_0 and μ_0 are respectively the unperturbed constant scalar electric permittivity and magnetic permeability. Their choice depends on the problem in hand. In the case of obstacles occupying but part of the cavity they will be chosen equal to the electric permittivity and magnetic permeability of the empty cavity. The tensor electric permittivity, $\boldsymbol{\epsilon}$, and the tensor magnetic permeability, $\boldsymbol{\mu}$, of the obstacle are given by

$$\boldsymbol{\epsilon} = \epsilon_0\mathbf{I}+\boldsymbol{\epsilon}',$$
$$\boldsymbol{\mu} = \mu_0\mathbf{I}+\boldsymbol{\mu}',$$

where $\mathbf{I}$ is the unit dyadic.

Here $\boldsymbol{\epsilon}'$ and $\boldsymbol{\mu}'$ are functions of position, and are zero in the region outside the obstacle. We assume an $e^{j\omega t}$ time dependence and observe that the fields obey the vector wave equations

$$\nabla\wedge\nabla\wedge\mathbf{E}-\omega^2\epsilon_0\mu_0\mathbf{E} = \omega^2\mu_0\boldsymbol{\epsilon}'.\mathbf{E}-j\omega\nabla\wedge(\boldsymbol{\mu}'.\mathbf{H}), \qquad (2a)$$
$$\nabla\wedge\nabla\wedge\mathbf{H}-\omega^2\epsilon_0\mu_0\mathbf{H} = \omega^2\epsilon_0\boldsymbol{\mu}'.\mathbf{H}+j\omega\nabla\wedge(\boldsymbol{\epsilon}'.\mathbf{E}). \qquad (2b)$$

In setting up the variational expression from which one obtains the integral equations satisfied by the fields, we shall also require a knowledge of the adjoint fields, $\mathbf{E}^\dagger$ and $\mathbf{H}^\dagger$, which we choose as the solutions of the equations

$$\begin{aligned} \nabla \wedge \mathbf{E}^\dagger &= j\omega\mu_0 \mathbf{H}^\dagger + j\omega \mathbf{H}^\dagger . \boldsymbol{\mu}' \\ \nabla \wedge \mathbf{H}^\dagger &= -j\omega\epsilon_0 \mathbf{E}^\dagger - j\omega \mathbf{E}^\dagger . \boldsymbol{\epsilon}' \\ \nabla . \mathbf{B}^\dagger &= \nabla . \mathbf{D}^\dagger = 0. \end{aligned} \tag{3}$$

In those problems where $\boldsymbol{\epsilon}$ and $\boldsymbol{\mu}$ are hermitian, we find that $\mathbf{H}^\dagger = \mathbf{H}^*$ and $\mathbf{E}^\dagger = \mathbf{E}^*$. In the case of dissipative ferrites, we find

$$\mathbf{H}^\dagger(x, y, z, \omega) = \mathbf{H}(x, y, z, -\omega)$$

and

$$\mathbf{E}^\dagger(x, y, z, \omega) = \mathbf{E}(x, y, z, -\omega)$$

as the off diagonal elements of the antisymmetric magnetic permeability tensor are odd in ω, and the diagonal elements are even in ω (**6**).

To solve equation (2 a) we introduce the electric dyadic Green's function (**3, 7**) which satisfies the differential equation

$$\nabla \wedge \nabla \wedge \mathbf{N}^\dagger \quad k^2 \mathbf{N}^\dagger = \mathbf{I}\delta(\mathbf{r} - \mathbf{r}') \tag{4}$$

and the boundary condition

$$\mathbf{n} \wedge \mathbf{N}^\dagger(\mathbf{r} \mid \mathbf{r}') = 0$$

when $\mathbf{r}$ lies on the boundary of the cavity.

Multiplying equation (2 a) by $\mathbf{N}_a^\dagger = \mathbf{N}^\dagger \mathbf{a}$, where $\mathbf{a}$ is an arbitrary vector introduced in order to simplify the handling of the dyadic Green's function, equation (4) by $\mathbf{E}(\mathbf{r})$ and subtracting the result, we find, after integrating over the volume of the cavity, that

$$\mathbf{E}(\mathbf{r}') = \omega^2 \mu_0 \int (\boldsymbol{\epsilon}' . \mathbf{E}) . \mathbf{N}^\dagger(\mathbf{r} \mid \mathbf{r}')\, d\tau - j\omega \int (\boldsymbol{\mu}' . \mathbf{H}) . [\nabla \wedge \mathbf{N}^\dagger(\mathbf{r} \mid \mathbf{r}')]\, d\tau. \tag{5}$$

In those problems where $\mathbf{E}(\mathbf{r}')$ is everywhere divergenceless, we shall also choose the electric dyadic Green's function to be divergenceless.

The normal mode expansion of the dyadic Green's function as obtained by Schwinger (**3**), is

$$\mathbf{N}^\dagger(\mathbf{r} \mid \mathbf{r}') = \sum_n \frac{\mathbf{E}_n^\dagger(\mathbf{r}) \mathbf{E}_n(\mathbf{r}')}{(k_n^2 - k^2)\Lambda_n^2} - \frac{1}{k^2} \sum_n \frac{\mathbf{f}_n^\dagger(\mathbf{r}) \mathbf{f}_n(\mathbf{r}')}{\Omega_n^2}, \tag{6}$$

where $\mathbf{E}_n$ and $\mathbf{f}_n$ are respectively the divergenceless and curl-less vector eigenfunctions of the empty cavity which satisfy the differential equation

$$\nabla \wedge \nabla \wedge \mathbf{A}_n - k_n^2 \mathbf{A}_n = 0$$

and have zero tangential components on the surface of the cavity; Λ_n and Ω_n are normalization constants, k_n^2 the eigenvalues, and

$$\mathbf{A}_n^\dagger(\mathbf{r}, \omega_n) = \mathbf{A}_n(\mathbf{r}, -\omega_n).$$

In those regions where $\mathbf{E}(\mathbf{r})$ is divergenceless we shall omit the second sum in the normal mode expansion of the dyadic Green's function, except for the curl-less eigenfunction, $\mathbf{f}_0$, which is also divergenceless.

To solve for the magnetic field, we may utilize equation (1) or repeat the above steps utilizing equation (2 b) and the magnetic dyadic Green's function (3). It is readily shown that the two methods are equivalent (3).

In terms of the normal mode expansion of the dyadic Green's function we have

$$\mathbf{E}(\mathbf{r}') = \sum_{n=0}^{\infty} \frac{J_n^e \mathbf{E}_n(\mathbf{r}')}{(k_n^2 - k^2)} - \frac{\omega^2 \mu_0}{k^2} \sum_{n=0}^{\infty} \frac{\left(\int \mathbf{f}_n^\dagger \cdot \boldsymbol{\epsilon}' \cdot \mathbf{E}\, d\tau \right)}{\Omega_n^2} \mathbf{f}_n(\mathbf{r}'), \tag{7}$$

where
$$J_n^e = \frac{\omega \mu_0}{\Lambda_n^2} \left[\omega \int \mathbf{E}_n^\dagger \cdot \boldsymbol{\epsilon}' \cdot \mathbf{E}\, d\tau + \omega_n \int \mathbf{H}_n^\dagger \cdot \boldsymbol{\mu}' \cdot \mathbf{H}\, d\tau \right] \tag{8}$$

and
$$j\omega_n \mu_0 \mathbf{H}_n^\dagger = \nabla \wedge \mathbf{E}_n^\dagger.$$

Taking the curl of equation (7) yields

$$\frac{\boldsymbol{\mu}' \cdot \mathbf{H}(\mathbf{r}')}{\mu_0} = \sum_{n=0}^{\infty} \frac{\omega_n}{\omega} \frac{J_n^e \mathbf{H}_n(\mathbf{r}')}{(k_n^2 - k^2)} - \mathbf{H}(\mathbf{r}'). \tag{9}$$

Let us note again that in those regions where $\mathbf{E}(\mathbf{r})$ is divergenceless we shall omit the last sum in equation (7) except for the divergenceless term. Proceeding as above we find that

$$\mathbf{E}^\dagger(\mathbf{r}) = \sum_{n=0}^{\infty} \frac{J_n^{e\dagger} \mathbf{E}_n^\dagger(\mathbf{r})}{(k_n^2 - k^2)} - \frac{\omega^2 \mu_0}{k^2} \sum_{n=0}^{\infty} \frac{\left(\int \mathbf{E}^\dagger \cdot \boldsymbol{\epsilon}' \cdot \mathbf{f}_n\, d\tau \right)}{\Omega_n^2} \mathbf{f}_n^\dagger(\mathbf{r}), \tag{10}$$

where
$$J_n^{e\dagger} = \frac{\omega \mu_0}{\Lambda_n^2} \left[\omega \int \mathbf{E}^\dagger \cdot \boldsymbol{\epsilon}' \cdot \mathbf{E}_n\, d\tau + \omega_n \int \mathbf{H}^\dagger \cdot \boldsymbol{\mu}' \cdot \mathbf{H}_n\, d\tau \right]$$

and
$$\frac{\mathbf{H}^\dagger(\mathbf{r}) \cdot \boldsymbol{\mu}'}{\mu_0} = \sum_{n=0}^{\infty} \frac{\omega_n}{\omega} \frac{J_n^{e\dagger} \mathbf{H}_n^\dagger(\mathbf{r})}{(k_n^2 - k^2)} - \mathbf{H}^\dagger(\mathbf{r}). \tag{11}$$

From the wave equation satisfied by the electromagnetic fields we find that

$$\nabla \cdot [\mathbf{E} \wedge (\nabla \wedge \mathbf{E}_n^\dagger) - \mathbf{E}_n^\dagger \wedge (\nabla \wedge \mathbf{E}) - j\omega \mathbf{E}_n^\dagger \wedge (\boldsymbol{\mu}' \cdot \mathbf{H})] + (k_n^2 - k^2) \mathbf{E}_n^\dagger \cdot \mathbf{E} = \omega \mu_0 [\omega \mathbf{E}_n^\dagger \cdot \boldsymbol{\epsilon}' \cdot \mathbf{E} + \omega_n \mathbf{H}_n^\dagger \cdot \boldsymbol{\mu}' \cdot \mathbf{H}].$$

It follows therefore that

$$J_n^e = (k_n^2 - k^2) \int \mathbf{E}_n^\dagger \cdot \mathbf{E}\, d\tau / \Lambda_n^2.$$

We can fix the amplitude of the field within the obstacle by restricting ourselves to fields satisfying the condition

$$\int \mathbf{E}_0^\dagger \cdot \mathbf{E}\, d\tau = \Lambda_0^2,$$

where $\mathbf{E}_0$ is the unperturbed solution whose perturbation we wish to compute. Thus

$$J_0^e = (k_0^2 - k^2), \tag{12}$$

and multiplying equation (7) by $\mathbf{E}^\dagger . \boldsymbol{\epsilon}'$, equation (9) by $\mathbf{H}^\dagger . \boldsymbol{\mu}'$ and adding yields

$$J_0^{e\dagger} \Lambda_0^2 = D_0^e \omega^2 \mu_0, \tag{13}$$

where

$$D_0^e = \int \mathbf{E}^\dagger . \boldsymbol{\epsilon}' . \mathbf{E}\, d\tau + \int \mathbf{H}^\dagger . \boldsymbol{\mu}' . \mathbf{H}\, d\tau + \frac{1}{\mu_0} \int \mathbf{H}^\dagger . \boldsymbol{\mu}' . \boldsymbol{\mu}' . \mathbf{H}\, d\tau -$$

$$- \frac{1}{\omega^2 \mu_0} \sum_{n \neq 0} \Lambda_n^2 J_n^e J_n^{e\dagger} / (k_n^2 - k^2) +$$

$$+ \sum_n \frac{\omega^2 \mu_0}{k^2 \Omega_n^2} \left[\int \mathbf{f}_n^\dagger . \boldsymbol{\epsilon}' . \mathbf{E}\, d\tau \right] \left[\int \mathbf{E}^\dagger . \boldsymbol{\epsilon}' . \mathbf{f}_n\, d\tau \right]. \tag{14}$$

Utilizing equations (10) and (11) it similarly follows that

$$J_0^e \Lambda_0^2 = D_0^e \omega^2 \mu_0.$$

Integral equations (7), (9), (10), and (11) for the electromagnetic field are by no means easier to solve than the original differential equations. Fortunately, however, we are able to construct a variational principle for the quantity $(k_0^2 - k^2)$, thus being able to obtain approximate solutions for the shift in the resonant frequency.

To construct such a variational principle, we combine equations (12) and (13) to obtain the stationary expression

$$(k_0^2 - k^2) = \frac{\Lambda_0^2}{\omega^2 \mu_0} \frac{J_0^e J_0^{e\dagger}}{D_0^e}. \tag{15}$$

It is readily shown that the first order variation of the right-hand side of equation (15) with respect to the fields, subject to the condition that

$$J_0^e = J_0^{e\dagger} = D_0^e \omega^2 \mu_0 / \Lambda_0^2 \tag{16}$$

yields the integral equations for the electromagnetic fields within the obstacle. Since expression (15) is amplitude-independent this condition is automatically satisfied.

3. Second variational principle

A second variational principle may be obtained from the integral equations satisfied by the electromagnetic field, which utilize the magnetic dyadic Green's function. Quite analogous to the foregoing we find that

$$\frac{\boldsymbol{\epsilon}' . \mathbf{E}(\mathbf{r}')}{\epsilon_0} = \sum_{n=0}^{\infty} \frac{\omega_n}{\omega} \frac{J_n^m \mathbf{E}_n(\mathbf{r}')}{(k_n^2 - k^2)} - \mathbf{E}(\mathbf{r}'), \tag{17}$$

and

$$\mathbf{H}(\mathbf{r}') = \sum_{n=0}^{\infty} \frac{J_n^m \mathbf{H}_n(\mathbf{r}')}{(k_n^2 - k^2)} - \frac{\omega^2 \epsilon_0}{k^2} \sum_{n=0}^{\infty} \frac{\left(\int \mathbf{g}_n^\dagger . \boldsymbol{\mu}' . \mathbf{H}\, d\tau \right) \mathbf{g}_n(\mathbf{r}')}{\eta_n^2}, \tag{18}$$

where $$J_n^m = \frac{\omega\epsilon_0}{\lambda_n^2}\Big[\omega_n \int \mathbf{E}_n^\dagger . \boldsymbol{\epsilon}' . \mathbf{E}\, d\tau + \omega \int \mathbf{H}_n^\dagger . \boldsymbol{\mu}' . \mathbf{H}\, d\tau\Big], \tag{19}$$

and λ_n^2 and η_n^2 are the normalization constants of $\mathbf{H}_n(\mathbf{r})$ and $\mathbf{g}_n(\mathbf{r})$ respectively. The functions $\mathbf{g}_n(\mathbf{r})$ are the curl-less magnetic eigenfunctions of the cavity. In those regions where $\mathbf{H}$ is divergenceless we shall omit the last sum in equation (18), except for the $\mathbf{g}_0$ term which is also divergenceless. Restricting ourselves to trial functions satisfying the condition

$$\int \mathbf{H}_0^\dagger . \mathbf{H}\, d\tau = \lambda_0^2,$$

we find that $$(k_0^2 - k^2) = J_0^m, \tag{20}$$

and $$J_0^m \lambda_0^2 = J_0^{m\dagger} \lambda_0^2 = \omega^2 \epsilon_0 D_0^m, \tag{21}$$

where $$J_n^{m\dagger} = \frac{\omega\epsilon_0}{\lambda_n^2}\Big[\omega_n \int \mathbf{E}^\dagger . \boldsymbol{\epsilon}' . \mathbf{E}_n\, d\tau + \omega \int \mathbf{H}^\dagger . \boldsymbol{\mu}' . \mathbf{H}_n\, d\tau\Big]$$

and

$$D_0^m = \int \frac{\mathbf{E}^\dagger . \boldsymbol{\epsilon}' . \boldsymbol{\epsilon}' . \mathbf{E}}{\epsilon_0} d\tau + \int \mathbf{E}^\dagger . \boldsymbol{\epsilon}' . \mathbf{E}\, d\tau + \int \mathbf{H}^\dagger . \boldsymbol{\mu}' . \mathbf{H}\, d\tau -$$

$$- \frac{1}{\omega^2\mu_0} \sum_{n \neq 0} \frac{\lambda_n^2 J_n^m J_n^{m\dagger}}{(k_n^2 - k^2)} + \sum_n \frac{\omega^2\epsilon_0}{k^2\eta_n^2}\Big(\int \mathbf{g}_n^\dagger . \boldsymbol{\mu}' . \mathbf{H}\, d\tau\Big)\Big(\int \mathbf{H}^\dagger . \boldsymbol{\mu}' . \mathbf{g}_n\, d\tau\Big).$$

The variational expression from which equations (17) and (18), and the corresponding adjoint equations are derivable is

$$(k_0^2 - k^2) = \frac{\lambda_0^2}{\omega^2\epsilon_0} \frac{J_0^m J_0^{m\dagger}}{D_0^m}. \tag{22}$$

We note that had we restricted ourselves to trial fields satisfying the condition

$$\int \mathbf{E}_0^\dagger . \mathbf{E}\, d\tau = \Lambda_0^2 \tag{23}$$

which we used for the first variational principle, we would have found

$$J_0^m = (k_0^2 - k^2) \int \mathbf{H}_0^\dagger . \mathbf{H}\, d\tau / \lambda_0^2 \tag{24}$$

and $$D_0^m = \frac{J_0^m J_0^{m\dagger} \lambda_0^2}{\omega^2\epsilon_0 (k_0^2 - k^2)} = J_n^{m\dagger} \int \mathbf{H}_0^\dagger . \mathbf{H}\, d\tau / \omega^2 \epsilon_0. \tag{25}$$

Variational expression (22), being amplitude independent, remains unaltered.

The fields which make expression (22) an extremum subject to conditions (23) or (25), are the same fields which make expression (15) an extremum.

We can therefore combine equations (12) and (24), utilizing equations (8) and (19), to find that

$$(k_0^2-k^2)\Big[\epsilon_0\Lambda_0^2+\mu_0\int \mathbf{H}_0^{\dagger}.\mathbf{H}\,d\tau\Big] = \omega\epsilon_0\mu_0(\omega+\omega_0)\Big[\int \mathbf{E}_0^{\dagger}.\boldsymbol{\epsilon}'.\mathbf{E}\,d\tau+\int \mathbf{H}_0^{\dagger}.\boldsymbol{\mu}'.\mathbf{H}\,d\tau\Big],$$

or

$$(\omega_0-\omega) = \omega\,\frac{\int \mathbf{E}_0^{\dagger}.\boldsymbol{\epsilon}'.\mathbf{E}\,d\tau+\int \mathbf{H}_0^{\dagger}.\boldsymbol{\mu}'.\mathbf{H}\,d\tau}{\int \epsilon_0\mathbf{E}_0^{\dagger}.\mathbf{E}\,d\tau+\int \mu_0\mathbf{H}_0^{\dagger}.\mathbf{H}\,d\tau}. \tag{26}$$

This is the well known Bethe–Schwinger perturbation formula (**5**) generalized to tensor media. The full use of the variational method consists of the substitution of trial functions with unknown variational parameters with respect to which we then make the variational expression an extremum. We may nevertheless at times obtain good first order results by simply substituting completely determined trial functions into either equation (12) or (20) subject to condition (16) or (21) respectively. Since the variational principle permits the computation of the amplitude of the field within the perturbing medium, we should expect its results to be better than those predicted by the perturbation formula.

I should like to express my appreciation to my colleagues at the Lincoln Laboratory for their stimulation and encouragement. Specifically, I should like to thank Drs. L. Gold, G. S. Heller, B. Lax, and H. J. Zeiger, and Mr. K. J. Button for their interest and help.

REFERENCES

1. J. O. Artman and P. E. Tannenwald, *J.A.P.* **26** (1955) 1124.
2. W. Hauser, *Variational Principles for Guided Electromagnetic Waves in Anisotropic Materials*, M.I.T. Lincoln Laboratory Group Report M35–61, August 1956.
3. J. Schwinger, *The Theory of Obstacles in Resonant Cavities and Waveguides*, M.I.T. Rad. Lab. Report 43–34.
   P. M. Morse and H. Feshbach, *Methods of Theoretical Physics* (McGraw-Hill (1953), vol. ii, ch. xiii.
4. A. D. Berk, *Proc. I.R.E. AP* **4** (1956) 104.
5. H. A. Bethe and J. Schwinger, *Perturbation Theory for Cavities*, Cornell Univ. Contractor's Report D1–117, March 1943.
   J. O. Artman and P. E. Tannenwald, *J.A.P.* **26** (1955) 1124.
6. B. Lax, *Proc. I.R.E.* **44** (1956) 1368.
7. H. Levine and J. Schwinger, 'On the theory of electromagnetic wave diffraction by an aperture in an infinite plane', *Communications on Pure and Applied Mathematics*, **3**, No. 4 (1950).
   R. D. Kodis, 'An introduction to variational methods in electromagnetic scattering', *J. Soc. Indust. Appl. Math.* **2** (1954).

DETERMINATION OF THE OPTIMUM RESPONSE OF LINEAR SYSTEMS

(ZERO-VELOCITY-ERROR AND ZERO-ACCELERATION-ERROR SYSTEMS)†

By A. W. BABISTER (*The University, Glasgow*)

[Received 29 November 1956]

SUMMARY

In (1) two response functions L and L_1 were defined by the equations

$$L = \int_0^\infty e^2\,d\tau \quad \text{and} \quad L_1 = \int_0^\infty \left(\frac{de}{d\tau}\right)^2 d\tau,$$

where e is the error at time τ. In (2) it was shown how these response functions could be used to obtain the optimum response for zero-displacement-error systems. The analysis is here applied to zero-velocity-error and zero-acceleration-error systems. The systems having the optimum response in velocity or in acceleration have a non-zero displacement lag. It is shown how the method can be extended to allow for the requirement of a zero-displacement-error in the final steady state.

1. Introduction

In (1) two response functions L and L_1 were defined by the equations

$$L = \int_0^\infty e^2\,d\tau \tag{1}$$

and

$$L_1 = \int_0^\infty \left(\frac{de}{d\tau}\right)^2 d\tau, \tag{2}$$

where e is the error at time τ. Formulae were given for L and L_1 in terms of (i) the coefficients of the characteristic equation, and (ii) the frequency response spectrum. In (2) it was shown how the response functions could be used to obtain the optimum response for zero-displacement-error systems. We shall show how the method can be extended to zero-velocity-error and zero-acceleration-error systems.

For simplicity we shall confine our attention to linear systems with one degree of freedom. As in (1) and (2), the system considered is one for which the equation of motion is

$$a_n \frac{d^n x}{d\tau^n} + a_{n-1} \frac{d^{n-1} x}{d\tau^{n-1}} + a_{n-2} \frac{d^{n-2} x}{d\tau^{n-2}} + \ldots + a_1 \frac{dx}{d\tau} + a_0 x = f(\tau), \tag{3}$$

† This paper forms part of a thesis for which the degree of Ph.D. of the University of Glasgow was awarded.

where $a_0, a_1, a_2, \ldots, a_n$ are constants and $a_n \neq 0$. We shall consider two cases: (i) where $f(\tau)$ is a linear function of τ, and (ii) where $f(\tau)$ is a quadratic function. We see that, for a stable system, when the transient motion has died away these two cases correspond respectively to systems with (i) constant velocity, and (ii) constant acceleration. Particular forms of $f(\tau)$ are chosen so that the system ultimately has no position error when subjected to either a constant velocity or a constant acceleration input.

2. Response of zero-velocity-error systems to a linearly increasing disturbance (constant velocity input)

In this case

$$f = 0 \quad \text{for } \tau \leqslant 0,$$
$$f = f_1 + f_0\tau \quad \text{for } \tau > 0, \tag{4}$$

where f_0 and f_1 are constants. For simplicity we shall take

$$\frac{f_0}{a_0} = \frac{f_1}{a_1} = a, \text{ say.} \tag{5}$$

For a stable system when the transient has died away, the steady motion is given by

$$x = a\tau$$

and

$$Dx = a,$$

where $D \equiv d/d\tau$.

We see that the system may be considered as being subjected to a constant velocity input, there being ultimately no position error (since $x = a\tau$). Such a system is sometimes called a 'zero-velocity-error system' (see (**3**), (**4**), and (**5**)).

As in (**2**) we shall find it convenient to normalize the equation of motion (3), but in a different manner from that for the zero-displacement-error system.

Let ω_1 be a frequency defined by

$$a_1 = \omega_1^{n-1} a_n \tag{6}$$

so that ω_1 would be the undamped natural frequency of a system with $a_0 = 0$. We define a new time scale by the relation

$$u_1 = \omega_1 \tau. \tag{7}$$

From (3)–(7), the normalized equation of motion is

$$\frac{d^n x}{du_1^n} + r_{n-1}\frac{d^{n-1}x}{du_1^{n-1}} + r_{n-2}\frac{d^{n-2}x}{du_1^{n-2}} + \ldots + r_2\frac{d^2x}{du_1^2} + \frac{dx}{du_1} + r_0 x$$
$$= \frac{f_1}{a_1\omega_1}(1 + r_0 u_1) \quad (\tau > 0), \tag{8}$$

where

$$r_m = \frac{a_m}{a_n \omega_1^{n-m}} \quad (m = 0 \text{ to } n). \tag{9}$$

Now the magnitude of the response x is proportional to f_1, but the nature of the response (percentage overshoot, damping time) is independent of f_1. We shall take

$$f_1 = a_1. \tag{10}$$

Then from (5), $\quad a = 1 \quad$ and $\quad f_0 = a_0.$

Thus we shall determine the response of the system given by (8) to a disturbance

$$f(\tau) = a_1 + a_0\tau. \tag{11}$$

As shown in (1) the response of the system is identical in form with that in the free motion with $Dx_0 = -1$ and $x_0, D^2x_0, D^3x_0, \ldots, D^{n-1}x_0$ zero where the suffix 0 denotes the values at time $\tau = 0$.

For a zero-velocity-error system subjected to a constant velocity input we are usually interested (in servomechanism theory) in the velocity response at a given time. We shall therefore consider the velocity response in the equivalent free motion, finding expressions for

$$L_1 = \int_0^\infty \left(\frac{dx}{d\tau}\right)^2 d\tau = \int_0^\infty v^2\, d\tau \tag{12}$$

and

$$L_2 = \int_0^\infty \left(\frac{d^2x}{d\tau^2}\right)^2 d\tau, \tag{13}$$

where

$$v = \frac{dx}{d\tau}. \tag{14}$$

Second-order zero-velocity-error system

From (1), with $Dx_0 = -1$, $x_0 = 0$, the response functions are given by

$$2L_1 a_1 = a_2,$$

i.e.

$$L_1 = \frac{1}{2\omega_1} \tag{15}$$

and

$$2L_2 a_2 = \frac{a_1^2 + a_0 a_2}{a_1}$$

or in terms of the normalized coefficient r_0 given by (9),

$$\frac{2L_2}{\omega_1} = 1 + r_0. \tag{16}$$

We see that for a system with a given value of ω_1 (i.e. for a second-order system, with a given damping factor), L_1 is a constant and L_2 is a function of r_0 (which for a mechanical system is proportional to the undamped natural frequency). L_2 is increased by increasing r_0. Now for stability

$r_0 > 0$. Consider the case $r_0 = 0$. Equation (8) becomes, using (14),

$$\frac{dv}{du_1} + v = 1 \qquad (u_1 > 0).$$

This first-order differential equation shows that v tends monotonically to unity as $u_1 \to \infty$ as shown in Fig. 1 (a). Thus the system $r_0 = 0$ is admissible and is the optimum system if we are only interested in the response in

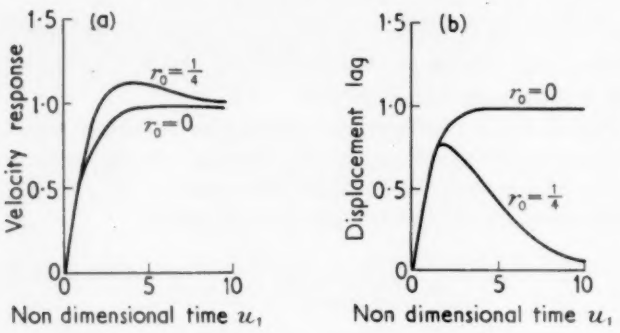

FIG. 1.

velocity, i.e. it is the system for which L_2 is least for a given value of L_1. For such a system the displacement x tends to $(u_1-1)/\omega_1$, i.e.

$$\omega_1(\tau - x) \to 1,$$

giving a displacement lag in the following of a velocity input as shown in Fig. 1 (b).

In a given system it may be either physically impossible or undesirable to have r_0 equal to zero. We have seen that when r_0 is zero there is a constant position error (at large times) between the output and the input; this is often unacceptable. As shown above, as r_0 increases L_1 remains constant but L_2 increases. As with the analysis of zero-displacement-error systems (2) we shall choose a value of r_0 ($= \frac{1}{4}$) so that the characteristic equation corresponding to (8) has equal roots. The velocity response and displacement lag are shown in Fig. 1 plotted against the non-dimensional time u_1. The velocity response has an overshoot of 14 per cent when $r_0 = \frac{1}{4}$. The maximum displacement lag $\omega_1(\tau - x)$ is 0·74, the lag becoming less than 0·10 when $u_1 \geqslant 9$. Systems having smaller (non-zero) values of r_0 would have a smaller overshoot in velocity but a higher maximum displacement lag. Considering the velocity response we are therefore led to the criterion

$$0 < r_0 \leqslant 0{\cdot}25$$

for satisfactory performance for a second-order zero-velocity-error system, the precise choice of r_0 being governed by the maximum acceptable displacement lag at any time.

Higher-order zero-velocity-error systems

The above analysis can easily be extended to higher order systems. From (1), with $Dx_0 = -1$, we have

$$x_0 = D^2x_0 = D^3x_0 = \ldots = D^{n-1}x_0 = 0,$$

$$2L_1a_0 \begin{vmatrix} a_1 & a_3 & a_5 & a_7 & \cdot & \cdot & \cdot \\ a_0 & a_2 & a_4 & a_6 & \cdot & \cdot & \cdot \\ 0 & a_1 & a_3 & a_5 & \cdot & \cdot & \cdot \\ 0 & a_0 & a_2 & a_4 & \cdot & \cdot & \cdot \\ \cdot & \cdot & \cdot & \cdot & \cdot & \cdot & \cdot \end{vmatrix} = \begin{vmatrix} -a_3 & a_0 & a_4 & a_6 & \cdot & \cdot & \cdot \\ -a_2 & 0 & a_3 & a_5 & \cdot & \cdot & \cdot \\ a_1 & 0 & a_2 & a_4 & \cdot & \cdot & \cdot \\ a_0 & 0 & a_1 & a_3 & \cdot & \cdot & \cdot \\ \cdot & \cdot & \cdot & \cdot & \cdot & \cdot & \cdot \end{vmatrix}$$

and

$$2L_2a_0 \begin{vmatrix} a_1 & a_3 & a_5 & a_7 & \cdot & \cdot & \cdot \\ a_0 & a_2 & a_4 & a_6 & \cdot & \cdot & \cdot \\ 0 & a_1 & a_3 & a_5 & \cdot & \cdot & \cdot \\ 0 & a_0 & a_2 & a_4 & \cdot & \cdot & \cdot \\ \cdot & \cdot & \cdot & \cdot & \cdot & \cdot & \cdot \end{vmatrix} = \begin{vmatrix} -a_3 & a_0 & a_2 & a_6 & a_8 & \cdot & \cdot & \cdot \\ -a_2 & 0 & a_1 & a_5 & a_7 & \cdot & \cdot & \cdot \\ a_1 & 0 & a_0 & a_4 & a_6 & \cdot & \cdot & \cdot \\ a_0 & 0 & 0 & a_3 & a_5 & \cdot & \cdot & \cdot \\ \cdot & \cdot & \cdot & \cdot & \cdot & \cdot & \cdot & \cdot \end{vmatrix}$$

or in terms of the normalized coefficients $r_0, r_2, \ldots, r_{n-1}$ given above,

$$2L_1\omega_1 \begin{vmatrix} 1 & r_3 & r_5 & r_7 & \cdot & \cdot & \cdot \\ r_0 & r_2 & r_4 & r_6 & \cdot & \cdot & \cdot \\ 0 & 1 & r_3 & r_5 & \cdot & \cdot & \cdot \\ 0 & r_0 & r_2 & r_4 & \cdot & \cdot & \cdot \\ \cdot & \cdot & \cdot & \cdot & \cdot & \cdot & \cdot \end{vmatrix} = \begin{vmatrix} r_2 & r_3 & r_5 & r_7 & \cdot & \cdot & \cdot \\ -1 & r_2 & r_4 & r_6 & \cdot & \cdot & \cdot \\ -r_0 & 1 & r_3 & r_5 & \cdot & \cdot & \cdot \\ 0 & r_0 & r_2 & r_4 & \cdot & \cdot & \cdot \\ \cdot & \cdot & \cdot & \cdot & \cdot & \cdot & \cdot \end{vmatrix} \tag{17}$$

and

$$\frac{2L_2}{\omega_1} \begin{vmatrix} 1 & r_3 & r_5 & r_7 & \cdot & \cdot & \cdot \\ r_0 & r_2 & r_4 & r_6 & \cdot & \cdot & \cdot \\ 0 & 1 & r_3 & r_5 & \cdot & \cdot & \cdot \\ 0 & r_0 & r_2 & r_4 & \cdot & \cdot & \cdot \\ \cdot & \cdot & \cdot & \cdot & \cdot & \cdot & \cdot \end{vmatrix} = \begin{vmatrix} r_2 & 1 & r_5 & r_7 & \cdot & \cdot & \cdot \\ -1 & r_0 & r_4 & r_6 & \cdot & \cdot & \cdot \\ -r_0 & 0 & r_3 & r_5 & \cdot & \cdot & \cdot \\ 0 & 0 & r_2 & r_4 & \cdot & \cdot & \cdot \\ \cdot & \cdot & \cdot & \cdot & \cdot & \cdot & \cdot \end{vmatrix} \tag{18}$$

where the determinants in (17) and (18) are all of order $n-1$ and r_1 has been put equal to 1. For stable systems of order n (> 2), i.e. systems having all the test functions positive, it can be shown that both L_1 and L_2 decrease as r_0 tends to zero. The system with $r_0 = 0$ is equivalent to an $(n-1)$th order system in v ($= Dx$). The velocity response for systems making L_1 a minimum and for systems having equal damping in the least

damped modes (referred to later as $L_{1\min}$ and L_{1d} systems) follows immediately from the analysis of (**2**) (e.g. the $L_{\min}$ and L_d systems shown in Tables 2, 3, and 4 and Fig. 2 of (**2**)). The displacement lag $\omega_1(\tau-x)$ tends to r_2 ($\neq 0$).

As with the second-order zero-velocity-error system it may be either physically impossible or undesirable to have r_0 equal to zero. Now from the analysis of (**2**) we see that for systems with r_0 zero the L_{1d} system is the most satisfactory. To derive a satisfactory velocity-error system with r_0 positive (denoted by L_{1e} system) we replace the zero root of the characteristic equation of the L_{1d} system by a real root having the same damping as the two most lightly damped modes of the L_{1d} system, and normalize the resulting equation (with $r_1 = 1$). Thus the characteristic equation for a third-order zero-velocity-error L_{1d} system is

$$\lambda^3+2\lambda^2+\lambda = (\lambda+1)^2\lambda = 0.$$

We replace the factor λ by $\lambda+1$ and normalize the resulting equation; the characteristic equation is then

$$\lambda^3+1{\cdot}73\lambda^2+\lambda+0{\cdot}19 = (\lambda+0{\cdot}58)^3 = 0$$

and the system has three equally damped modes of motion. The values of the normalized coefficients and the corresponding roots of the characteristic equation for higher-order systems are given in Tables 1 and 2.

TABLE 1

Values of the normalized coefficients r_m for zero-velocity-error systems of order n having three modes with equal damping (L_{1e} systems)

n	r_0	r_1	r_2	r_3			
3	0·19	1	1·73	1	r_4		
4	0·17	1	1·89	1·53	1	r_5	
5	0·18	1	2·14	2·97	1·52	1	r_6
6	0·11	1	3·55	2·90	3·66	1·24	1

TABLE 2

Roots of the characteristic equation for a zero-velocity-error L_{1e} system of order n

n	*Roots*
3	$-0{\cdot}58,\ -0{\cdot}58,\ -0{\cdot}58$
4	$-0{\cdot}38,\ -0{\cdot}38,\ -0{\cdot}38\pm 1{\cdot}01i$
5	$-0{\cdot}30,\ -0{\cdot}30\pm 0{\cdot}47i,\ -0{\cdot}30\pm 1{\cdot}35i$
6	$-0{\cdot}37,\ -0{\cdot}17,\ -0{\cdot}17\pm 0{\cdot}82i,\ -0{\cdot}17\pm 1{\cdot}53i$

As the order of the system increases, the damping of the least-damped mode decreases, the percentage overshoot in velocity increases as does the maximum displacement lag.

It is also of interest to normalize the coefficients of the characteristic

equation to make the numerical coefficient unity, as with the zero-displacement-error system discussed in (2). This enables a comparison to be made with the results of Whiteley in (3).

TABLE 3

Values of the normalized coefficients q_m for zero-velocity-error systems of order n having three modes with equal damping (L_{1e} systems)

n	q_0	q_1	q_2	q_3			
3	1	3	3	1	q_4		
4	1	3·8	4·6	2·4	1	q_5	
5	1	4·0	6·0	5·9	2·1	1	q_6
6	1	6·2	10·8	8·7	7·6	1·8	1

Whiteley's corresponding coefficients are much larger than those shown in Table 3, giving modes with very small damping and hence a velocity response with a long 'tail'. This is closely connected with the fact that Whiteley's calculations are based on 10 per cent maximum velocity overshoot whereas in the above analysis much better overall damping has been achieved at the expense of a larger overshoot. No curves of displacement lags are given in (3) but these would be correspondingly large. Comparing the above results with the ITAE curves (5) we find that the velocity response of the ITAE system is rather more oscillatory than the L_{1e} curves with a maximum overshoot of about the same order. The L_{1e} curves are not unlike those based on binomial filters and are, in general, thought to be a reasonable compromise between Whiteley's curves and the ITAE ones.

3. Response of zero-acceleration-error systems to a quadratic type disturbance (constant acceleration input)

In this case

$$f = 0 \quad \text{for } \tau \leqslant 0;$$

$$f = f_2 + f_1\tau + \tfrac{1}{2}f_0\tau^2 \quad \text{for } \tau > 0, \tag{19}$$

where f_0, f_1, and f_2 are constants. For simplicity we shall take

$$\frac{f_0}{a_0} = \frac{f_1}{a_1} = \frac{f_2}{a_2} = b, \text{ say.} \tag{20}$$

For a stable system when the transient has died away, the steady motion is given by

$$x = \tfrac{1}{2}b\tau^2$$

and

$$D^2x = b.$$

We see that the system may be considered as being subjected to a constant acceleration input, there being ultimately no position error. Such a system is sometimes called a 'zero-acceleration-error system' (see (3), (4), and (5)).

The analysis is carried out in a precisely similar manner to that given above. We find it convenient to normalize the equation of motion (3) in

such a way that the coefficients of d^2x/du_2^2 and d^nx/du_2^n are unity, where

$$u_2 = \omega_2 \tau \tag{21}$$

and

$$a_2 = \omega_2^{n-2} a_n. \tag{22}$$

From (3), (19)–(22), the normalized equation of motion is

$$\frac{d^nx}{du_2^n} + s_{n-1}\frac{d^{n-1}x}{du_2^{n-1}} + s_{n-2}\frac{d^{n-2}x}{du_2^{n-2}} + \ldots + s_3\frac{d^3x}{du_2^3} + \frac{d^2x}{du_2^2} + s_1\frac{dx}{du_2} + s_0 x$$

$$= \frac{f_2}{a_2\omega_1^2}(1 + s_1 u_2 + s_0 u_2^2) \quad (\tau > 0), \tag{23}$$

where

$$s_m = \frac{a_m}{a_n \omega_2^{n-m}} \quad (m = 0 \text{ to } n). \tag{24}$$

We take

$$f_2 = a_2.$$

As shown in (1) the response of the system is identical in form with that in the free motion with $D^2x_0 = -1$ and x_0, Dx_0, D^2x_0,..., $D^{n-1}x_0$ zero.

For a zero-acceleration-error system subjected to a constant acceleration input we are usually interested in the acceleration response at a given time. We shall therefore consider the acceleration response in the equivalent free motion, finding values of

$$L_2 = \int_0^\infty \left(\frac{d^2x}{d\tau^2}\right)^2 d\tau \tag{25}$$

and

$$L_3 = \int_0^\infty \left(\frac{d^3x}{d\tau^3}\right)^2 d\tau. \tag{26}$$

By a similar analysis to that given above we find that both L_2 and L_3 decrease as s_0 and s_1 tend to zero. Considering the case $s_0 = s_1 = 0$ we find that the relations for L_2 and L_3 become identical with those given in (2) for L and L_1 for a zero-displacement-error system of order $n-2$, q_m and ω_0 being replaced by s_{m+2} and ω_2.

For systems with $s_0 = s_1 = 0$, neither the displacement lag nor the velocity lag tends to zero as $\tau \to \infty$. This can be remedied as above by replacing the two zero roots of the characteristic equation by two real roots having the same damping as the two most lightly damped modes of the corresponding L_{2d} system and normalizing the resulting equation (with $s_2 = 1$). The values of the normalized coefficients and the corresponding roots of the characteristic equation are given in Tables 4 and 5.

As the order of the system increases (for $n > 4$) the damping of the least-damped mode decreases, s_0 and s_1 only decrease slightly, and the percentage overshoot in acceleration increases.

TABLE 4

Values of the normalized coefficients s_m for zero-acceleration-error systems of order n having four modes with equal damping (L_{2f} systems)

n	s_0	s_1	s_2	s_3	s_4	s_5	s_6
3	0·037	0·33	1	1			
4	0·028	0·27	1	1·63	1		
5	0·026	0·27	1	1·72	1·59	1	
6	0·026	0·27	1	2·08	2·67	1·61	1

Note: the third-order system in the above table has, of course, only three equally damped modes.

TABLE 5

Roots of the characteristic equation for a zero-acceleration-error L_{2f} system of order n

n	*Roots*
3	$-0{\cdot}33,\ -0{\cdot}33,\ -0{\cdot}33$
4	$-0{\cdot}41,\ -0{\cdot}41,\ -0{\cdot}41,\ -0{\cdot}41$
5	$-0{\cdot}32,\ -0{\cdot}32,\ -0{\cdot}32,\ -0{\cdot}32\pm0{\cdot}84i$
6	$-0{\cdot}27,\ -0{\cdot}27,\ -0{\cdot}27\pm0{\cdot}41i,\ -0{\cdot}27\pm1{\cdot}20i$

TABLE 6

Values of the normalized coefficients q_m for zero-acceleration-error systems of order n having four modes with equal damping (L_{2f} systems)

n	q_0	q_1	q_2	q_3	q_4	q_5	q_6
3	1	3	3	1			
4	1	4	6	4	1		
5	1	5·0	8·9	7·4	3·3	1	
6	1	5·6	11·5	13·1	9·1	3·0	1

Note: the third-order system in the above table has, of course, only three equally damped modes.

In Table 6 the coefficients for both third- and fourth-order systems are binomial coefficients; this follows immediately from the condition of equal damping. Whiteley's corresponding coefficients (3) are much larger than those in Table 6. As stated above, this leads to modes with much smaller damping than those shown in Table 5 (allowing for the different time scale). The L_{2f} curves are not unlike those based on the binomial filters, which are generally thought to be a suitable compromise between overshoot and damping.

REFERENCES

1. A. W. BABISTER, 'Response functions of linear systems with constant coefficients having one degree of freedom', *Quart. J. Mech. App. Math.* **10** (1957) 360.

2. A. W. Babister, 'Determination of the optimum response of linear systems (zero-displacement-error systems), *Quart. J. Mech. App. Math.* **10** (1957) 504.
3. A. L. Whiteley, 'Theory of servo systems, with particular reference to stabilization', *J. Inst. Elec. Engnrs.* **93** (1946) 353.
4. G. J. Thaler and R. G. Brown, *Servomechanism Analysis* (McGraw Hill, 1953).
5. D. Graham and R. C. Lathrop, 'The synthesis of optimum transient response: criteria and standard forms', *A.I.E.E. Trans.* **72** (1953) 273.

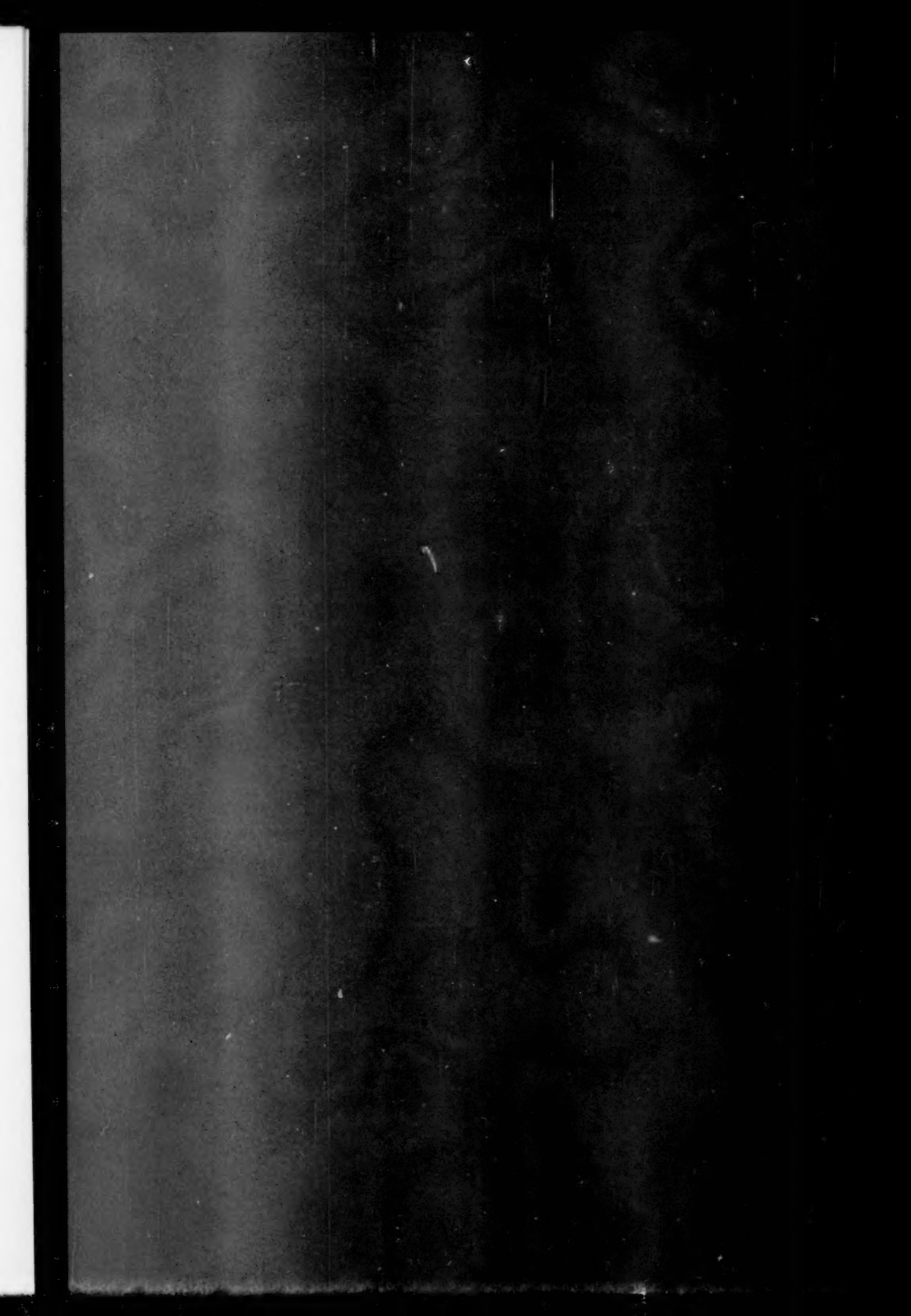

THE QUARTERLY JOURNAL OF MECHANICS AND APPLIED MATHEMATICS

VOLUME XI PART 1 FEBRUARY 1958

CONTENTS

A. KOGAN: An Application of Crocco's Stream Function to the study of Rotational Supersonic Flow past Airfoils . 1

L. C. WOODS: On the Deflexion of Jets by Aerofoils . . 24

K. STEWARTSON: On the Motion of a Sphere along the Axis of a Rotating Fluid 39

D. E. BOURNE and D. R. DAVIES: Heat Transfer through the Laminar Boundary Layer on a Circular Cylinder in Axial Incompressible Flow 52

J. L. ERICKSEN: Hypo-elastic Potentials 67

J. B. CALDWELL: Diffusion of Load from a Boom into a Rectangular Sheet 73

J. E. ADKINS: A Three-dimensional Problem for Highly Elastic Materials subject to Constraints . . . 88

J. N. KAPUR: Unified Theory of Internal Ballistics . . 98

W. HAUSER: On the Theory of Anisotropic Obstacles in Cavities 112

A. W. BABISTER: Determination of the Optimum Response of Linear Systems. Zero-velocity-error and Zero-acceleration-error Systems 119

The Editorial Board gratefully acknowledge the support given by: Blackburn & General Aircraft Limited; Bristol Aeroplane Company; Courtaulds Scientific and Educational Trust Fund; English Electric Company; Hawker Siddeley Group Limited; Metropolitan-Vickers Electrical Company Limited; The Shell Petroleum Co. Limited; Vickers-Armstrongs (Aircraft) Limited.